

# FOG

## Freiberg Online Geology



FOG is an electronic journal registered under ISSN 1434-7512

2005, VOL 14

Böhme, Beate

## Geo-ecology of the Lake Urema / Central Mozambique

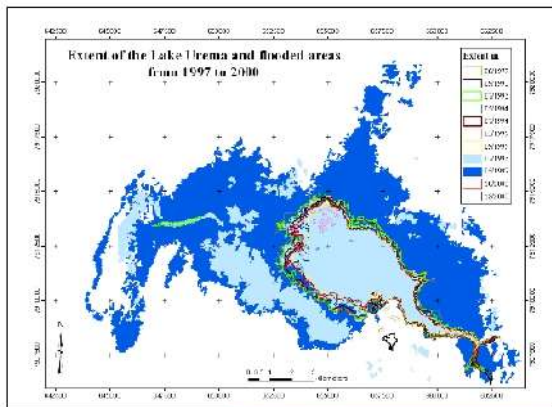


## Table of Contents

1	Abstract.....	10
2	Introduction.....	11
3	Assumptions and research questions.....	13
4	Study area.....	14
	4.1 Lake Urema in the Gorongosa National Park.....	14
	4.2 Geology and Geomorphology.....	16
	4.3 Climate.....	20
	4.4 Soils.....	22
	4.5 Hydrology / Hydrogeology.....	23
	4.6 Ecology and Land Use.....	26
	4.7 Human factor.....	29
5	Methods.....	30
	5.1 Remote Sensing and GIS.....	30
	5.1.1 Data sources and software products.....	30
	5.1.2 Analysis of remotely sensed data.....	30
	5.1.2.1 Geometric and atmospheric correction.....	30
	5.1.2.2 Extraction of the lake's contour from NDVI.....	31
	5.1.2.3 Extraction of the lake's contour and of the floodplain grasslands using supervised classification.....	31
	5.1.2.4 Calculation of a DTM from ASTER data .....	32
	5.1.2.5 Extraction of the drainage system and the catchment area from SRTM data (Shuttle Radar Topography Mission).....	32
	5.1.2.6 Calculation of the lake's volume.....	32
	5.2 Field sampling & Mapping.....	34
	5.2.1 Sampling schedule and logistics.....	34
	5.2.2 Hydrology and hydrochemistry.....	34
	5.2.2.1 Lake level height.....	34
	5.2.2.2 Bathymetry.....	34
	5.2.2.3 Measurement of discharge.....	35
	5.2.2.4 On-site measurement of water chemistry.....	36
	5.2.3 Sediment cores.....	37
	5.2.4 Vegetation transects and mapping of reference biotopes.....	38
	5.3 Laboratory analyses.....	38
	5.3.1 Water chemistry: major ions, TIC, DOC.....	38
	5.3.2 Sediment analyses.....	40
	5.3.2.1 Grainsize distribution, determination of TC and TIC.....	40
	5.3.2.2 X-ray diffraction (XRD).....	40
6	Results.....	41
	6.1 Tectonics.....	41
	6.2 Morphology.....	42
	6.2.1 The rift valley .....	42
	6.2.2 Definition of the catchment area.....	47
	6.2.3 Lake basin.....	49
	6.3 Change detection.....	52
	6.4 Hydrology.....	61

6.4.1	Change of the lake level height during the period of investigation.....	61
6.4.2	How much rain is required to fill the lake's 1997 extent?.....	64
6.5	Water chemistry.....	65
6.6	Sedimentation.....	78
6.6.1	Sediment coring.....	78
6.6.2	Siltation.....	83
6.7	Vegetation investigation.....	84
6.7.1	Transects .....	84
6.7.2	Reference sites in the floodplain around Lake Urema.....	87
6.8	Fisheries.....	88
7	Discussion.....	89
7.1	Evaluation of methods.....	89
7.1.1	Remote Sensing and GIS.....	89
7.1.2	Field sampling and mapping.....	90
7.1.3	Hydrology and hydrochemistry.....	91
7.1.4	Sediment analyses.....	92
7.2	Does Lake Urema undergo changes?.....	92
7.3	Which factors influence the hydrological regime of Lake Urema?.....	94
7.3.1	Neo-tectonics.....	94
7.3.2	Morphology and Sedimentation.....	95
7.3.3	Quantity of surface water.....	97
7.3.4	Water chemistry.....	98
7.3.5	Groundwater fed?.....	101
7.3.6	Ecological responses of Lake Urema.....	102
7.4	Will Lake Urema disappear?.....	104
8	Conclusions and recommendations.....	106
9	Sources.....	108
10	Acknowledgments.....	113

## Illustration Index

Figure 1: Location of the Gorongosa National Park (green colored in the right picture) in Central Mozambique, Southern Africa (map created with GMT by Wobbe).....	14
Figure 2: Location of Lake Urema in the Gorongosa National Park (rivers and park boundaries from IGN.FI CENACARTA, 1999, some additional rivers digitized from DINAGECA, 1997/98).....	15
Figure 3: Geologic-tectonic correlation of the Mozambique Basin (from Lächelt, 2004).....	17
Figure 4: Cross-section of the Urema Rift (from Lächelt, 2004).....	18
Figure 5: Geology of the Urema Rift and adjacent units (SRTM data (90 m resolution) superposed with geology data from Edição, 1968a).....	19
Figure 6: Average monthly rainfall for the major landscape units in the Gorongosa Ecosystem; derived from FAO LocClim Climate estimator (from Owen, 2004).....	20
Figure 7: Flow measurements at the Urema River (station E81, elevation 12 m a.s.l., close to the southern boundary of the Gorongosa National Park, see figure 2) 10/1956-09/1978, data from ARAC, 2004.....	24
Figure 8: Land use around Lake Urema (after IGN.FI CENACARTA, 1999).....	26
Figure 9: Dry season distribution and abundance of hippo from aircounts in November 1972 (after Tinley (1977), figure 9.11).....	28
Figure 10: Differences in water volume and extent of Lake Urema between 05/1997 and 10/2000.....	33
Figure 11: Dugout canoe for the transport on Lake Urema (photo: Beate Böhme).....	34
Figure 12: Lake level gauge at Lake Urema (photo: Beate Böhme).....	34
Figure 13: Current meter (photo: Beate Böhme).....	35
Figure 14: Measurement of water clarity with Secchi-disc (photo: Beate Böhme).....	37
Figure 15: Sediment core (photo: Beate Böhme).....	37
Figure 16: Vegetation transect V01, supposed path of hippo (photo: Beate Böhme).....	38
Figure 17: Seismic activity in the Urema Rift between 1973 and 2004, data acquired from Harvard Seismology CMT catalog [web_11], underlying relief from GTOPO30 [web_12], map processed in GMT.....	41
Figure 18: Overview of Urema Rift from SRTM data, rivers from IGN.FI CENACARTA (1999) and digitized from DINAGECA (1997/98).....	43
Figure 19: Detail of the Urema Basin, with lake's extent of 05/1997, from SRTM data, rivers from DINAGECA 1997/98.....	44
Figure 20: Stream profile of the Pungoe River within Mozambique.....	45
Figure 21: Stream profile of the Nhandugue River.....	46
Figure 22: Stream profile of the Nhampasa River.....	46
Figure 23: Stream profile of the Muredeze River.....	46
Figure 24: Elevation Profile through the so-called “Muredeze-plug”.....	46
Figure 25: Catchment of the Lake Urema with subcatchments and drainage system as derived from SRTM, sun elevation angle 30°, sun azimuth angle 90°.....	48
Figure 26: Morphology around Lake Urema as derived from SRTM, sun elevation angle 30°, sun azimuth angle 90°.....	49
Figure 27: Location of the four depth profiles in Lake Urema, curves smoothed using a moving average , profiles from left to right: no 1 - 2 – 3 – 4 .....	50

Figure 28: Depth profiles measured from the southwestern shoreline to the northeastern shoreline, curves smoothed with moving average (over 10 measurements) and csplines.....	51
Figure 29: Open water surface of Lake Urema from NDVI.....	52
Figure 30: Comparison of the area of Lake Urema from supervised classification and NDVI.....	53
Figure 31: Output of the supervised classification, lake's extent from 1960 from topographical map (DINAGECA, 1960?).....	56
Figure 32: Floodplain grassland at the northeastern part of the Lake Urema from airplane, height above ground 150-200 m (photo: Beate Böhme).....	55
Figure 33: Location of profiles in BGY and BGW images, background image from Landsat TM 05/28/1994, Brightness (red), Greenness (green) and Wetness (blue).....	57
Figure 34: Pattern of Brightness (red), Greenness (green) and Yellowness (1979: blue)/Wetness (other years: blue) along profiles in the floodplain around Lake Urema, profiles show west-east-orientation.....	59
Figure 35: Pattern of Brightness (red), Greenness (green) and Yellowness (1979: blue)/Wetness (other years: blue) along profiles in the floodplain around Lake Urema, profiles show west-east-orientation.....	60
Figure 36: WP 96; Urema River about 7 km downstream the mouth of the Lake Urema (photo: Beate Böhme)....	62
Figure 37: Hydrometric station E 81 at the Urema River in September 2004 (photo: Beate Böhme).....	62
Figure 38: Cross-section of the Vunduzi River at site 318.....	63
Figure 39: Sample sites at Lake Urema, white numbers are labels of water sample sites, V01-V06 are vegetation transects, background Landsat ETM+ 4/3/2, 12/30/2000, image stretch by standard deviation (n=2)....	66
Figure 40: Air temperature vs. water temperature of Lake Urema.....	67
Figure 41: Measurements of water temperature at Lake Urema between 08-10/2004, Landsat ETM+ 4/3/2, 12/30/2000, image stretch by standard deviation (n=2).....	68
Figure 42: Measurements of pH at Lake Urema between 08-10/2004, background Landsat ETM+ 4/3/2, 12/30/2000, image stretch by standard deviation (n=2).....	68
Figure 43: Measurements of electrical conductivity (EC) at Lake Urema between 08-10/2004, Landsat ETM+ 4/3/2, 12/30/2000, image stretch by standard deviation (n=2).....	69
Figure 44: Measurements of Secchi-disc transparency at Lake Urema between 08-10/2004, background Landsat ETM+ 4/3/2, 12/30/2000, image stretch by standard deviation (n=2).....	70
Figure 45: Top view at a water filter (200 nm mash size, magnification 8 x) after filtration of 90 ml water from site 115 (photo: Beate Böhme).....	71
Figure 46: Measurements of redox potential at Lake Urema between 08-10/2004, background Landsat ETM+ 4/3/2, 12/30/2000, image stretch by standard deviation (n=2).....	72
Figure 47: Correlation of saturation of dissolved oxygen, pH and water temperature.....	73
Figure 48: Measurements of saturation of dissolved oxygen at Lake Urema between 08-10/2004, background Landsat ETM+ 4/3/2, 12/30/2000, image stretch by standard deviation (n=2).....	73
Figure 49: Correlation of saturation of dissolved oxygen, pH and water temperature.....	73
Figure 50: Concentration of major anions in the water of Lake Urema and tributaries.....	75
Figure 51: Concentration of major cations in the water of Lake Urema and tributaries.....	76
Figure 52: Concentration of total dissolved solids along the transect through Lake Urema and its tributaries.....	77
Figure 53: Comparison of the measured electrical conductivity EC with the calculated electrical conductivity ....	78
Figure 54: Location and appearance of the sediment cores at Lake Urema, sediment distribution after Januario (2004), background picture Landsat ETM+ 4/3/2, 12/30/2000, image stretch by standard deviation (n=2).....	79

Figure 55: Mineral composition of S00-2 and S01-2 according to the results of XRD.....	80
Figure 56: Mineral composition of S04-2 and S04-3 according to the results of XRD.....	81
Figure 57: Mineral composition of S03-2 and S03-3 according to the results of XRD.....	82
Figure 58: Mineral composition of the whole samples.....	83
Figure 59: Vegetation transect V01 (photos: Beate Böhme).....	85
Figure 60: Vegetation transect V06 (photos: Beate Böhme).....	86
Figure 61: Vegetation transect V07 (photos: Beate Böhme).....	87
Figure 62: Interpolated, estimated rainfall for climate zone 05 for the period 1993 to 1998, from web_6.....	94
Figure 63: Hippo path in the floodplain southwest of Lake Urema close to Mira Hippo (photo: Beate Böhme). .	103

## Index of Tables

Table 1: Overview about ecosystems and vegetation types in the rift valley (after Tinley, 1977).....	27
Table 2: Population estimates for Hippopotamus in the Gorongosa National Park from 1968 to 2004, 1 Figures from Tinley, (1977), 2 figures from SWECO&Associates_X (2004), 3 figure from Falker (2005).....	28
Table 3: Modified coverage scale after Braun-Blanquet.....	38
Table 4: Area of subcatchments and sum of length of all rivers in these subcatchments after modeling from SRTM data and from IGN.FI CENACARTA (1999).....	47
Table 5: Length of the depth profiles 1 to 4, Lake Urema.....	50
Table 6: Average and standard deviation of the depth profiles 1 to 4, Lake Urema.....	51
Table 7: Area of Lake Urema; lake contour derived from satellite images through application of a NDVI threshold (1979 NDVI < 0.03, otherwise NDVI < 0) or of a supervised classification, figure for 1960 from topographical map [DINAGECA, 1960?].	54
Table 8: Water loss through Potential Evaporation (Epot), water input through precipitation (P) and surface runoff (R) during September to October 2004, all numbers referred to an lake area of 18.5 km <sup>2</sup> .....	64
Table 9: Water depth, pH and electrical conductivity EC in the trophogenic and tropholytic zone, site 109a and b close to each other.....	74
Table 10: Saturation of dissolved oxygen in the trophogenic and tropholytic zone.....	74
Table 11: Error of analysis, modeled in PhreeqC, analysis is satisfying if error is below 2% (+).....	77
Table 12: Composition of rainwater in Beira, sampled in March 2005, concentration in mg/l,.....	78
Table 13: Concentration of Total Organic Carbon (TOC).....	83

# 1 Abstract

Lake Urema is one of the most important ecological features of the Gorongosa National Park, Central Mozambique. It is located in the Urema Rift which is a part of the East African Rift System. The understanding of the geo-ecology of the lake and its tributaries is particularly important for the conservation of its floodplain habitats. There are recent concerns that the lake has changed during the last years. A multi-temporal and multi-disciplinary approach was applied to investigate the dynamics and control mechanisms of the lake. Principal methods adopted were: remote sensing analyses of time series of Landsat and ASTER data, geomorphological interpretations of SRTM (Shuttle Radar Topography Mission) data as well as field investigations such as water and sediment analyses and vegetation mapping.

The study showed that the water of Lake Urema and its in- and outflow has very low concentrations of total dissolved solids (TDS) between 20 to 100 mg/l. The pH is on average about 7, regulated by a  $\text{CO}_2$  -  $\text{HCO}_3^-$  -  $\text{CO}_3^{2-}$  buffering system. The water transparency is very low, mostly less than half a meter. During the period of investigation no outflow of the lake was observed, but the Vunduzi River, one of the tributaries to Lake Urema, had a considerable discharge. A decrease of the lake level height was detected over a period of two months. In addition to the evaporation from the open water surface of the lake, water is probably also lost through spreading into the adjacent floodplain grasslands, through evapotranspiration as well as through infiltration. A significant enrichment of the water constituents in the dry season did obviously not occur.

The widespread distribution of clayey sediments over large parts of the lake and the evidence of sandy sediments in the narrowing part of the lake towards its outflow suggest a temporally and spatially constrained pattern of transport and deposition. It is supposed that the axial part of the lake is characterized by a more energetic flow and the lateral areas by quiescent conditions.

The results of the supervised classification of the satellite images from 1979 to 2000 did not indicate a trend for the variations of the lake's size. The area of Lake Urema ranged from 17.4 km<sup>2</sup> (09/1995) to 25.1 km<sup>2</sup> (08/1979). A rainfall anomaly was responsible for the outstanding lake size in May 1997. Investigations showed that alluvial fans limit the Urema Basin from all sides and make Lake Urema a kind of “reservoir lake”.

Further studies should focus on the enlightenment of the water balance of the lake system. Especially the contribution of groundwater to the water balance of the lake is not yet understood.

## 2 Introduction

Approximately 1% of the African surface area is floodplain<sup>1</sup> [SHUMWAY, 1999]. Floodplains are assigned to freshwater wetlands<sup>2</sup> whose conservation and use is object of the Ramsar Convention<sup>3</sup> [web\_17].

The importance of wetlands arises from their contribution to groundwater recharge and discharge regulation, flood- and erosion control as well as to the retention of sediments, nutrients and toxic substances. Wetlands provide habitats for wildlife and are characterized by a high biological diversity [MATIZA & CRAFTER, 1994]. Causes of global wetland losses through human activities are drainage, groundwater abstraction, discharge of pollutants, impacts of hydraulic engineering facilities and filling [BREEN at al., 1997]. Droughts, erosion and biotic effects are common natural causes for the loss of wetlands.

Lake Urema and the adjacent floodplains are very important, if not even the most important ecological feature in the Gorongosa National Park. The Gorongosa National Park is located in Central Mozambique at the southern end of the East African Rift Valley. This wetland is part of the Lower Zambeze-Gorongosa-Buzi-Pungue Flood Plain System [BREEN at al., 1997]. Prior to the civil war in Mozambique (1976-1992), the Gorongosa National Park was called the “jewel in the crown of Mozambique’s National Parks”. Until then, Urema Floodplains inhabited – at least periodically - a variety of wildlife comprising hippo, buffalo, elephant, zebra, waterbuck, impala, oribi, sable, wildebeest and eland [TINLEY, 1977]. The armed conflicts came along with the decimation of local populations of animals in the National Park. Numbers of large mammals were reduced by as much as 95% [web\_1]. Bird species remained largely untouched by the poaching and killing and spectacular concentrations of waterbirds can be observed on the Urema Floodplain.

Former studies on the Gorongosa Ecosystem in the 1960s-1970s [TINLEY, 1977] indicated that the size of Lake Urema varies strongly between dry and rainy season with extensions ranging from approximately 10 km<sup>2</sup> to 200 km<sup>2</sup>. These variations are triggered by the timing and amount of the water flows from the adjacent mountains, which therefore hold a key position for the maintenance of the floodplain ecosystem.

---

1 “A floodplain is any region along the course of a river where large seasonal variations in rainfall result in overbank flooding into the surrounding plains”. [SHUMWAY, 1999]

2 “For the purpose of this Convention wetlands are areas of marsh, fen, peatland or water, whether natural or artificial, permanent or temporary, with water that is static or flowing, fresh, brackish or salt, including areas of marine water the depth of which at low tide does not exceed six meters.”[web\_17]

3 The mission of the Ramsar Convention “is the conservation and wise use of all wetlands through local, regional and national actions and international cooperation for the conservation and wise use of wetlands and their resources”.

Now that the park experiences an ecological rehabilitation and attempts to attract tourists are undertaken, an update inventory of the lake's ecosystem seemed to be expedient.

This is essential as concerns about a change of the lake's extent and its hydrological regime are expressed.

The analysis of a multi-temporal remote sensing image dataset for change detection is reasonable as other data sources about the lake's state in the last 20 years are sparse. The approach of wetland change detection with remote sensing data was well proven e.g. by NELLIS et al. (1998), MUNYATI (2000) and FRAZIER & PAGE (2000).

Subsequently, the objectives of this thesis about Lake Urema are presented. The study area will be characterized in chapter 4. Chapter 5 describes the methods which were applied. Results are presented in chapter 6 and comprehensively discussed in chapter 7. The achievements of the study are highlighted. This report ends with recommendations for future investigations.

### 3 Assumptions and research questions

There is a recent concern in the local park staff community that the extent of Lake Urema has decreased over the last decades. Another concern deals with sediment accumulation which would trigger the siltation of the lake. Reasons for such developments can be diverse: natural factors include climate, neo-tectonical movements and morphology. Land use changes in the catchment area (deforestation, flood regulation) and the nearly complete eradication of hippopotamus, a key species in the wetland ecosystem, during the civil war are possible anthropogenic causes.

Already BURLISON et al. (1977) attempted to solve the question whether a drying up of the area of the Gorongosa National Park occurred. In their work they discussed possible reasons without a definite conclusion. However, the concern was expressed, that a drying out of the floodplain grasslands could lead to bush encroachment with all its consequences for the ecosystem, e.g. a shift from grassland species towards savanna woodland species.

Since the comprehensive study of TINLEY (1977) few studies were undertaken to understand the lake's ecosystem. SWECO&ASSOCIATES (2004) dealt with the hydrological regime of the Pungoe River Basin and OWEN (2004) with that of the Gorongosa Ecosystem.

But still the hydrological regime of Lake Urema is not yet fully understood. Therefore an interdisciplinary approach was used to solve the following questions:

- 1) What is regulating the hydrological regime of Lake Urema (groundwater, surface water, morphology, neo-tectonical movements)?
- 2) How much did the extent of Lake Urema vary over the last 20 years?
- 3) Are there changes in the lake's system and what are potential reasons?
- 2) What is the state of Lake Urema in dry season 2004 regarding hydrochemistry, sedimentation and littoral vegetation?

Due to the poor knowledge on the lake's recent state field investigations were conducted in the dry season 2004. They comprised analyses of water chemistry, sediments and littoral vegetation. The field work was completed by laboratory analyses of water- and sediment samples.

Eleven satellite scenes from dry and rainy seasons (1979-2000) were used to describe the intra- and inter-annual variations of the extent of Lake Urema. A Digital Terrain Model served for the description and interpretation of the morphology of the lake and its surroundings.

The results of this study were to be discussed comprehensively in the context of the catchment area of Lake Urema. Finally, recommendations for further investigations should be given.

## 4 Study area

### 4.1 Lake Urema in the Gorongosa National Park

Lake Urema is located in southern Africa, at 18°52'S and 34°30'E in the Sofala Province / Central Mozambique. It is part of the Gorongosa National Park (established in 1960) which covers an area of 5370 km<sup>2</sup> [SWECO&ASSOCIATES\_X, 2004]. The Pungoe River represents the southern border of this protected conservation area [Figure 1, Figure 2].<sup>4</sup>

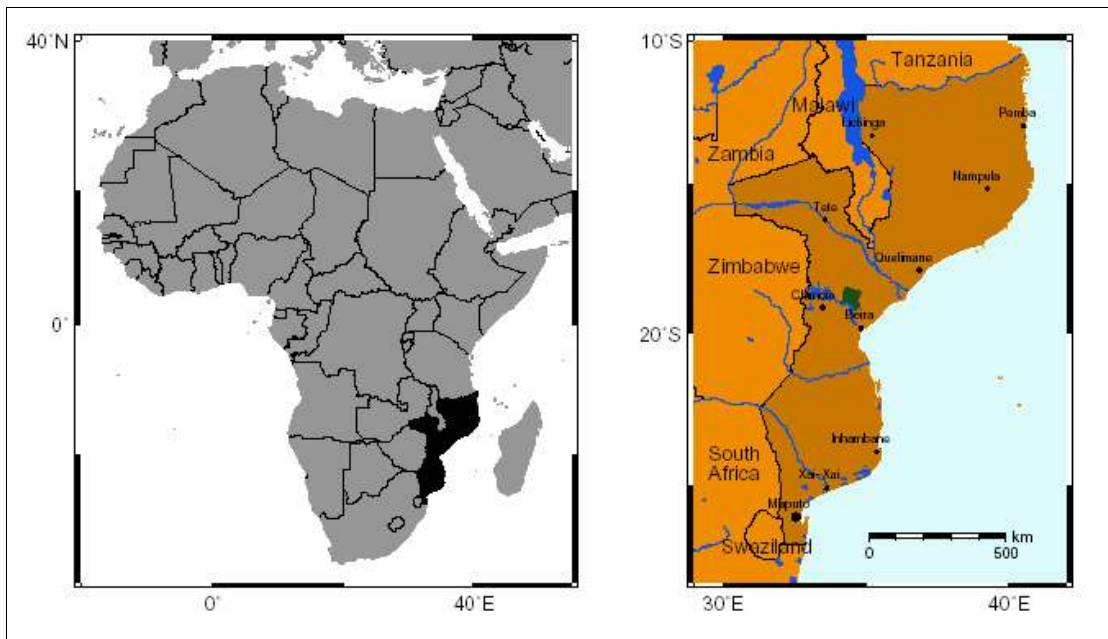


Figure 1: Location of the Gorongosa National Park (green colored in the right picture) in Central Mozambique, Southern Africa (map created with GMT by Wobbe)

<sup>4</sup> all location names were adopted from topographical map 1 : 250 000 [DINAGECA, 1997/1998].

4 Study area

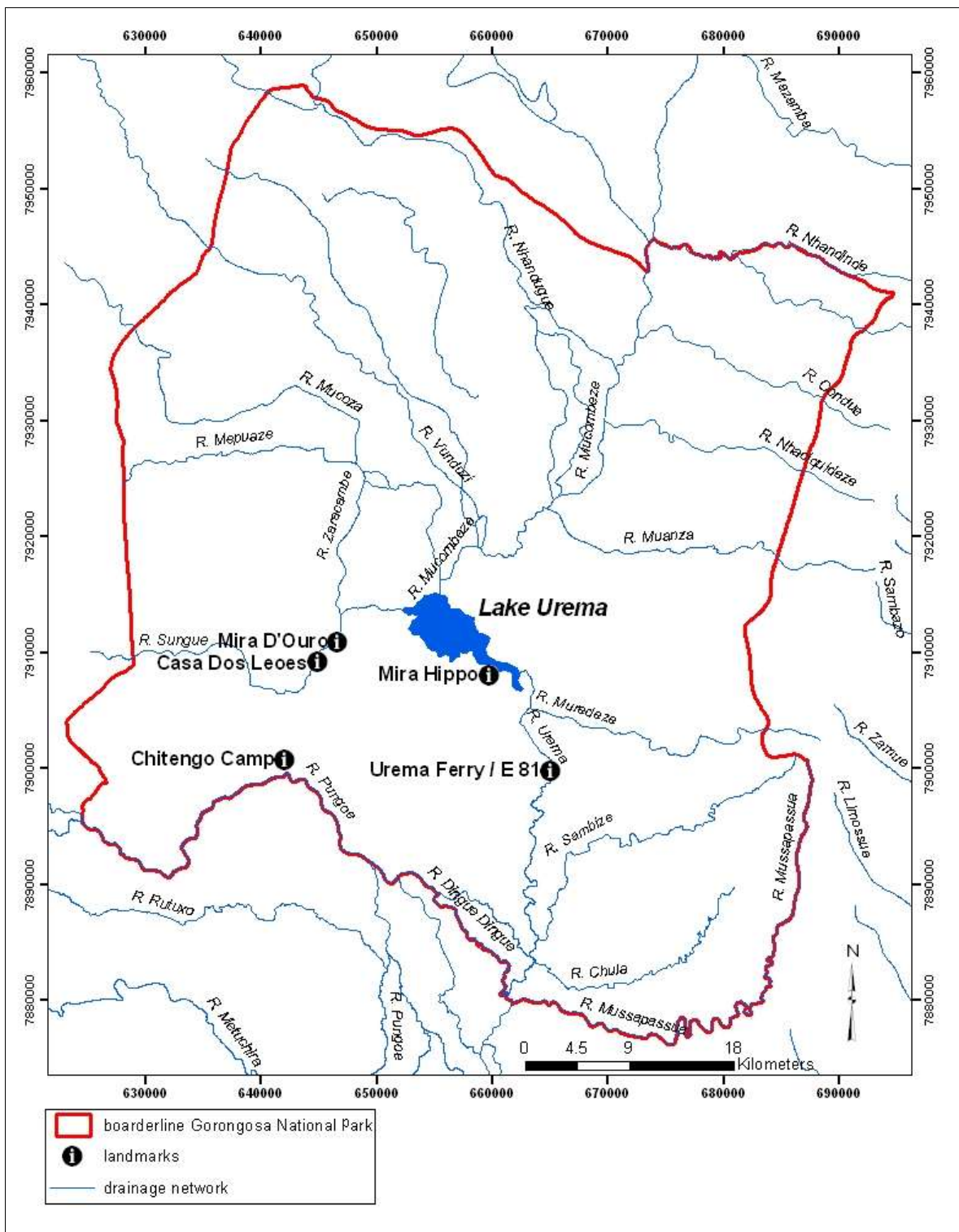


Figure 2: Location of Lake Urema in the Gorongosa National Park (rivers and park boundaries from IGN.FI CENACARTA, 1999, some additional rivers digitized from DINAGECA, 1997/98)

## ***4.2 Geology and Geomorphology***

LÄCHELT (2004) considers the rifts in Mozambique to be an integrated part of the East African Rift System (EARS). They are characterized by less volcanic activity than the further northern parts of the EARS, and those south of 15°S also show less seismic activity. Rifting is mainly implied by grabens, fractures and volcanic pipes.

During the Gondwana Period (Karoo Period, Upper Carboniferous-Middle Jurassic: 300-175 Ma), when southern Africa was located in the interior of the supercontinent Gondwana, large intracratonic basins developed which were filled with sediments and volcanics composing the Karoo supergroup. In Mozambique this period lasted up to the Lower Cretaceous (140 Ma) [LÄCHELT, 2004].

Seafloor spreading related to the disintegration of Gondwana followed an initial phase of extensive rifting between 300 and 205 Ma which left rift structures located in the southern continuation of the later East African Rift and Mozambique Channel [LÄCHELT, 2004].

During the Post-Gondwana Period (Lower Cretaceous to Cenozoic) the western flank of the Urema Rift formed by reactivation of a structure from the Gondwana Period while the eastern flank was initiated [LÄCHELT, 2004] [Figure 3].

In the last rifting phase of the Post-Gondwana Period, referred to as “Neorifting phase” (35-5 Ma), the EARS formed and pre-existing rift faults were repeatedly activated [LÄCHELT, 2004].

Figure 4 visualizes the halbgraben-like profile of the Urema Rift which is due to differences in timing and amount of displacement at the eastern and western boundary faults. Urema Rift has a N-S extension of 280 km and ranges from the Zambeze-Chire junction to the Indian Ocean at Beira and Sofala.

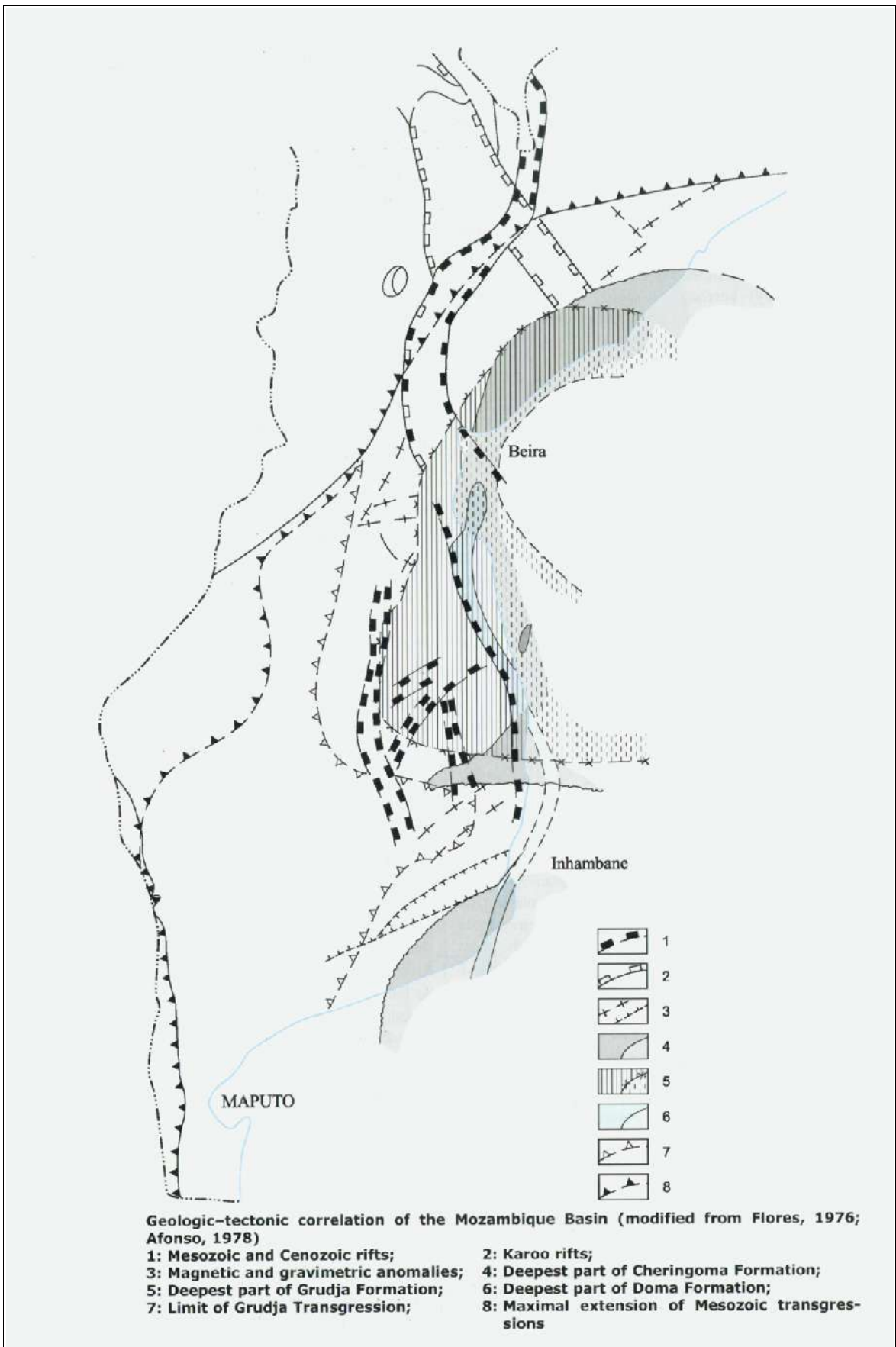


Figure 3: Geologic-tectonic correlation of the Mozambique Basin (from LACHELT, 2004)

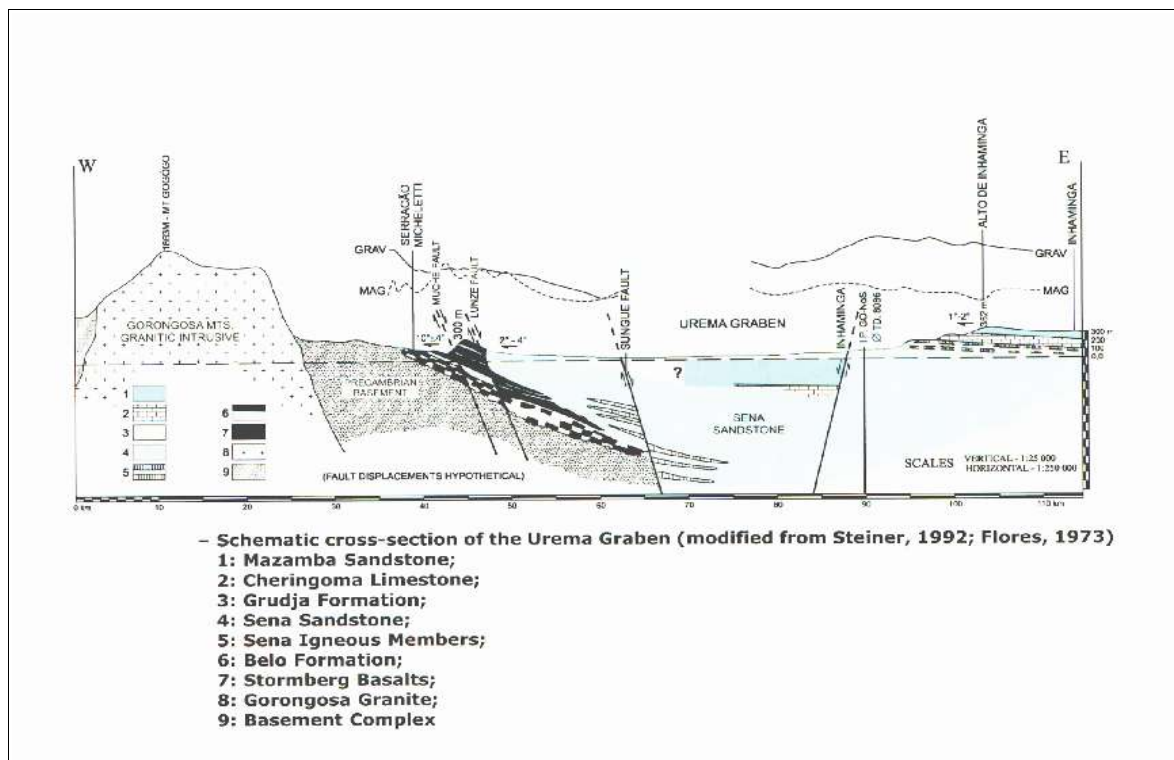


Figure 4: Cross-section of the Urema Rift (from LÄCHELT, 2004)

The **rift floor** is covered with unconsolidated pleistocene to recent alluvial deposits [DNA, 1987] [Figure 5]. The sediment distribution shows coarse proximal facies sediments of the alluvial fans at the margins of the rift floor and fine-grained silts and clays in the central part forming slacks and basins. Sediments are underlain by Mazamba Sandstone (Miocene) and Cheringoma Limestone (Eocene) over cretaceous continental arkosic sandstones and conglomerates (within a calcareous matrix) of the Sena Formation [LÄCHELT, 2004].

The **Báruè Midlands** are part of the former Miocene planation surface [TINLEY, 1977]. Westwards the Midlands turn over into the Great Escarpment. The Báruè Formation consists of Precambrian quartzose, feldspatic and micaceous gneisses and migmatites [LÄCHELT, 2004]. Quartzites and marbles occur locally. The landform is undulating to incised.

The **Gorongosa Massif** is a cretaceous granitic intrusive complex (gabbro, granite) extending 30 km in N-S direction and 20 km E-W. The highest elevation is at GoGoGo peak with 1863 m a.s.l. The massif rises about 1400 m above the surrounding Midlands. The slopes of the Gorongosa Mountain are approximately 30-40 degrees.

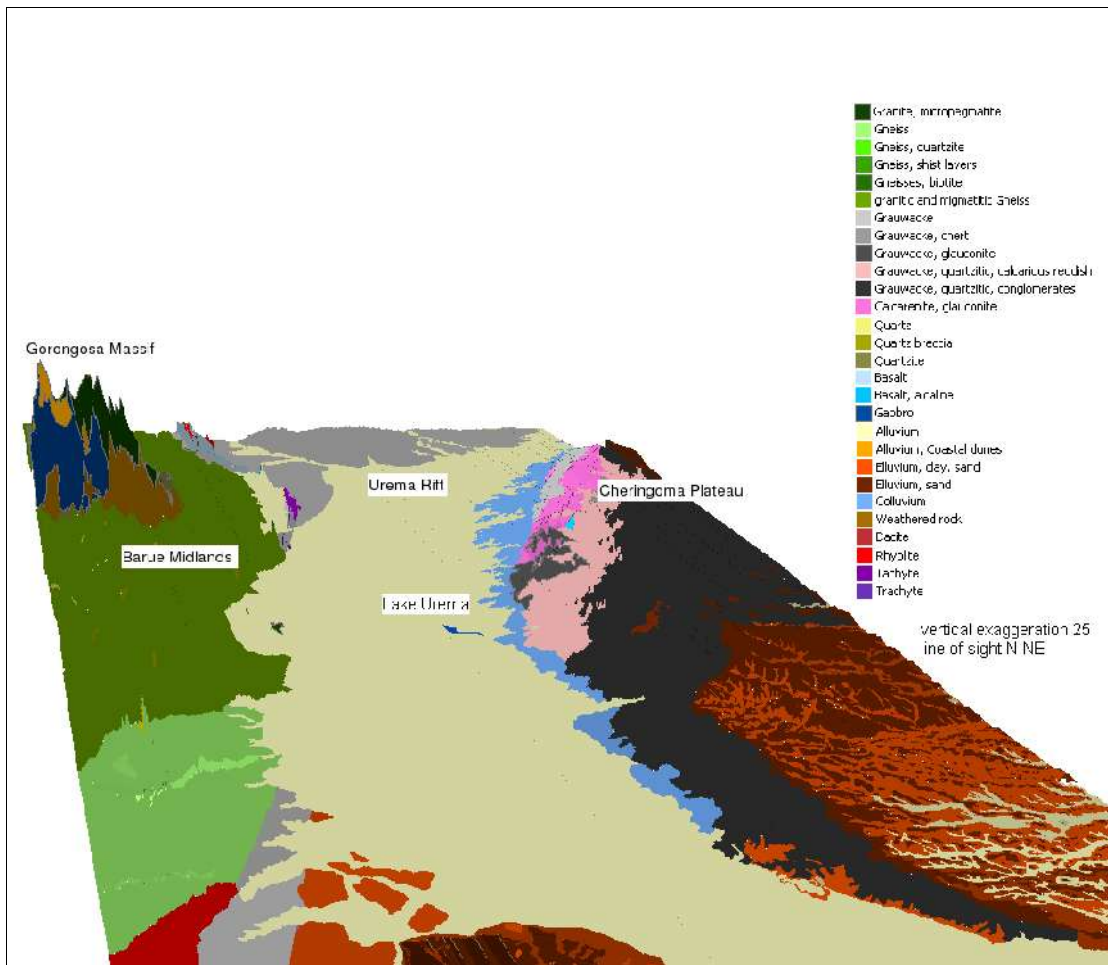


Figure 5: Geology of the Urema Rift and adjacent units (SRTM data (90 m resolution) superposed with geology data from Edição, 1968a)

The Urema Rift is flanked by the **Cheringoma Plateau** to the east, which rises up to 300 m a.s.l. The Cheringoma Plateau is underlain by a 1-2° seaward dipping sequence from Cretaceous to Pleistocene [EDIÇÃO, 1968a]. Pleistocene sandy alluvium and Miocene Mazamba Sandstone (arkosic and conglomeratic sands containing relics of molluscs) lay on top of the Cheringoma Formation (Middle-Upper Eocene). The Cheringoma Formation is characterized by the presence of nummulitic limestones or limestones containing gastropodes and echinoderm fauna. The limestones include layers of clay and calcareous sandstone. Towards the north the limestone bedrock of the Cheringoma Plateau caused the development of karst features which can be seen at the interrupted drainage system (pans, sinkholes) [OWEN, 2004]. The cretaceous Grudja Formation on top of Sena Sandstones contains calcareous and glauconitic sandstones.

### 4.3 Climate

The study area is influenced by the monsoon circulation. With the southward migration of the Inter-Tropical Convergence Zone (ITCZ) across Southern Mozambique from December to February, the northeast monsoon causes air stream flow from the high pressure centers of the Indian Continent. This period represents the principal rainy season in southern Africa.

In austral winter the wind systems are reversed thus flowing as southwest monsoons from the equator to Arabia, India and Burma.

The de Martonne's Index of Aridity ( $P/(T+10)$ ; T = air temperature, P = precipitation) indicates that the Gorongosa Mountain, the Bárúè Midlands, the Cheringoma Plateau and the rift valley are different physiographic regions [TINLEY, 1977]. The average monthly rainfall for all units is shown in Figure 6.

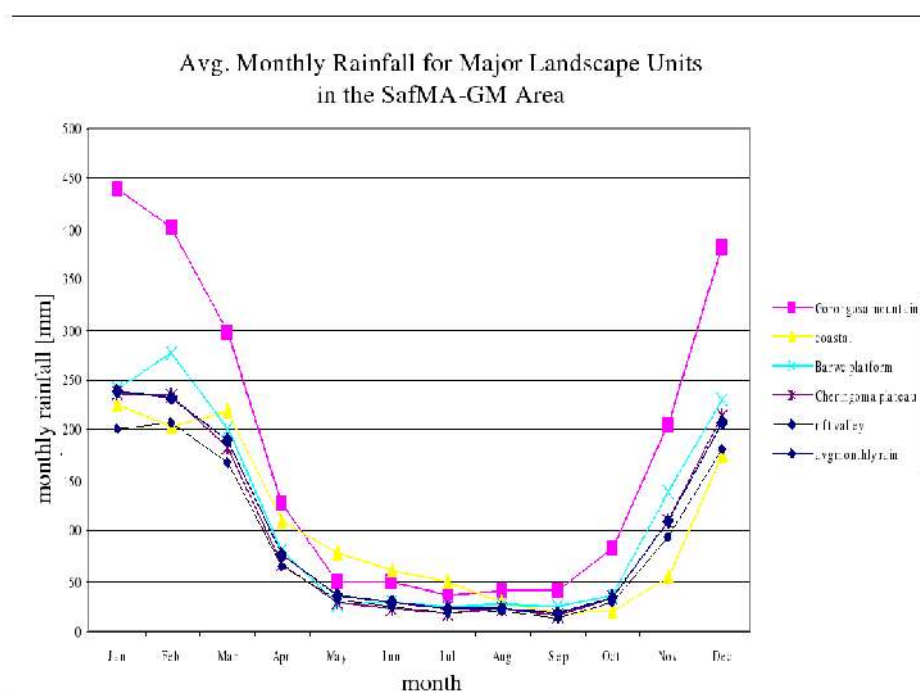


Figure 6: Average monthly rainfall for the major landscape units in the Gorongosa Ecosystem; derived from FAO LocClim Climate estimator (from OWEN, 2004), location of landscape units in Figure 5

**The floor of the Urema Rift** is the driest section among the four described physiographic regions. After KÖPPEN it is assigned to Wet-Dry Tropical Savanna Climates (Aw) with a moist, warm season from November to April and a cool, dry period from May to October [COBA, 1977?]. The annual precipitation is between 600 and 1000 mm/y [OWEN, 2004]. The mean annual air temperature at Chitengo, located at the rift floor, is 25.7 °C (21.5 °C in winter, 28.6 °C in summer) [COBA, 1977?].

The water deficit<sup>5</sup> at the floor of the rift valley comprises 600-800 mm on an annual basis, with a dry season deficit of 700 to 850 mm and a wet season surplus of 0-150 mm (results from global FAO LocClim Climate estimator [OWEN, 2004]).

The sum of annual rainfall in the **Báruè (Barwe) Midlands** is between 800 and 1200 mm [OWEN, 2004] whereas rainfall is decreasing with distance from the sea but is also subject to orographic effects in western direction [TINLEY, 1977].

**Gorongosa Mountain** receives up to 2000 mm rainfall per year due to orographic rainfalls [TINLEY, 1977]. The most constant among the moisture-bearing winds come from SE.

The lowest numbers for the annual potential evaporation among the four physiographic regions were modeled with FAO LocClim Climate estimator for the Gorongosa Mountain (around 1000 mm/y) and the highest values for the rift valley (up to 1600 mm/y) [OWEN, 2004]. The modeled P-PET water balance indicates that only the Gorongosa Mountain has an annual water surplus of 300 to 500 mm.

The crest of the **Cheringoma Plateau** receives on average between 1000 and 1400 mm rainfall [OWEN, 2004].

---

<sup>5</sup> water deficit = precipitation – potential evaporation

#### **4.4 Soils**

The soils of the Gorongosa Mountain and the Midlands developed under the influence of denudation and colluvation while those of the rift valley are influenced by accretion and hydromorphism (flood-ebb regime, seasonal climatic regimes) [TINLEY, 1977]. The soils of the Cheringoma Plateau developed under the influence of eluviation and illuvation. For the soil formation at the riftward slopes erosive processes were important.

The **rift floor** is built up by fluvio-lacustrine alluvium [DNA, 1987]. Differential sorting of coarse and fine sediments occurred in the course of alluvial fan formation or shifting of river courses [TINLEY, 1977]. The coarser, leached sandy soils are associated with the alluvial fans, splays and colluvium at the rift sides as well as with river stream beds. Soils with fine clayey texture are located in interdistributary slacks and interfan slacks or basins. They are saturated with calcium, magnesium and sodium [FERNANDES, 1968]. In addition, their extractable phosphorous content is relatively high. Hydromorphic clays are mostly built up of montmorillonite which can form a gilgai microrelief due to the expansion and contraction of clays overlaying a sand layer [TINLEY, 1977]. Floodplain grasslands are bound to saline, black, hydromorphic, humic clays.

The diversity of deposits on the rift floor is responsible for the high variance of pH and salinity whereas the salinity is quite high compared to the other morphological units of the Gorongosa Ecosystem [FERNANDES, 1968].

The gneisses and migmatites of the crystalline **Báruè Midlands** were the base for the formation of mostly sandy skeletal fersiallitic soils [TINLEY, 1977]. Their excessive permeability results in rapid infiltration and is therefore responsible for the strongly seasonal nature of the rivers which originate in the Midlands.

The general nutrient deficiency of the Midland soils is ameliorated by basic and pegmatitic dykes contributing to deeply weathered latosols.

At the **Gorongosa Mountain** ferrallitic soils developed on fine grained acid granite. The intensive weathering which lead to the soil formation also gave rise to the leaching of bases.

Prior to the downthrow of the **Cheringoma Plateau** alluvial sandy fan material was cemented by calcic clay of the Mazamba formation [TINLEY, 1977]. When the calcareous material was leached laterally and downward, an impermeable clayey illuvial subsoil with lime concretions formed. The sesquioxide-rich quartz sands build up leached, infertile (deficient in extractable phosphorous) soils at the surface. From the colluvium of the Cheringoma Plateau heavy textured melanic black soils developed. Where marls are exposed they form aridosols.

## 4.5 Hydrology / Hydrogeology

Lake Urema is part of the Pungoe River catchment which has an area of 31,150.5 km<sup>2</sup> with 1,460.7 km<sup>2</sup> (4.7%) in Zimbabwe and 29,689.8 km<sup>2</sup> (95.3%) in Mozambique [SWECO&ASSOCIATES\_I, 2004].

The main water sources of Lake Urema are located in the Gorongosa Mountain, in the Bárúè Midlands, in the Cheringoma Plateau and in the rift valley. Due to the different underlying geology and landscape geomorphology, in addition to the distribution of rain, the contribution of these rivers to the waterbalance of Lake Urema differs in time and amount. According to TINLEY, (1977) the extent of the lake varied between 10 km<sup>2</sup> (dry season minimum) and 200 km<sup>2</sup> (maximum during flooding).

On the **rift floor** a shallow watershed separates the southern Urema catchment from the northern Zangoe catchment which is part of the Zambeze catchment. During high floods both catchments can be linked although BURLISON et al. (1977) considered that with the closure of the Kariba dam “on the Zambeze in 1958, flooding was reduced, and the quantity of water passing through decreased.”

The underlying hardrock fracture system and the seaward dip of the strata control the south-east trend of the rivers crossing the rift valley [TINLEY, 1977]. The low elevation gradient of the rift floor gives rise to a meandering of the streams which traverse the rift valley and retards water in swampy areas, wetlands, “shallow lakes, flow reversals, interrupted drainages and other features associated with impeded drainage.” [OWEN, 2004] Thus an estimation of the runoff coefficient is only between 20 to 30% of effective rainfall<sup>6</sup>.

The river Mucombeze originates at the rift valley floor and discharges directly into the lake. After its confluence with the Nhandugue River, it forms an extensive delta with the Mucoza and the Vunduzi<sup>7</sup> at the head of Lake Urema [Figure 2].

Urema River is the only outflow of the lake and drains into the Pungoe River. According to flow measurements in the 1950s to 1970s its flow varied between less than 5 m<sup>3</sup>/s at the peak of the dry season and up to 56 m<sup>3</sup>/s in high flood period [Figure 7] [ARAC, 2004]. Low flow periods with less than 5 m<sup>3</sup>/s lasted from July to November, peak flow period from January to May (26 to 56 m<sup>3</sup>/s).

<sup>6</sup> Effective rainfall is estimated by OWEN (2004) as monthly P-100 mm, 100 mm/month interception

<sup>7</sup> There are two Vunduzi Rivers within/close to the catchment area of Lake Urema. One of them is draining Gorongosa Mountain in eastern direction. The other one is flowing in southern direction (OWEN, 2004 refers to it as Vanduzi River). In this work emphasis is given to the eastern Vunduzi.

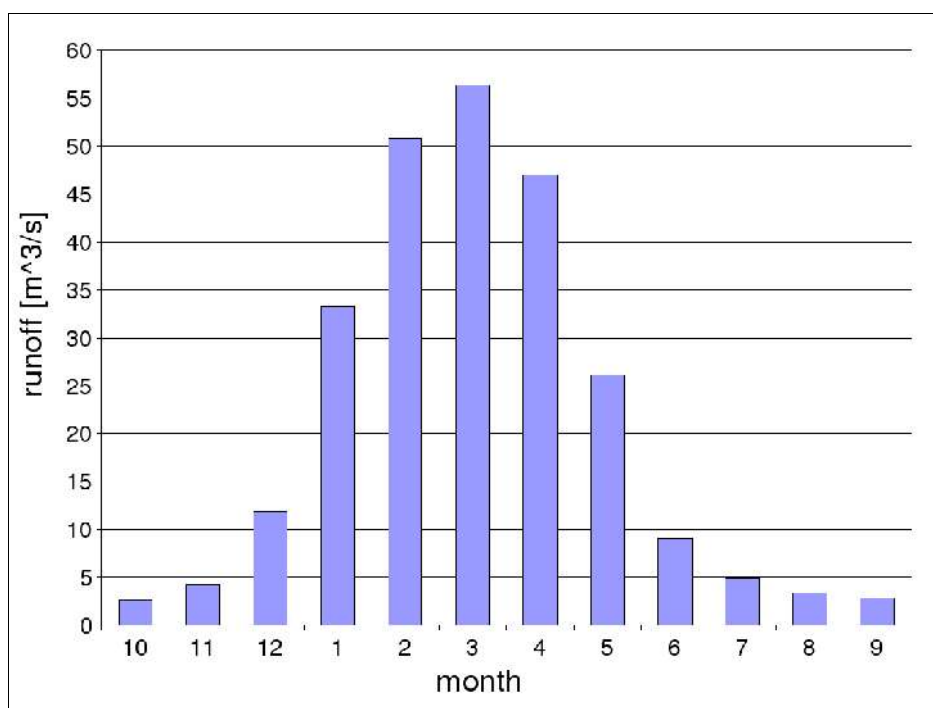


Figure 7: Flow measurements at the Urema River (station E81, elevation 12 m a.s.l., close to the southern boundary of the Gorongosa National Park, see figure 2) 10/1956-09/1978, data from ARAC, 2004

At Chitengo Camp in the rift valley the phreatic watertable laid at about 8 m below the surface [TINLEY, 1977]. TINLEY reasoned “that an impervious stratum occurs below that level.” Groundwater recharge should occur at the edges of the trough. The surface soils of the rift floor are characterized as impervious to percolation beyond 1 m depth. However, cracks in the vertisols of the floodplain and slack-basins could enable recharge during the time of flooding in the rift before the sealing off of the clays by swelling. The underlying Sena Sandstones are characterized as “not very favorable for groundwater development” [SWECO&ASSOCIATES\_IV] because of their low permeability.

The rivers raising in the **Báruè Midlands** strongly follow rainfall changes and show little system memory [OWEN, 2004]. Impermeable and shallowly weathered crystalline gneisses cause relatively high runoff coefficients (0.505 of effective rainfall). The Nhandugue River [Figure 2], which is originating in the Midlands, plays an important role for the water supply during flood periods [TINLEY, 1977]. It is partly a dry sand river with accessible water below the sand. During floods it carries large amounts of sandy sediments. Occurrence of groundwater in the Báruè Midlands is mostly associated with geologically weak zones, expressed by folds, faults and fractures or occurs in valley bottoms [OWEN, 2004].

The steep slopes of the **Gorongosa Mountain** release water all year through orographic rains. Thus it is acting as one of two major aquifers in the Gorongosa region. The runoff coefficient is with estimated 0.65 of effective rainfall high to very high [OWEN, 2004].

The Vunduzi River, which is originating at the Gorongosa Mountain, is the only *perennial* surface flow to Lake Urema [TINLEY, 1977]. Through headward erosion it capped a part of the upper catchment of the Nhandare River which has a high rainfall catchment.

The **Cheringoma Plateau** is the second major aquifer in the Gorongosa system due to the highly permeable surface of quartz rich sands [TINLEY, 1977]. Rivers originating at the Cheringoma Plateau mostly trickle away in the sandy beds and alluvial fans at the rift margins during dry season and therefore do not reach the rift floor. They are only perennial in their middle courses. The runoff coefficient should be low due to rapid infiltration (0.3 of the effective rainfall, in OWEN, 2004).

Due to the seaward dip of the underlying strata of the Cheringoma Plateau it is assumed that the subsurface drainage is feeding into the coastal plain and discharging into the ocean [OWEN, 2004].

LÄCHELT (2004) specifies 53 thermal springs in Mozambique. The thermal waters in the Sofala and Manica districts are characterized as chloride-sulphate alkaline water with sodium as the major cation and chloride as the major anion [MARTINELLI et al., 1995]. Silica content is below 100 mg/kg.

The Chicheri springs are located at the southwestern boundary of the Gorongosa National Park (approximately 19° 01' 00" S, 34°11'00 E) [LÄCHELT, 2004]. The springs are associated with the western flank of the Urema Rift and have a water temperature of 50°C. Their localization is determined by bordering zones between basement and sedimentary sequences.

#### 4.6 Ecology and Land Use

The land use and land cover database of CENACARTA (1999) shows that the different vegetation types around Lake Urema are circularly arranged [Figure 8]. The inner zone is described as “aquatic meadow” which is joined by “bare soils” southwest to northeast of the lake and in further distance to the lake by “meadow, liable to flood”. Southeast to southwest of the lake “wooded grasslands” are attached to the zone of “aquatic meadow”. The outermost zone consists of “inundable sparse meadow”.

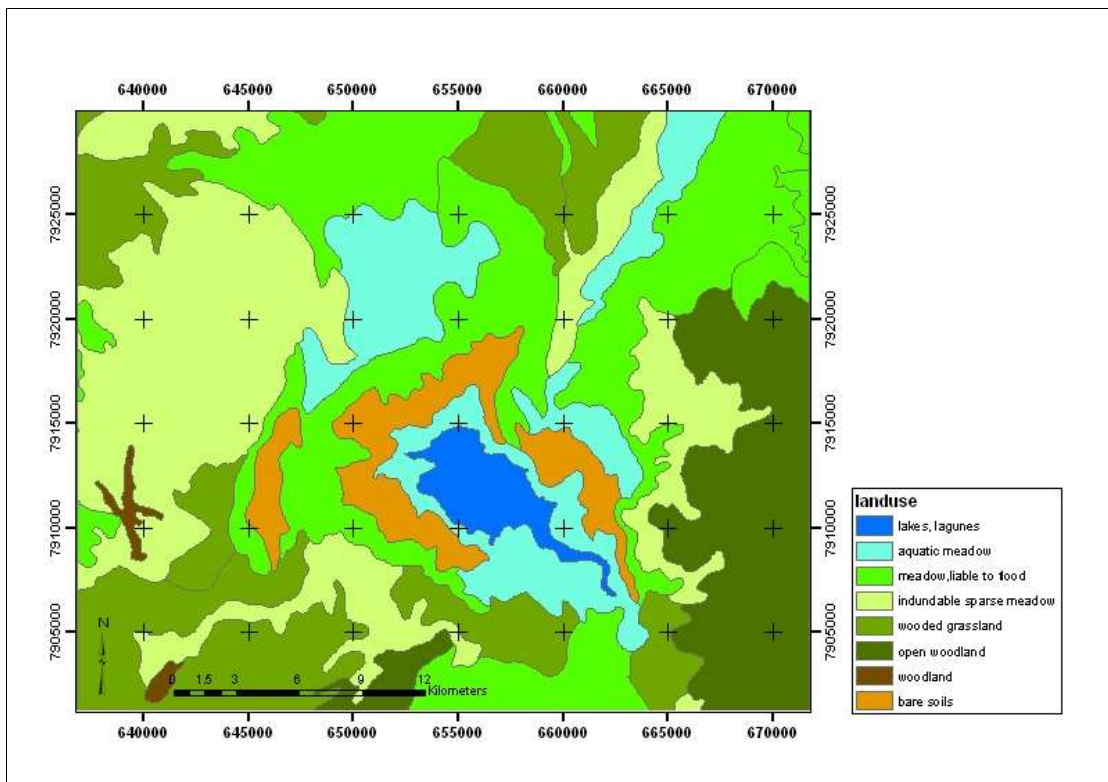


Figure 8: Land use around Lake Urema (after IGN.FI CENACARTA, 1999)

The rift floor, the driest part of the Gorongosa Ecosystem, is built up of different base saturated alluvial soils which together with changing flood levels enable the development and preservation of a mosaic of ecosystems [Table 1].

Table 1: Overview about ecosystems and vegetation types in the rift valley (after TINLEY, 1977)

ecosystem	vegetation types
<b>Forest</b>	- Dry - Riverine
<b>Thicket &amp; Shrub-Thicket</b>	- Riverine - Termitaria - Fan & Splay - Secondary
<b>Savanna</b>	- Tall Piliostigma-Acacia - Palm Savannas - Short Acacia - Mopane Woodland - Sand Savanna
<b>Rockfaces</b>	
<b>Grassland</b>	- Drainage line - Floodplain - Saline
<b>Warm Freshwater System</b>	- Lakes, pans, marshes - Rivers, streams

The requirements towards the soil moisture balance differ between forest habitats and savanna/grassland: Forests prefer well drained sites, e.g. duplex sands of fan deposits or riverine sites on free draining loamy soils. In contrast, open grasslands and savanna develop on clayey soils as well as on deep horizonless sands [TINLEY, 1977].

This study focuses on the open, high productive floodplain grasslands which require seasonal flooding and thus demarcate the total seasonally inundated area of the rift floor. The extension of the flooded area is marked by a “tree-line junction of the savannas and other woody cover.” [TINLEY, 1977]

When flood water ebbs away, a zone of changing widths follows the ebb line, leaving a green flushing zone on moist soil around Lake Urema [TINLEY, 1977]. This zone plays an important role for the support of the population of waterbuck, impala and hippo during the peak of the dry season [TINLEY, 1977].

A number of 35 000 wild ungulates on the rift floor is given for the time prior to the civil war (1976-1992) [TINLEY, 1977]. 27 ungulate species inhabited the mosaic of forest, thicket, savanna and floodplain grassland. Their population numbers were radically reduced in times of civil war when the Gorongosa National Park was occupied by opposing armed forces. The numbers for hippopotamus (*Hippopotamus amphibius*) are presented in Table 2.

Table 2: Population estimates for Hippopotamus in the Gorongosa National Park from 1968 to 2004, 1 Figures from TINLEY, (1977), 2 figures from SWECO&ASSOCIATES\_X (2004), 3 figure from FALKER (2005)

year	11/1968 <sup>1</sup>	1970 <sup>2</sup>	10/1972 <sup>1</sup>	1979 <sup>2</sup>	2003 <sup>2</sup>	2004 <sup>3</sup>
population estimate	2972	3200	3483	4800	25	62

According to TINLEY (1977), 80% of the hippos in the Gorongosa Ecosystem were confined to the margins of Lake Urema – thus representing the single largest hippo population in Mozambique at that time [Figure 9].

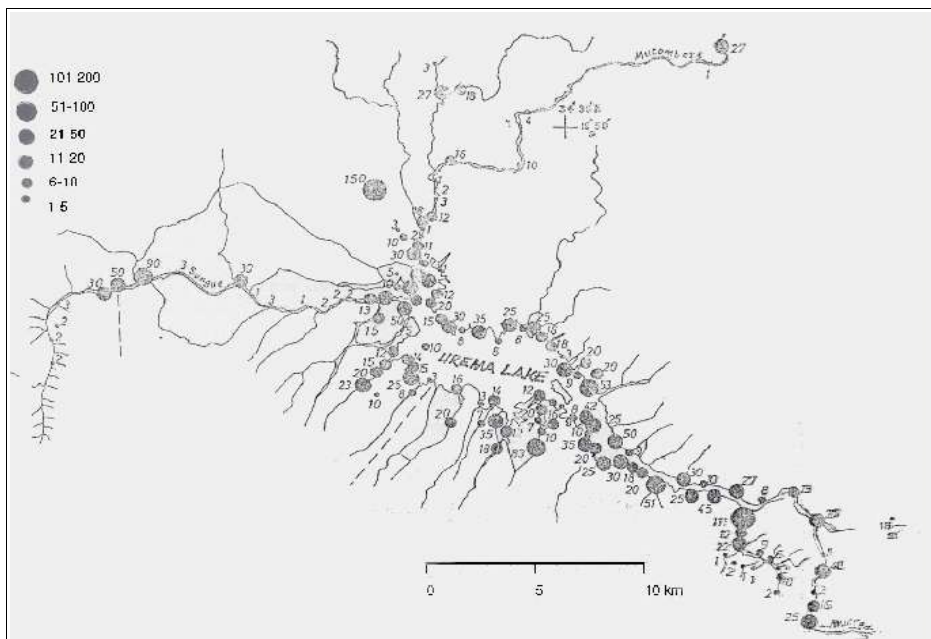


Figure 9: Dry season distribution and abundance of hippo from aircounts in November 1972 (after TINLEY (1977), figure 9.11), circles represent # of individuals

Adequate aquatic habitats for hippos are deep enough to cover their bodies and are within a certain distance from pastures. By means of their habitually wandering between the grazing grounds on land (during the night) and the open water of rivers, lakes and basins (at daytime) hippos transfer soil matter and nutrients from the land to the aquatic environment. When ground is soft during the rains and flood periods their paths become channels which aid spreading and draining of flood- and rain water [TINLEY, 1977]. Thus, hippos act as “ecosystem engineers”.

### ***4.7 Human factor***

10 000 to 15 000 people are supposed to live within the Gorongosa National Park (GNP) while “Several communities live within the boundaries of GNP, whilst others straddle the boundaries” [LYNAM et al., 2003].

Agriculture (cultivation of crops, vegetables and fruits, domestic animals), fishing, hunting, collection of wild foods, timber extraction and bee keeping are the basics for the livelihood of the people living in and around the Gorongosa National Park, although there exist regulations and prohibitions in the park area, e.g. regarding the killing of animals and cutting of timber [LYNAM et al., 2003].

During the period of investigation (August to November 2004) temporary camps of fisherman were encountered at Lake Urema. Four teams with two fishermen worked at the lake for few days. After successful catches they moved back to their village (Muaredzi). They are permitted to fish on Lake Urema, but such activities are regulated.

During the civil war (1976-1992) the flora and fauna of the park was seriously affected and the infrastructure destroyed. Since the end of the civil war big efforts were and still are undertaken to rehabilitate the Gorongosa National Park through demining, re-establishment of management activities, rebuilding of the infrastructure, anti-poaching operations and restocking of wildlife. Sustainable land use in the buffer zone of the park is enforced [web\_1, web\_4].

## 5 Methods

### *5.1 Remote Sensing and GIS*

#### **5.1.1 Data sources and software products**

Eleven satellite images from Landsat sensors MSS, TM, ETM+ and ASTER were available. Topographical information were available as SRTM data (90 m resolution).

Image analyses were conducted using PCI Geomatica, V9.1.x. ESRI ArcGIS, V8.6 was used for data storage, administration and presentation. Parameters for datum shift were used from TNTmips V6.8. Graphics were created in GMT 3.4.4, Gimp 2.2, Gnuplot 4.0 and OpenOffice.org 1.1.3, statistics in STATGRAPHICS Plus 5.1, hydrochemical modeling in PhreeqC V2.2.

#### **5.1.2 Analysis of remotely sensed data**

##### ***5.1.2.1 Geometric and atmospheric correction***

Topographical maps of the study area were available at the scale of 1 : 50 000 and 1 : 250 000 ([DINAGECA, 1997/98], [DINAGECA, 1960?]). The maps were digitized with a pixel size of 10 m x 10 m (1 : 50 000) and 50 m x 50 m (1 : 250 000). A datum shift to WGS 84 Datum was necessary as the maps were registered to Tete Datum.

With these maps the satellite images were geometrically corrected. The pixel size of the output image was chosen according to the spatial resolution of the input scene. The ground control points (GCPs) were distributed over the whole scene. The nearest neighbour resampling algorithm was used and residuals were less than 2 pixel.

Subsets of the satellite scenes (upper left limit: 7930110N, 636750E; lower right limit: 7901040N, 671760E) were created to reduce memory requirements and calculating capacity.

The module ATCOR2 in PCI Geomatica [RICHTER, 2005] was applied to perform radiometric correction through calculating an atmospheric correction for flat areas. Calibration files were available for Landsat 4/5 MSS, Landsat 4/5 TM and ASTER.

It was not possible to correct the scenes 09/04/1995 and 10/02/2000 for haze with this method (error warning). The scenes from 09/09/1991, 07/04/1996 and 12/30/2000 could not be corrected for influences of haze and clouds as there were gaps in the spectral coverage or not assignable bands. However, the lake area was without atmospheric disturbance through clouds.

### **5.1.2.2 Extraction of the lake's contour from NDVI**

The Normalized Difference Vegetation Index (NDVI) - where possible calculated from radiometrically corrected scenes - proved to be a suitable instrument to distinguish the open water surface from terrestrial habitats [Equation 1].

#### *Equation 1*

$$\text{NDVI} = (\text{NIR} - \text{Red}) / (\text{NIR} + \text{Red})$$

where:

NIR = reflectance in the near infrared portion of the spectrum (band 4 Landsat 5 and 7, band 3 Landsat 2, band 3 ASTER)

Red = reflectance in the red portion of the spectrum (band 3 Landsat 5 and 7, band 2 Landsat 2, band 2 ASTER)

In general, NDVI values are in the range between -1 and +1. A threshold value THR for the NDVI was chosen to extract the water body of the Lake Urema (Landsat TM areas: THR = 0, Landsat MSS = 0.03). Pixel with gray values below the THR (= water) were extracted and converted into vector shapes. Only directly connected pixel were considered as part of the water body of Lake Urema. The NDVI could not be calculated from the Landsat scenes from 1991 and 1996 due to gaps in the spectral coverage and not assignable bands.

### **5.1.2.3 Extraction of the lake's contour and of the floodplain grasslands using supervised classification**

There was a rough notion about the distribution of floodplain grassland around Lake Urema from several field trips between August and November 2004 and from an overflight over the lake in November 2004.

However, the spatial distribution of different grassland types (short grassland, tall grassland, medium high grassland) was not known.

To distinguish open water from floodplain grassland and surrounding savanna a Maximum Likelihood Classification with null classes was used. It considers the variability of Brightness values in the training areas of each class in addition to the mean values. A classification with null classes gives the user the chance to avoid that all pixel must be assigned to classes. This was especially important as it was known that much more classes would have been to be distinguished for ground coverage of the satellite images [CUNCLIFFE, 2004]. Due to the gaps in spectral coverage and not assignable bands different procedures were applied to the scenes in advance of the classification, such as Tasseled Cap Transformation, PCA and NDVI.

The Tasseled Cap Transformation produces images with three bands interpreted as Brightness, Greenness and Yellowness (Landsat 2) and Brightness, Greenness, Wetness (Landsat 5 and Landsat 7) [CAMPBELL, 2002]. The method may be sensitive to atmospheric turbidity and angle of illumination. Therefore a direct comparison of spectral values between scenes from different times is only possible for the radiometrically corrected images.

A sieve filter was applied to the output of the classification procedure. Image value polygons smaller than a certain threshold (THR) were merged with the largest neighbouring polygon. The THR for the class “open water” in Landsat TM was eight pixel (= 7200 m<sup>2</sup>, pixel size 30 m x 30 m), in Landsat MSS it was three pixel (= 9747 m<sup>2</sup>, pixel size 57 m x 57 m), in ASTER 32 pixel (= 7200 m<sup>2</sup>, pixel size 15 m x 15 m).

For “grassland” a THR of 22500 m<sup>2</sup> was chosen (equals to 25 pixel in Landsat TM, 100 pixel in ASTER, in Landsat MSS no class grassland distinguished). The intention for the use of different THR values for grassland and water was to detect large water bodies as well as little ponds while only large grassland areas should be extracted.

#### **5.1.2.4 Calculation of a DTM from ASTER data**

Although of a good relative quality, the ASTER DTM was too erroneous in the flat terrain of the rift valley floor for precise absolute height measurements.

#### **5.1.2.5 Extraction of the drainage system and the catchment area from SRTM data (Shuttle Radar Topography Mission)**

Subsets of USGS SRTM data (90 m resolution) for the area covered by Landsat path 167 and 168, row 072 and 073 were available and used to extract the catchment area of the Lake Urema and its drainage system [JENSON & DOMINGUE, 1988].

#### **5.1.2.6 Calculation of the lake's volume**

It was observed in the Landsat scene from May 1997 that the extent of Lake Urema was significantly larger at that time than in the other years. The question was how big the difference in the water volume between May 1997 and a “normal” year (e.g. October 2000) was.

The DTM generation from the ASTER scene (10/02/2000) was imprecise at the floor of the rift valley around Lake Urema. Therefore the SRTM data were used for the calculation of the difference in water volume [Figure 10].

First of all, the altitude of the lake's shoreline<sup>8</sup> in October 2000 was determined from SRTM data.

---

<sup>8</sup> shoreline = delineation between the open water surface and swampy grassland

This was done by creating an elevation profile around the lake and extracting the mean elevation of this contour line (= 21 m). In order to fill the holes in the DTM at the lake and to get a plane water surface, the DTM elevation values under a mask with the lake's extent in October 2000 (result from supervised classification) were replaced with the value of 21 m.

Contourlines (1 m interval) were generated from this modified DTM. The contourline at 24 m a.s.l. proved to fit best with the contourline of Lake Urema in May 1997.

Consequently, the difference in altitude between the shoreline in October 2000 and May 1997 was about 3 m.

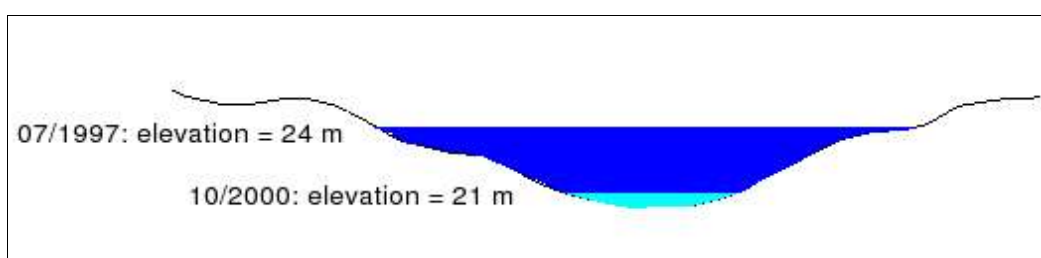


Figure 10: Differences in water volume and extent of Lake Urema between 05/1997 and 10/2000

GEOMATICA FOCUS algorithm VLM (Volume Report) calculates the volume between a DTM and a specified elevation base under a user-selected bitmap mask.

The elevation base for the volume calculation was set at 24 m (settings: pixel size 90 m, elevation step size 1 m). The bitmap mask had the extent of Lake Urema in May 1997. The volume between the mask and the terrain surface approximates the difference of water volume between 2000 and 1997. There is a certain percentage of pixel which lie above this mask but can be disregarded.

## 5.2 Field sampling & Mapping

### 5.2.1 Sampling schedule and logistics

The field work in dry season 2004 was conducted with the help of the staff of the Gorongosa National Park, to point out Fernando Januario. The field work on the lake was performed with a rubber boat of the type AVON Rover VER R3.41 or a dugout canoe [Figure 11], depending on the requirements. For the positioning a handheld GPS of the type GARMIN etrex (12 channel GPS) was used.



Figure 11: Dugout canoe for the transport on Lake Urema (photo: Beate Böhme)

### 5.2.2 Hydrology and hydrochemistry

#### 5.2.2.1 Lake level height

A lake level gauge was established at the 4<sup>th</sup> of September at the southwestern shoreline not far from Mira Hippo [Figure 12]. The wooden stick had a length of 2 m and was anchored approximately 0.3 m in the lake bottom. The lake level height was measured until the 28<sup>th</sup> of October.



Figure 12: Lake level gauge at Lake Urema (photo: Beate Böhme)

#### 5.2.2.2 Bathymetry

The depth profiles 1-4 were measured at the 16<sup>th</sup> of August. The lake was traversed with a rubber boat in SW-NE direction at a velocity of approximately 8 km/h. A sonar, type LCX-18C, was used. The data were post-processed by removing zero and faulty values as well as including the correction for the transducer depth (= 0.25 m).

In order to get an overview of the lake's extent at that time, the shoreline was tracked with the Garmin GPS. The distance of the track to the shoreline varied between 20 and 30 m. It was not possible to get closer because of shallow water, floating mats of vegetation and several times because of disturbance of a hippo.

### 5.2.2.3 Measurement of discharge

The current meter, type Teledyne Gurley 622 [Figure 13], was made available by ARA-Centro, Beira (Administração Regional de Aguas do Centro). The cross-section of the Vunduzi River river was subdivided into segments with a certain depth and width. Within these segments the number of rotations of the current meter was counted acoustically in a definite period of time (15 to 40 s). The velocity was then calculated with the rating curve equation [Equation 2]<sup>9</sup>.

*Equation 2 (for cable measurements):*

$$R < 0,025 \quad \rightarrow v = 0.0$$

$$R < 5 \quad \rightarrow v = 0.00828 \text{ m/s} + 0.67463 \text{ m} \cdot R$$

where  $R$  = number of rotations per second [1/s]

$$v = \text{flow velocity [m/s]}$$

For each segment the cross-sectional area  $A$  [m<sup>2</sup>] was multiplied by the velocity  $v$  [m/s] of the water [Equation 3] to get the discharge. Finally, the discharges of all segments were added up.

*Equation 3: Calculation of discharge*

$$D = A \cdot v$$

where  $D$  = discharge [m<sup>3</sup>/s]

$$A = \text{area of flow profile [m}^2\text{]}$$

$$v = \text{flow velocity [m/s]}$$

The water velocity was additionally estimated with a floating piece of wood.



Figure 13: Current meter  
(photo: Beate Böhme)

<sup>9</sup> measurement device non-calibrated

#### **5.2.2.4 On-site measurement of water chemistry**

The sampling scheme for the water analyses was more and more refined during the period of investigation. A first **screening** of the parameters

- water temperature
- pH
- electrical conductivity EC
- Secchi-disc transparency

was conducted at the 12<sup>th</sup>, 14<sup>th</sup> and 15<sup>th</sup> of August when the lake was surrounded by boat. Redox potential  $E_h$  was not measured as it requires some more time for stabilization which was not feasible during the trip over the lake.

The water analyses between the 6<sup>th</sup> and the 10<sup>th</sup> of September focused on the water chemistry **along the four depth profiles**.

The following parameters were measured:

- water temperature
- pH
- electrical conductivity EC
- redox potential  $E_h$
- concentration of dissolved oxygen
- Secchi-disc transparency

At those sites which seemed to be **representative for certain compartments** of the lake (**littoral, pelagial, inflow region, outflow region, bays...**), measurements of ammonium, nitrate, phosphate and sulphate were conducted at the 15<sup>th</sup> and 16<sup>th</sup> of September in addition to the determination of the above listed parameters.

Between the 6<sup>th</sup> and 11<sup>th</sup> of October the **water samples for laboratory analyses** were taken at the lake, one of its tributaries, Vunduzi River, and its outflow, Urema River. Nutrient concentrations, pH, temperature, EC,  $E_h$ , water transparency and concentration of dissolved oxygen were measured on site.

At the end of the period of investigation, at the 28<sup>th</sup> of October, all field-parameters were **repeatedly** measured at two sample sites to check whether the lake underwent significant changes since the last measurements.

The measurement of water temperature, pH, EC and concentration of dissolved oxygen in the **tropholytic zone** was conducted with a one liter water bottle, which was weighted by a heavy stone. After 10 to 15 minutes the bottle was lifted and the measurements conducted. Redox potential was not measured with this method.

The **water transparency** was measured with a Secchi-disc [Figure 14]. This white plate was lowered into the water until its contours disappeared. It was lowered some more and then raised while the depth at which it reappeared was observed. The average of both depths was calculated. The Secchi-disc transparency was measured at different locations and at different times of the day so that the light conditions varied. This error source was unavoidable during the field work.

During all samplings air-temperature, wind conditions and currents as well as the cloud coverage were noted. The water depth was measured with a bamboo stick.



Figure 14: Measurement of water clarity with Secchi-disc (photo: Beate Böhme)

During the period of investigation ARA-Centro (Administração Regional de Aguas do Centro), Beira, measured precipitation at Chitengo, located at about 18 km distance from the lake on the floor of the rift valley (7900934.6N, 642380.0E, 34.4 m a.s.l.).

### 5.2.3 Sediment cores

A polyacrylate-core with a length of 0.5 m and a diameter of 0.06 m was used for sediment sampling [Figure 15]. The equipment was only applicable at a water depth of less than one meter and sampling therefore limited to the shallower areas of the lake.

The core was manually pressed into the sediment as deep as possible. One cap closed the top of the core already under water. When the core was lifted to the water surface, the lower end of the core was closed with the second cap.

A PVC hose was used to remove the water column above the sediment. Afterwards the sediments were pushed out of the core with the help of a stopper, analyzed with respect to sediment texture (finger probe), color (Munsell color chart), characteristics like hydromorphic signs, roots and colonization and finally packed in pre-labelled PVC bags. For later laboratory analyses in Freiberg, Germany, the sediments were air-dried for at least one week.



Figure 15: Sediment core (photo: Beate Böhme)

## 5.2.4 Vegetation transects and mapping of reference biotopes

Vegetation transects at the transition from the littoral zone to temporally inundated areas were investigated along accessible paths of hippopotamus, elephant and one path of fishermen [Figure 16].

The length of the transects varied between 20 and 300 m. The distances were estimated with the step length. In deeper water, the investigation was conducted from the boat otherwise by wading.

The coverage of the plant species was estimated at a scale of five intervals according to the method of Braun-Blanquet [Table 3]. The length of adjacent plots comprised 1.5 to 2 m, the width 1 m.

Water depth, vegetation height and additional significant characteristics were noted for each plot of the transect.



Figure 16: Vegetation transect V01, supposed path of hippo (photo: Beate Böhme)

Table 3: Modified coverage scale after Braun-Blanquet

scale	percentage of coverage
1	<5%
2	5-25%
3	25-50%
4	50-75%
5	75-100%

The **reference sites** represent some of the habitat types located in the floodplain grasslands southwest of the lake. They were included into the supervised classification of the satellite images. The sites were mapped with a GPS, documented with photos and verbally described (dominant species, estimation of ground coverage, height of vegetation layers).

## 5.3 Laboratory analyses

### 5.3.1 Water chemistry: major ions, TIC, DOC

The filtered (pore size 200 nm, cellulose acetat membrane) water samples for the measurement via Ion Chromatography (IC) were stored in polyethylene (PE) bottles in the refrigerator until being analyzed.

The unfiltered samples for the determination of the carbon species were stored in glass bottles in the refrigerator.

The major ions  $\text{Li}^+$ ,  $\text{Na}^+$ ,  $\text{K}^+$ ,  $\text{Ca}^{2+}$ ,  $\text{Mg}^{2+}$ ,  $\text{Cl}^-$ ,  $\text{SO}_4^{2-}$ ,  $\text{NO}_3^-$ ,  $\text{Br}^-$  were analyzed via Ion Chromatograph, measurement device MERCK-HITACHI D 6000 (cation column: MERCK LiChrosil IC CA-2, RT 125-4.6; anion column: MERCK Polyspher IC AN-1, RT 100-4.6; detectors: anions: conductivity detector, UV-VIS detector (254 nm), cations: conductivity detector; eluent cations: 750 mg/l tartaric acid, 167 mg/l Pyridine-2,6-dicarboxylic acid, eluent anions: 415 mg/l phthalic acid, 278 mg/l Tris-(hydroxymethyl-aminomethane)).

The concentrations of  $\text{PO}_4^{3-}$  and  $\text{NH}_4^+$  were photometrically determined (measurement device Hach DR/ 2000) in addition to the field measurements. The determination of  $\text{NH}_4^+$  is based on the Nessler-Method (HACH mineral stabilizer (Cat. 23766-26), HACH Polyvinyl alcohol (Cat. 23765-26), HACH Nessler reagent (Cat. 21194-49)). The determination of  $\text{PO}_4^{3-}$  based on the Ascorbic Acid Method (HACH Foil Pillows Ammonia Salicylate Reagent (Cat. 26532-99), Ammonia Cyanurate (Cat. 26531-99)).

With the exception of  $\text{NH}_4^+$ , the above mentioned ions were determined both in the pure sample and in the enriched sample (enrichment factor 10 for IC; factor 5 for  $\text{PO}_4^{3-}$  except sample 402: without enrichment, sample 318 factor 2.4).

An ion-sensitive electrode and measurement device (WTW Microprocessor pH/ION Meter pMX 3000) was used for the determination of fluoride in the unfiltered pure water samples. 10 ml of TISAB (Total Ionic Strength Adjustment Buffer) were added to 25 ml of calibration solution/water sample. The measurement time was between 10 and 20 minutes until the result was stable. A calibration line was drawn over the range of 0.05 mg F/l to 10 mg F/l.

For the measurement of TIC (Total inorganic carbon) and DOC (Dissolved organic carbon) two replicates of each sample were analyzed. Each measurement was conducted twice with the measurement device liquiTOC (elementar Analysensysteme GmbH, detection limit for DOC 0.1 mg/l). The average of both results was calculated.

The error of analysis, the percentage of oxygen saturation (from oxygen concentrations) and the concentrations of  $\text{HCO}_3^-$  (from TIC) were modeled in PhreeqC, V2.2.

## **5.3.2 Sediment analyses**

### ***5.3.2.1 Grainsize distribution, determination of TC and TIC***

The grainsize distribution of the sediment samples was determined according to the guidelines in DIN ISO 11277 (2002). 20 to 25 g sediment sample were used. Pre-treatment with H<sub>2</sub>O<sub>2</sub> removed organic matter. 25 ml 0.4N Na<sub>4</sub>P<sub>2</sub>O<sub>7</sub> solution were added to disperse the samples. Grains with diameters smaller than 63 µm (silt and clay fraction) were fractionated by sedimentation. Grains of the sand fraction and bigger (63-2000 µm) were separated by dry sieving.

The concentrations of Total Carbon TC and Total Inorganic Carbon TIC were determined with C-Mat 5500 (Ströhlein). The difference between the concentration of TC and TIC equals to the concentration of Total Organic Carbon TOC. Detection limit for TIC was estimated with 0.05 mass% (subject to measuring conditions, composition of sample,...) [HAHNEWALD, 2005].

### ***5.3.2.2 X-ray diffraction (XRD)***

The fraction up to 63 µm (clay and silt) and the fraction between 63 to 2000 µm were separately handled for the X-ray diffraction (XRD). These subsamples were recovered in the course of the determination of the grainsize distribution. The air dried subsamples were finely ground in a McCrone Mill to a size between 6 to 20 µm and/or manually in an agate mortar to a size of 30 µm. The homogenized samples were analyzed via XRD (type of device: Philips PW 3020, cobalt tube, graphite secondary monochromator).

## 6 Results

### 6.1 Tectonics

Figure 17 gives an overview of the recent seismic activity in the Urema Rift. Earth tremors along the fracture lines in the rift occur repeatedly. Four earthquakes were detected close to Lake Urema in the 1980s: In March 1981 in the area of the Nhandugue River in the rift valley and south of the Muanza River (focus in 33 km depth), in April 1983 west of the Urema River and in May 1986 in the Dingue Dingue area (focus in 10 km depth). The magnitude of the earthquakes was 4.4 to 4.7 (for 1983 no information about magnitude available).

The Centroid Moment Tensor (CMT) focal mechanisms indicate a E-W expansion of the rift and attest its tectonic activity<sup>10</sup>

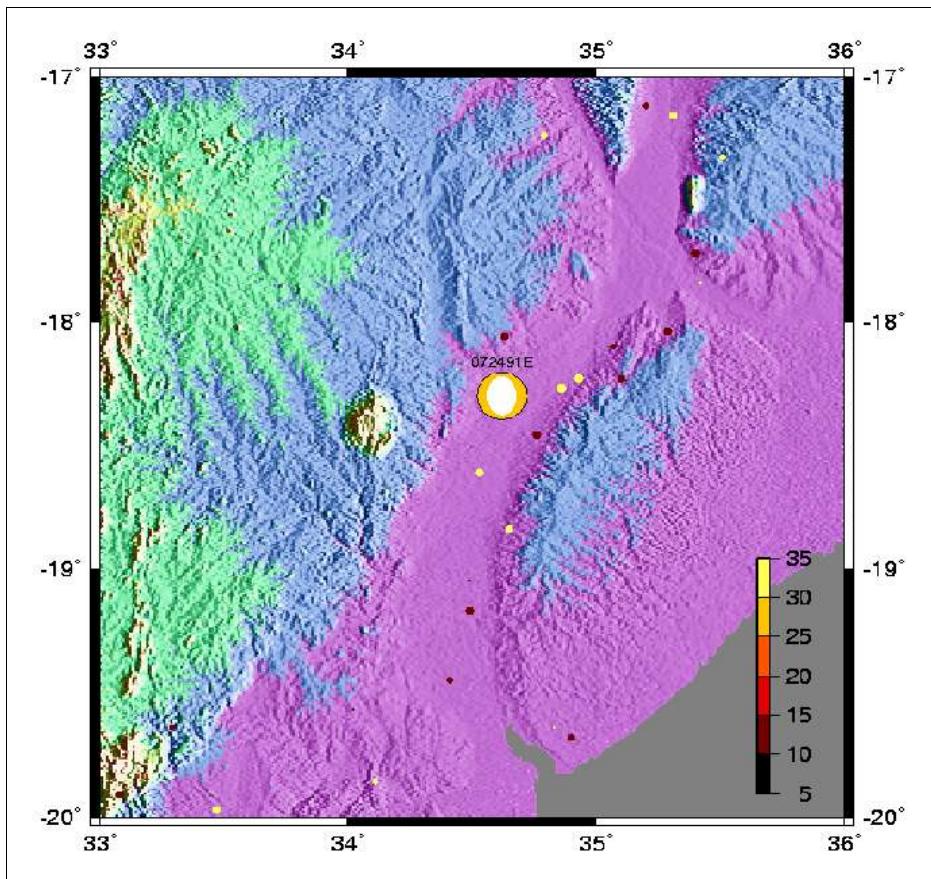


Figure 17: Seismic activity in the Urema Rift between 1973 and 2004, data acquired from Harvard Seismology CMT catalog [web\_11], the size of the bubbles represents the magnitude of the earthquake, the color represents its depth in km, underlying relief from GTOPO30 [web\_12], map processed in GMT

<sup>10</sup> details of CMT: Date: 1991/7/24, Centroid Time: 13:54:52.4 GMT, Lat= -18.30, Lon= 34.62, Depth= 24.7, Half duration= 2.3, Centroid time minus hypocenter time: 0.8, Moment Tensor: Expo=23, -5.632, 0.911, 4.721, 0.000, 0.000, -0.069, Mw = 5.1, mb = 5.1, Ms = 4.7, Scalar Moment = 5.18e+23, Fault plane: strike=180, dip=45, slip=-90, Fault plane: strike=0, dip=45, slip=-90

## 6.2 Morphology

### 6.2.1 The rift valley

Lake Urema is located at the floor of the Urema Rift flanked by the Cheringoma Plateau to the east and the Bárúè Midlands to the west. The overview in Figure 18 (lower left) shows the Urema Rift from the Zambeze-Chire junction to the sea. Initially, it shows a NNE-SSW trend which turns into a N-S trend near the Pungoe River and into a NW-SE trend where it joins Mozambique channel.

The deepest parts of the Urema Rift between the Pungoe-Zambeze-Watershed and the Pungoe delta are situated at the foot of the Cheringoma Plateau at the Lake Urema, Urema River and its outlet into Pungoe River (less than 28 m a.s.l.) (figure in the upper right). In the following, this area is referred to as Urema Basin. The longitudinal profiles (1v and 3v in Figure 18) through the rift show elevations of about 100 m a.s.l. at its margins. The central part decreases from about 60 m at the Pungoe-Zambeze-Watershed to less than 30 m a.s.l. in the area of the Lake Urema (profile 2v). Following the southward trend of profile 2v towards the Pungoe River, the terrain rises up to little less than 50 m. The width of the rift valley floor is about 40 km in the adjacency of the Urema Basin.

Profiles 2h, 3h and 4h indicate a steeper slope from the rift valley floor to the Cheringoma Plateau ( $0.42^\circ$ ) than to the Bárúè Midlands ( $0.37^\circ$ ) (numbers from cross-section 2h, Figure 18). TINLEY (1977) justifies this trend with geologically recent fault lines at the Cheringoma side. The outstanding elevation in Profile 4h at 15 000 m is the Buè Maria Ridge.

In the detailed subset in Figure 18 (upper right) the alluvial fans of the Pungoe River, the Nhandugue River and the Nhampasa River are clearly visible. Beside of them also the Vunduzi River, Mucoza River, Mepuaze und Sungue River built up fans from the west and Muanza, Nhaciquideze, Condue, Nhandinde and Mazamba River from Cheringoma side. Alluvial fans from the Nhampasa River, originating at the Midlands, and the Mazamba River, originating at the Cheringoma Plateau are responsible for the watershed between the Pungoe and the Zambeze catchment.

Generally, fans are characteristic accumulation forms of streams where they lose much gradient while flowing from the mountains on to a plain and therefore deposit parts of their load [AHNERT, 1998]. The alluvial fan of the Nhandugue River reaches up to 20 km east-southeast-wards from the margins of the rift valley floor. The fan of the Nhampasa River is even larger reaching to the middle of the rift floor. From the opposite site, from the Cheringoma Plateau, the fan of the Mazamba River elongates up to 14 km. The majority of the alluvial fans built up by the rivers from the Cheringoma Plateau are smaller than those from the Midlands and from the Gorongosa Mountain.

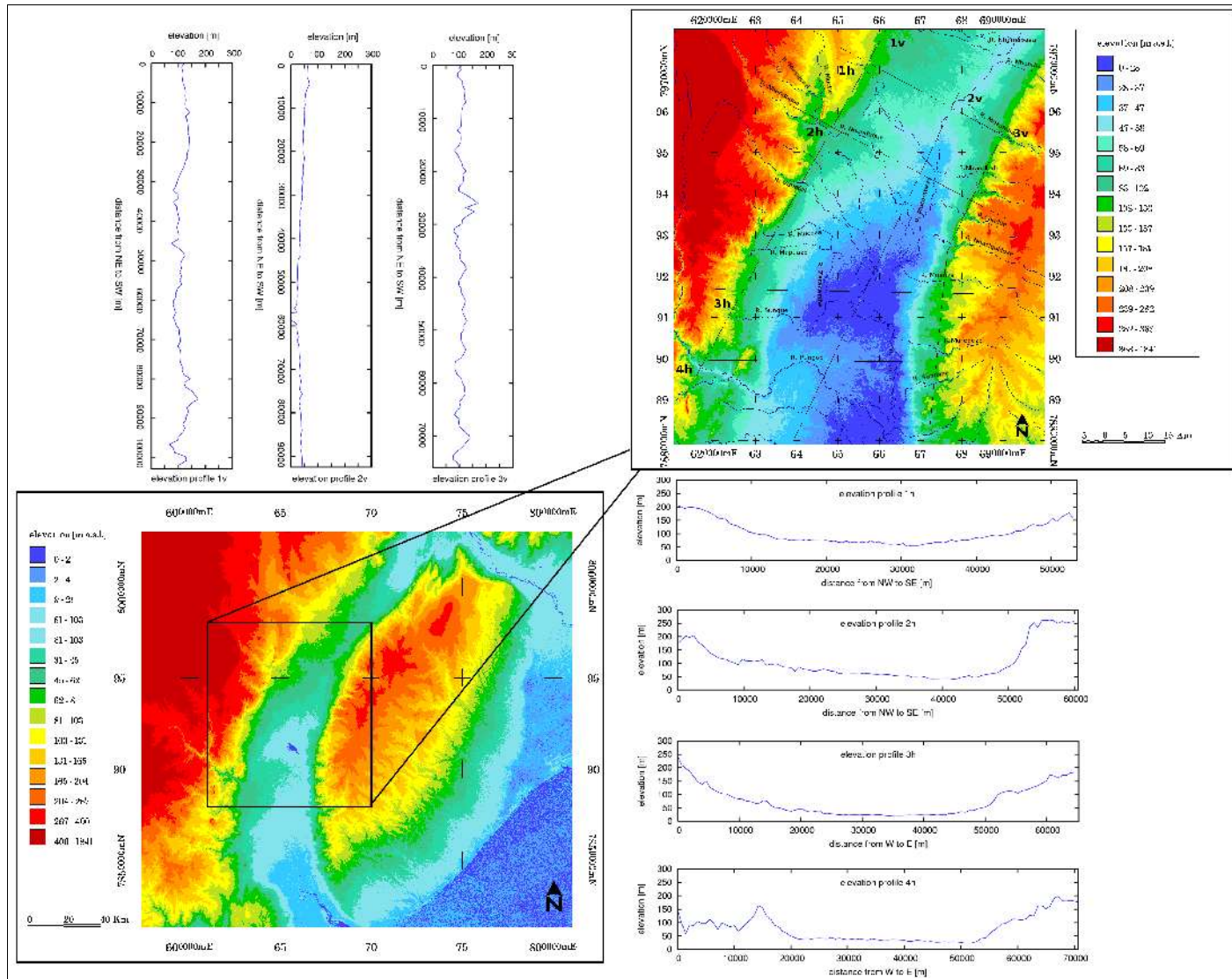


Figure 18: Overview of Urema Rift from SRTM data, rivers from IGN.FI CENACARTA (1999) and digitized from DINAGECA (1997/98)

The largest fan in Figure 19 is built up by the Pungoe River whose course is totally separated from the Urema Basin. The alluvial fan extends approximately 47 km from the western rift margin and fills nearly the whole width of the valley.

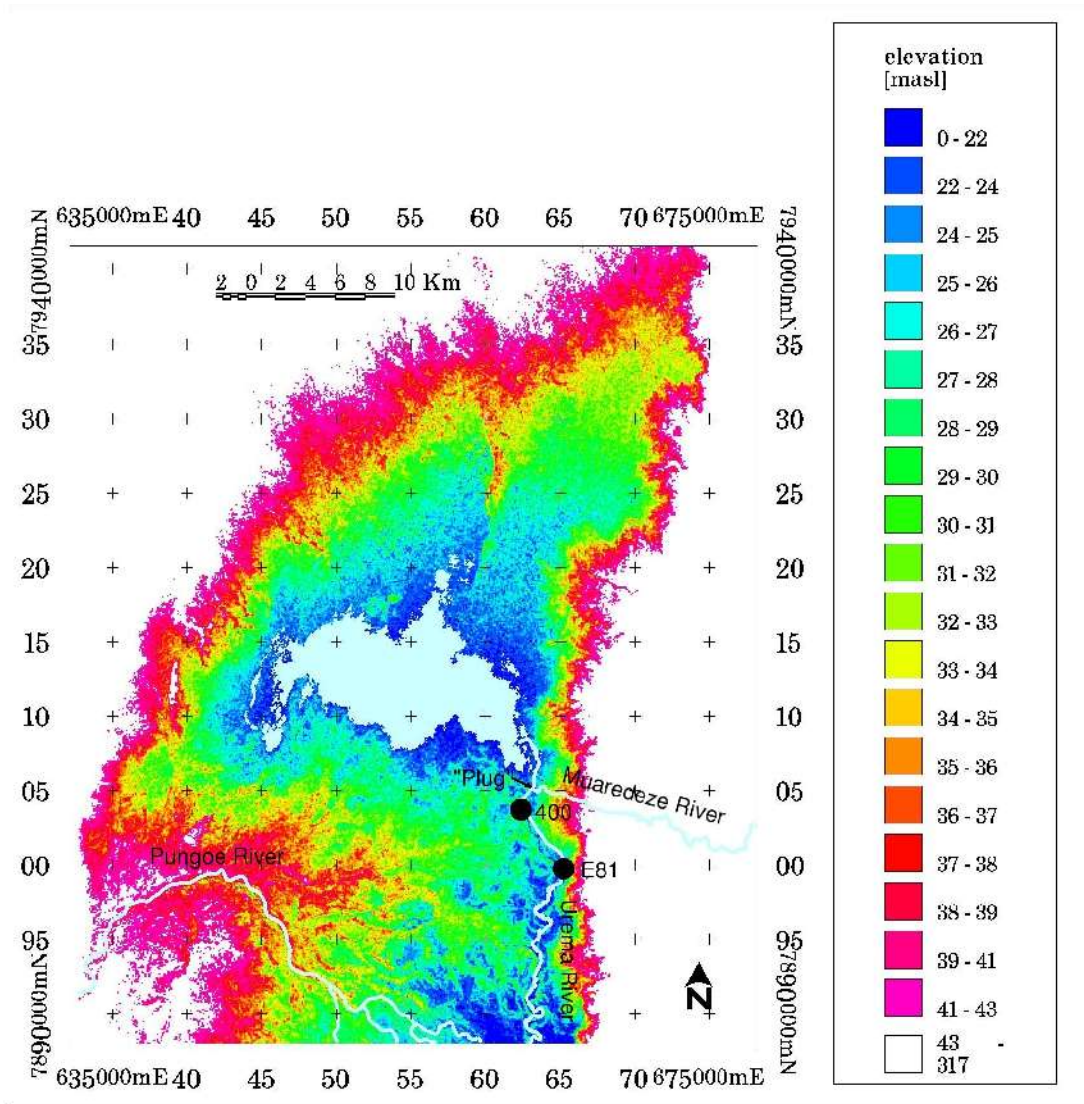


Figure 19: Detail of the Urema Basin, with lake's extent of 05/1997, from SRTM data, rivers from DINAGECA 1997/98

Conclusions about the effectivity of erosion, sedimentation and denudation can be drawn from longitudinal stream profiles. Stream profiles of rivers have to be differentiated from valley profiles because they also consider meandering of rivers within their valleys. Subsequently, the stream profiles for the Pungoe, Muredeze, Nhandugue and Nhampasa River are shown as they were created from topographical maps (DINAGECA, 1997/98), satellite imagery and SRTM topographical information [Figure 20, Figure 21, Figure 22, Figure 23].

The Nhandugue River and the Nhampasa River [Figure 21, Figure 22] show a concave stream profile in the upper reaches of their courses. The profile of the Nhandugue River then turns into a slightly convex form while that of the Nhampasa River is nearly linear. The Pungoe River is characterized by a convex profile on its course through Mozambique.

The Pungoe River [Figure 20] and the Nhandugue River show a clear break in slope where they enter the floor of the rift valley (from about  $0.27^\circ$  to  $0.06^\circ$ ,  $0.3^\circ$  to  $0.07^\circ$ ).

Among these four rivers the Muredeze River [Figure 23] has the steepest slope on the rift floor ( $0.17$  to  $0.28^\circ$ ).

After the classification scheme of slope types in AHNERT (1998) the four profiles can be assigned as follows:

- Pungoe: XvR
- Nhandugue: VXvR
- Nhampasa: VR
- Muredeze: XR

while X = convex, V = concave, R = rectilinear, v = concave slope break

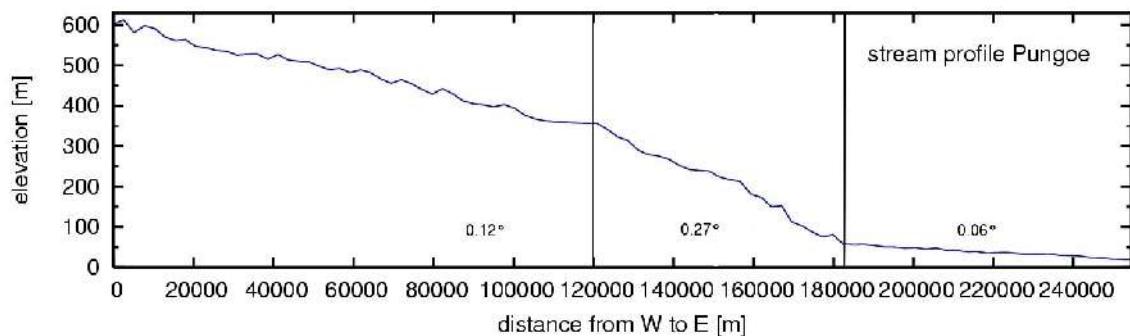


Figure 20: Stream profile of the Pungoe River within Mozambique

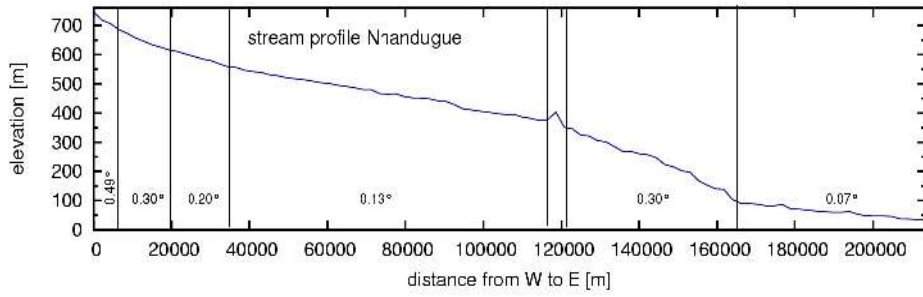


Figure 21: Stream profile of the Nhandugue River

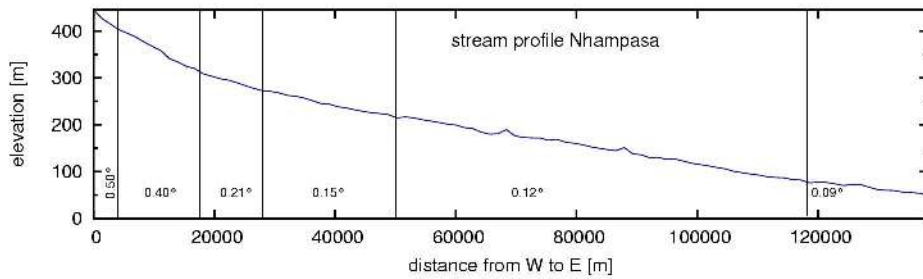


Figure 22: Stream profile of the Nhampasa River

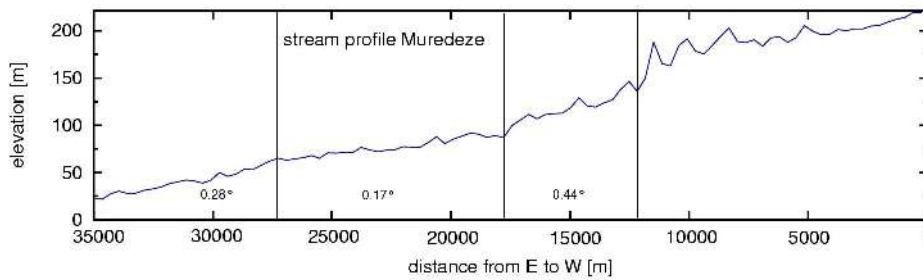


Figure 23: Stream profile of the Muredeze River

As indicated in Figure 24 the alluvial fan of the Muredeze River together with Pungoe sediments forms a “bottleneck” at the outflow of Lake Urema through Urema River. TINLEY (1977) ascribes this “alluvial plug” an important role in the control of the outflow and water storage of lake water. Figure 24 shows the depth of this bottleneck with approximately 5 m over a width of 500 m. To the west the terrain is undulating while the terrain to the east rises slightly up by 0.4°.

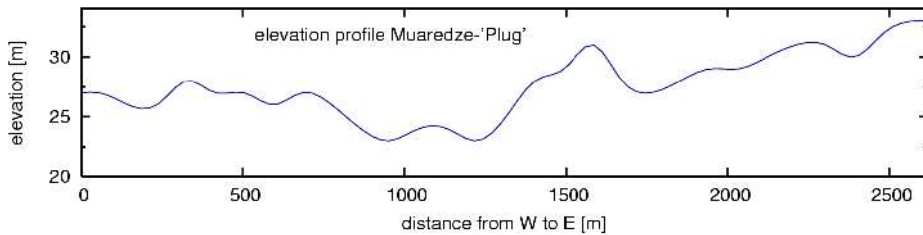


Figure 24: Elevation Profile through the so-called “Muredeze-plug”, location of cross-section shown in Figure 19

## 6.2.2 Definition of the catchment area

The modeling of the catchment area of the Lake Urema from SRTM data gave a result of 8755 km<sup>2</sup> [Figure 25, Table 4]. The extraction of the catchment divides at the floor of the rift valley retrieves a certain amount of risk due to small differences in altitude and a vertical resolution of the SRTM data of just 1 m.

According to IGN.FI CENACARTA data (1999), the Nhandugue River is the longest tributary within the catchment of the Lake Urema. Together with the Mucombeze River and some other smaller tributaries its catchment comprises about 68% of the whole lake's catchment area.

The subcatchment of the Sungue River and the Muredeze River comprises 18 percent of the total catchment area of Lake Urema. The rest of 14 percent is made up by the Vunduzi subcatchment.

*Table 4: Area of subcatchments and sum of length of all rivers in these subcatchments after modeling from SRTM data and from IGN.FI CENACARTA (1999)*

<b>subcatchment</b>	<b>area after SRTM [km<sup>2</sup>]</b>	<b>length of all rivers after SRTM [km]</b>	<b>length of main tributary after IGN.FI CENACARTA (1999) [km]</b>
<b>Vunduzi</b>	1224	229	Vunduzi: 90.6
<b>Nhandugue - Mucombeze</b>	5935	858	Nhandugue: 214.1 Mucombeze: 90.6
<b>Sungue-Muredeze</b>	1596	187	Sungue: 36.9
<b>total catchment of the Lake Urema</b>	<b>8755</b>	<b>1274</b>	
<b>total Urema catchment at hydrometric station E81; from SWECO&amp;ASSOCIATES_I (2004)</b>	<b>8060</b>		

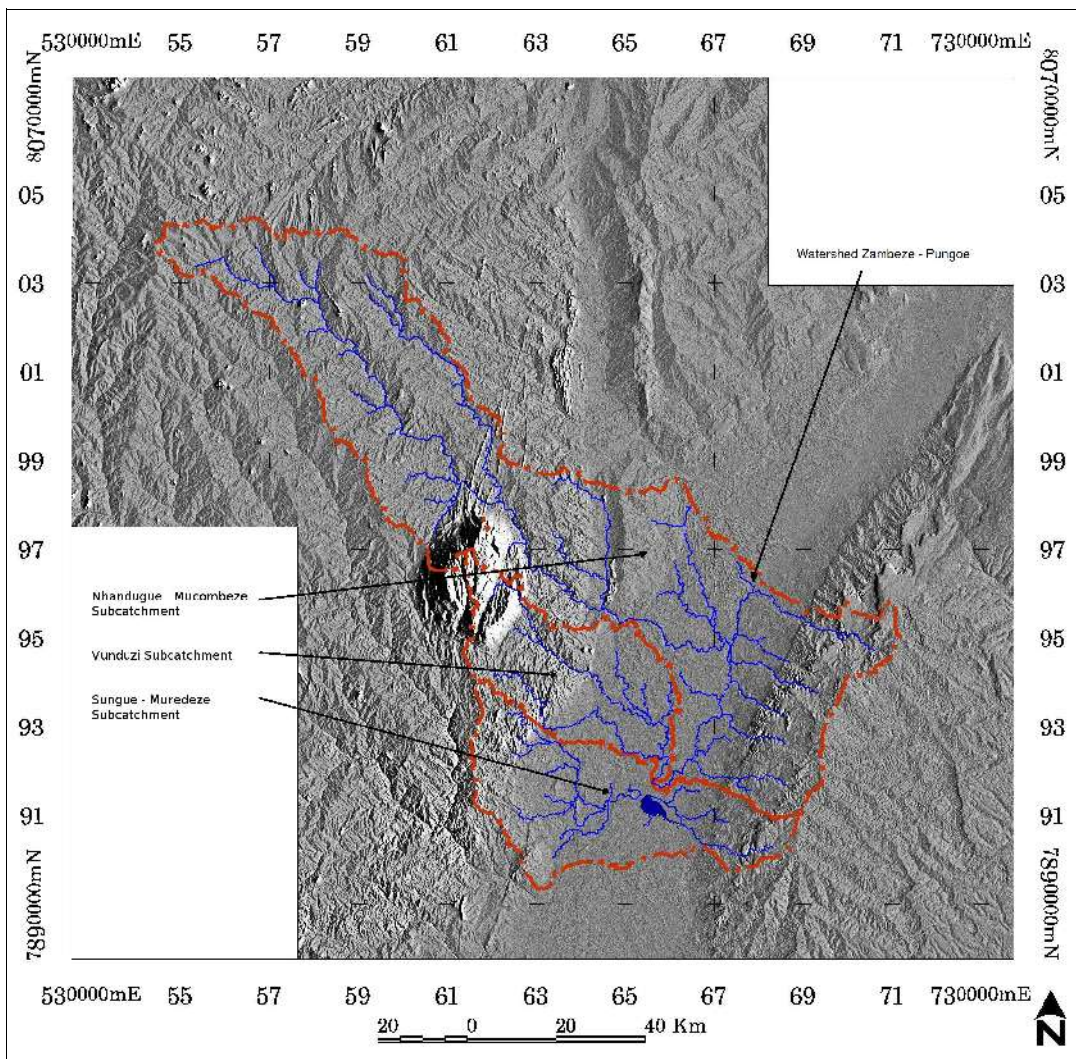


Figure 25: Catchment of the Lake Urema with subcatchments and drainage system as derived from SRTM data, sun elevation angle  $30^\circ$ , sun azimuth angle  $90^\circ$

Two outcrops are visible at the floor of the rift valley [Figure 26]. The western one is an inselberg formed by quartz breccia while the eastern one is a rounded horst block of Precambrian migmatitic gneiss with dykes of granophyre [TINLEY, 1977]. A fault line goes through the Sungue swamps. The ridge in the lower left corner is Buè Maria Ridge.

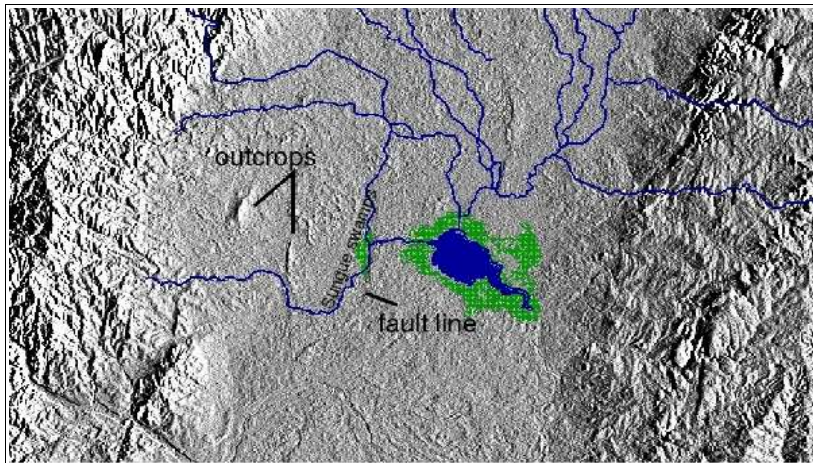


Figure 26: Morphology around Lake Urema as derived from SRTM, sun elevation angle  $30^\circ$ , sun azimuth angle  $90^\circ$

According to the results from the modeling of the drainage network the Vunduzi subcatchment owes the highest drainage density, followed by the Nhandugue – Mucombeze subcatchment and the Sungue - Muredeze subcatchment. As illustrated in Figure 25 the drainage network of Lake Urema shows a dendritic pattern. The watershed of the Cheringoma Plateau is N-S orientated with a riftward and a seaward drainage system.

### 6.2.3 Lake basin

The lake area as derived from ASTER data, acquired in October 2000, is a good approximation of the lake size during the period of investigation. This was recognizable when comparing the track of the shoreline in September 2004 with the shoreline extracted from satellite imagery.

Four depth profiles were measured from the southwestern shoreline to the northeastern shoreline of the Lake Urema [Figure 27, Figure 28].

Assuming that the profiles represent the lake bottom over a 100 m wide stripe and considering a lake size of approximately 18.5 km<sup>2</sup> (October 2000), the profiles cover 4% of the lake area during the period of investigation [Table 5]. Profile 1 and 2 are located in the northwestern and central part of the Lake Urema while the other two profiles are situated in the southeastern part where the lake is getting narrow, forming a lake arm.

Table 5: Length of the depth profiles 1 to 4, Lake Urema

profile ID	1	2	3	4
length [km]	2.8	2.7	1.1	0.72

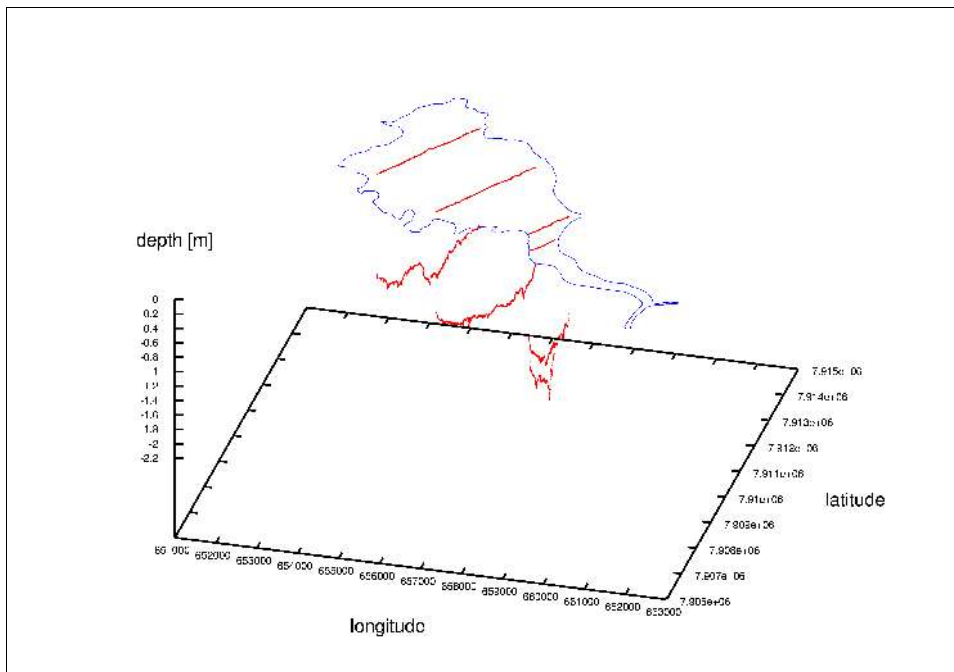


Figure 27: Location of the four depth profiles in Lake Urema, curves smoothed using a moving average (over 10 values), profiles from left to right: no 1 - 2 - 3 - 4

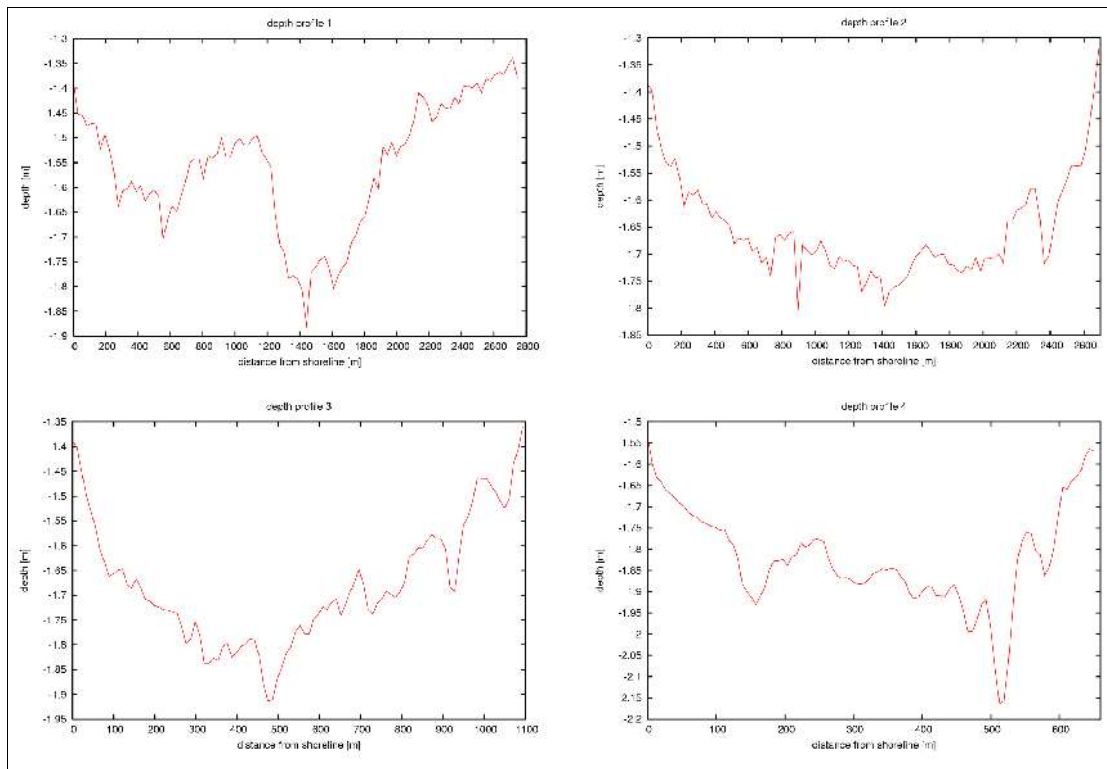


Figure 28: Depth profiles measured from the southwestern shoreline to the northeastern shoreline, curves smoothed with moving average (over 10 measurements) and csplines

The average depth of the four profiles measured 1.64 m with a standard deviation of 0.13 m [Table 6].

Table 6: Average and standard deviation of the depth profiles 1 to 4, Lake Urema

profile ID	1	2	3	4	average over 1 to 4
average depth [m]	1.59	1.66	1.69	1.82	1.64
minimum depth [m]	1.28	1.31	1.32	1.37	
maximum depth [m]	1.93	1.87	2.00	2.31	
standard deviation of depth [m]	0.12	0.09	0.13	0.13	0.13

Profile 1 is the shallowest profile [Table 6]. Profile 4 is the deepest profile. Its maximum depth is 2.31 m at about 180 m distance from the northeastern shoreline.

Generally, the variations in depth are very small. Nevertheless few remarkable structures of the lake bottom can be observed [Figure 28].

Two deepenings are conspicuous in profile 1. Over a length of about 750 m the water depth drops from about 1.5 m to 1.7 m and 1.9 m. Profile 2 is barely deeper than 1.8 m over most of its cross-section. Profiles 3 and 4 are characterized by steeper flanks than profiles 1 and 2.

The deepest part of profile 3 is approximately in its center, forming a channel of 80 m width there. Profile 4 has a more asymmetrical shaped cross-section.

Considering a lake area of 18.5 km<sup>2</sup> and an average depth of 1.64 m (mean of all four depth profiles) the water body of Lake Urema comprised 30.34\*10<sup>6</sup> m<sup>3</sup> during the period of investigation.

A modeling of the lake basin was not successful due to the lack of depth measurements between the four profiles.

### 6.3 Change detection

Figure 29 visualizes the extents of Lake Urema as they were derived from NDVI thresholds of satellite images. The lake size in May 1997 is the most striking observation. The lake's extents in 1993 and 1979 are somewhat larger than in the rest of the years which do not show much variations.

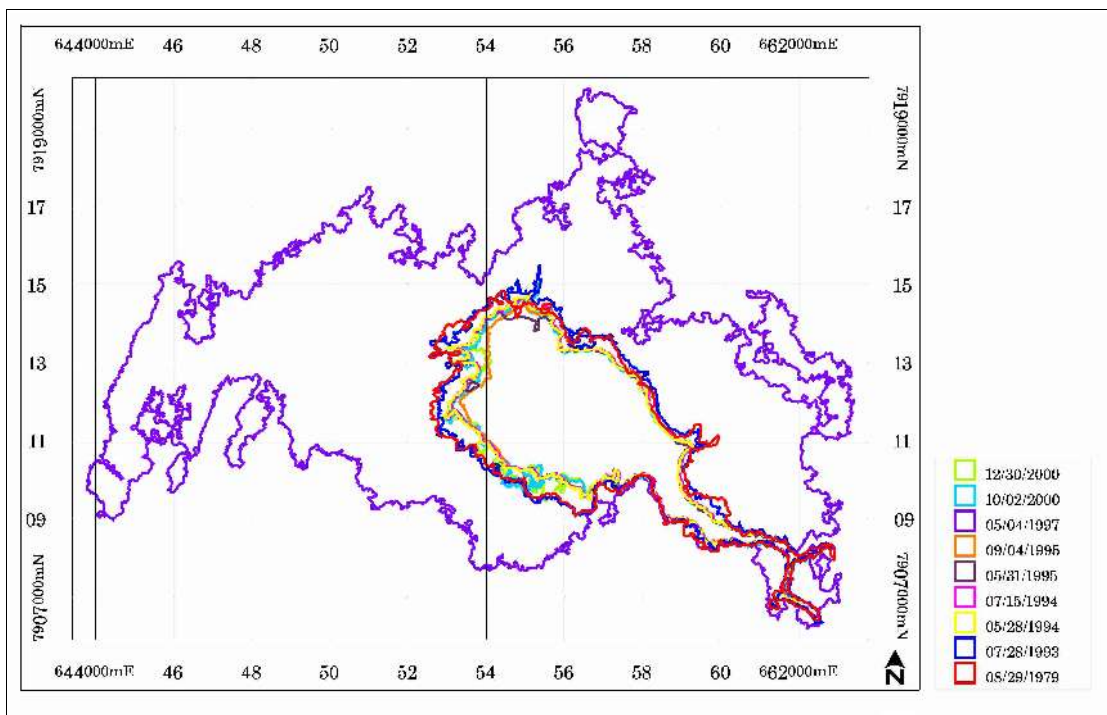


Figure 29: Open water surface of Lake Urema from NDVI, note that no NDVI was calculated for 1991 and 1996

The lake's extent as it was derived through supervised classification of the satellite scenes and from topographical maps [DINAGECA, 1960?] ranges from 7.9 km<sup>2</sup> (1960) to 104.1 km<sup>2</sup> (05/04/1997) [Table 7, Figure 30]. Excluding these two extremums the mean area comprises 20.5 km<sup>2</sup> with a standard deviation of 2.8 km<sup>2</sup>.

All differences in size smaller than about 1 km<sup>2</sup> can be disregarded for the reason of accuracy of the data source. A simple demonstration of that is as follows: A lake perimeter of 43 km corresponds to a line of 1433 pixel (pixel size 30 m x 30 m). A difference in the lake size of 1 km<sup>2</sup> corresponds to 1111 pixel (pixel size 30 m x 30 m). Thus a difference in the lake's size of 1 km<sup>2</sup> is comparable to a lake expansion or contraction by one pixel in the radius of the lake.

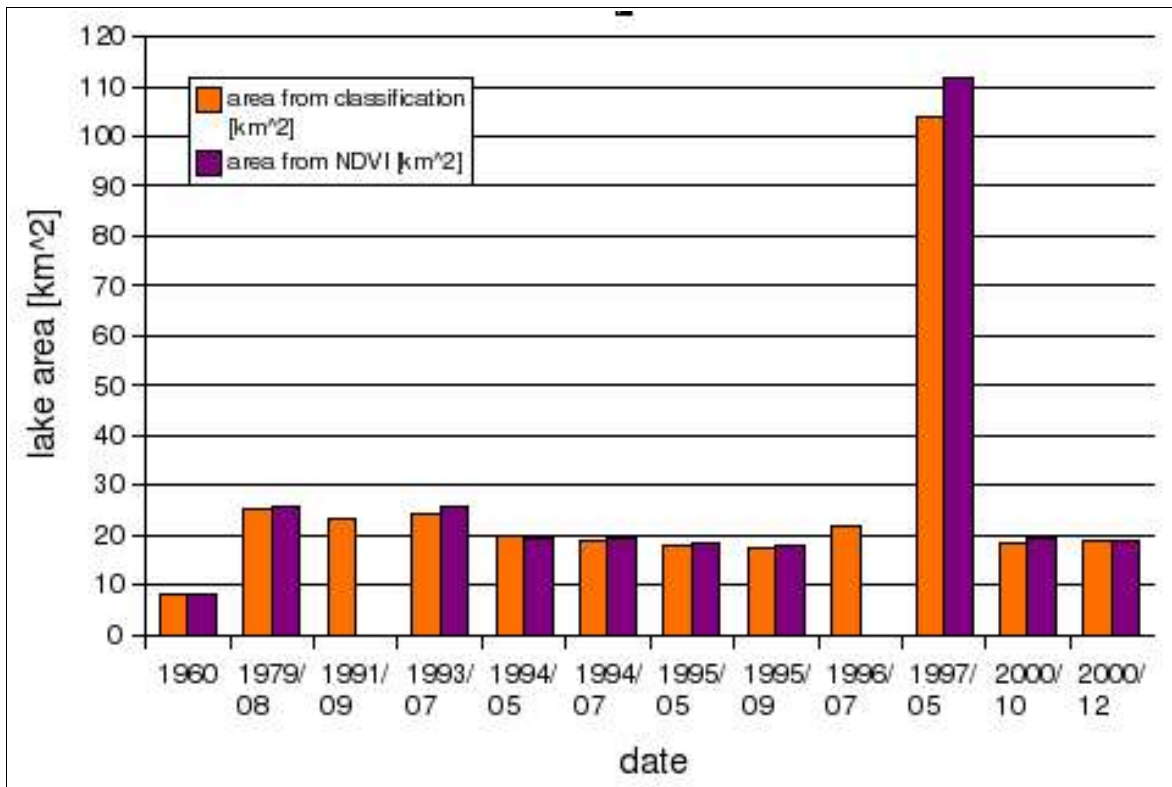


Figure 30: Comparison of the area of Lake Urema from supervised classification and NDVI, note that the area of 1960 is digitized from topographical maps (DINAGECA, 1960?)

For the majority of the images the lake area is bigger using the NDVI threshold than using the approach of a supervised classification (difference less than or equal to 1 km<sup>2</sup>) [Table 7].

Table 7: Area of Lake Urema; lake contour derived from satellite images through application of a NDVI threshold (1979 NDVI < 0.03, otherwise NDVI < 0) or of a supervised classification, figure for 1960 from topographical map [DINAGECA, 1960?], d = dry season, w = wet season, d/w = transition between dry and wet season, average and standard deviation without values for 1960 and 1997

	1960	1979/ 08/29	1991/ 09/09	1993/ 07/28	1994/ 05/28	1994/ 07/15	1995/ 05/31	1995/ 09/04	1996/ 07/04	1997/ 05/04	2000/ 10/02	2000/ 12/30
<b>A area [km<sup>2</sup>] from NDVI</b>	7.9	25.6		25.5	19.4	19.4	18.4	17.7		111.9	19.1	19.1
<b>B area [km<sup>2</sup>] from classi- fication</b>	7.9	25.1	23.0	24.3	19.6	18.9	18.0	17.4	22.0	104.1	18.5	18.6
<b>(A/B-1)*100 [%]</b>	-	2	-	5	-1	3	2	2	-	7	3	3
<b>season</b>	?	d	d	d	w/d	d	w/d	d	d	w/d	d/w	w
<b>average area from NDVI [km<sup>2</sup>]</b>				20.5		standard deviation of area from NDVI [km <sup>2</sup> ]					3.2	
<b>average area from classification [km<sup>2</sup>]</b>				20.5		standard deviation of area from classification [km <sup>2</sup> ]					2.8	

The difference between the smallest and the largest lake's extent for the years except 1960 and 1997 is 7.9 km<sup>2</sup> (NDVI) or 7.7 km<sup>2</sup> (classification).

When the lake's extent is compared within one year it is conspicuous that the seasonal difference comprises less than one square kilometer. A correlation with climate data could not be conducted due to a lack in precipitation data for the major part of the time series. Rainfall data for the study area are only available between 1956 and 1982 and since 1997.

In addition to the size of the Lake Urema, the course of the shoreline and the surrounding floodplain grasslands [Figure 32] were investigated via supervised classification. In this context the study area was limited to the Guinha and Sungue Floodplain grasslands as they are described in TINLEY (1977). Results are given in Figure 31. The Landsat MSS scene acquired in October 1979 did not allow to extract the floodplain grassland via supervised classification. This was also not possible for the scene from 1996 because of a gap in the spectral range. In 1997, the grassland area was completely flooded.

The images from 1993, 1995 and 2000 show a distinct white stripe between the classes “open water” and “grassland” which was not assigned to one of these classes in the course of the supervised classification [Figure 31]. The stripe is expanding from the first to the second image of the year. White patches are also located within the lake and are supposed to represent islands of aquatic vegetation or shallowly flooded areas.

Through the sieving process, ponds within the grassland class were only detected when they were larger than 0.72 hectares. In 1996 such open water surfaces were extensive southwest of the lake and in the Sungue plain. In the scene from 1993 open water was detected between the Sungue plain and the lake, and in the scenes from 1979, 1991 and October 2000 south of the lake. Not all of these open water areas were detected in the course of the classification procedure. They were later recovered through the comparison of the original images with the output of the classification. In Figure 31 such ponds appear as white patches within the floodplain grasslands: in July 1993 south of the narrowing part of the lake (where there is a pond in 1991), in October 2000 around the whole lake and in December south of the lake.



*Figure 32: Floodplain grassland at the northeastern part of the Lake Urema from airplane, height above ground 150-200 m (photo: Beate Böhme)*

What seems to be an uniform green area around the lake after supervised classification can actually be quite heterogeneous according to species composition, soil characteristics, exposure to flooding and so on. The results of the Tasseled Cap Transformation were subject of a more detailed analysis to discover differences within the floodplain grassland.

Four profiles were laid through the BGY/BGW (Brightness/Greenness/Yellowness; Brightness/Greenness/Wetness) images. They cover different parts of the floodplain grasslands adjacent to the Lake Urema [Figure 33].

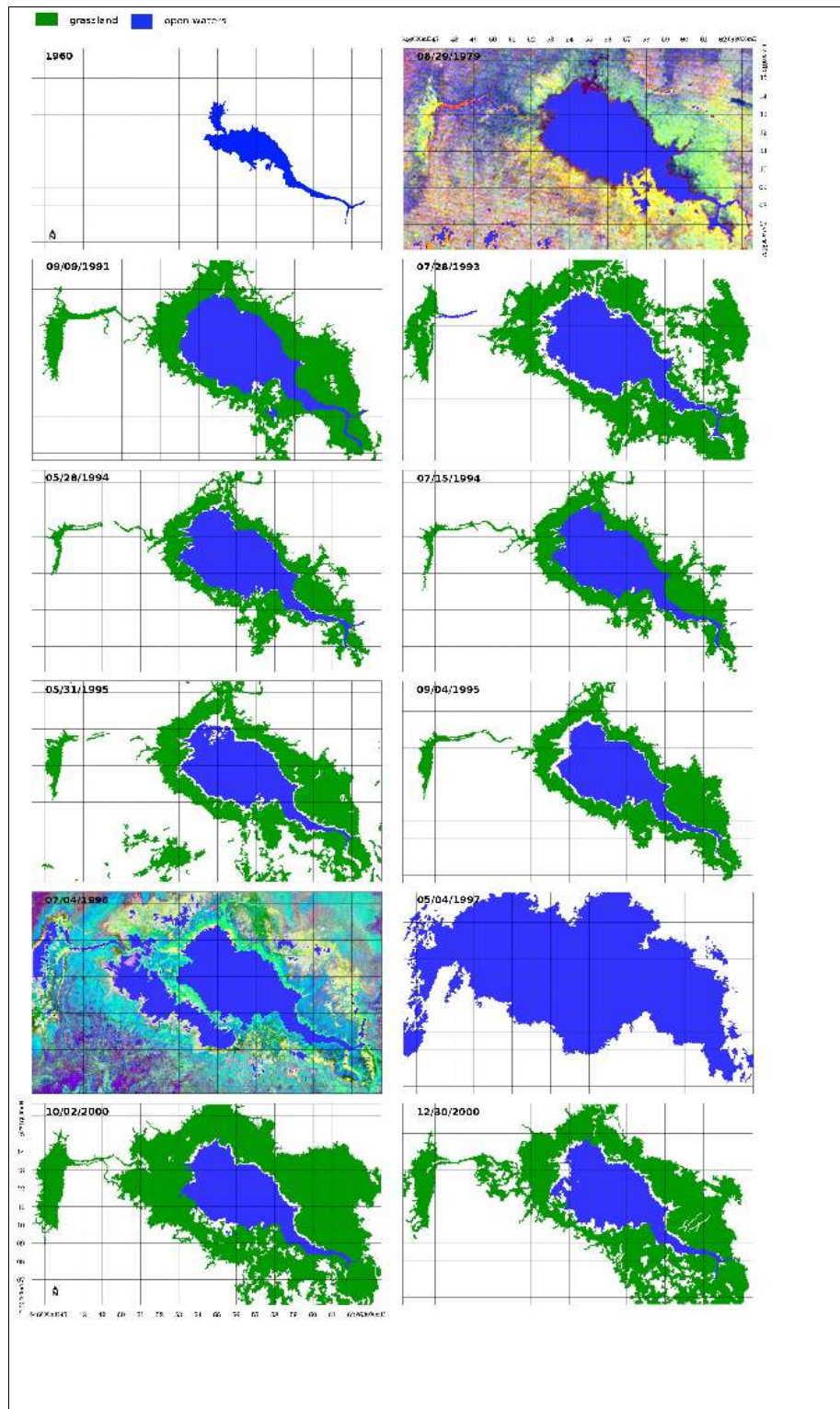


Figure 31: Output of the supervised classification, lake's extent from 1960 from topographical map (DINAGECA, 1960?)

The image from 1997 is outstanding due to its high Wetness values. The Greenness values in the four - completely water logged - profiles are lower than in the other images (exception profile 2). Peaks in Brightness and Greenness can probably be ascribed to only shallowly inundated areas or islands of vegetation within the flooded areas.

The image from September 1995 has clearly lower Greenness and higher Brightness values than the other years. It has to be emphasized that this image did not undergo haze correction. July 1993 seemed to have been moister which is shown by higher Wetness and Greenness values. Additionally, the lake was larger as the profiles 1 and 4 indicate by the sudden increase of the Wetness values at the lake's shoreline.

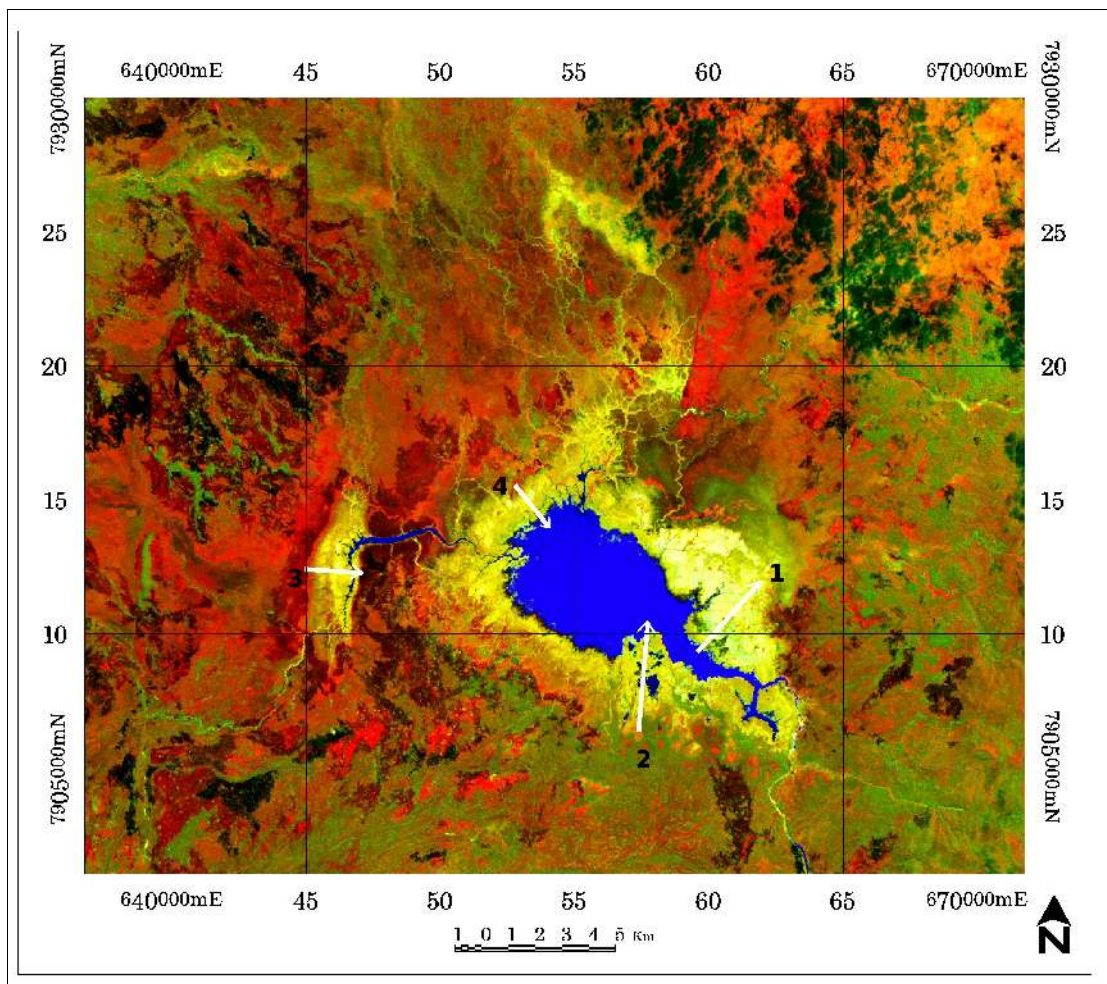


Figure 33: Location of profiles in BGY and BGW images, background image from Landsat TM 05/28/1994, Brightness (red), Greenness (green) and Wetness (blue)

With proceeding dry season the decreasing Greenness goes together with an increase in Brightness (1994, 1995). In this context note the shift of the lake's shoreline inwards from May 1994 to July 1994 and from May 1995 to September 1995 (profile 4).

Profile 3 shows the intra- and inter-annual behavior of the Sungue plain. The area which is most likely water logged or at least characterized by high moisture and vitality of the vegetation is at about 1800 m distance from the starting point of the profile. In all years, except in 1993 and 1997, it is characterized by a definite peak in Greenness. In 1993 there is a decrease in Greenness but instead a local peak in Wetness indicating open water conditions.

Comparing the lake's shoreline - as it is indicated by a sudden increase in Wetness in BGW images - with the results of the classification (gray lines in Figure 34, Figure 35) it can be seen that there is good consistence (profile 2 and 4).

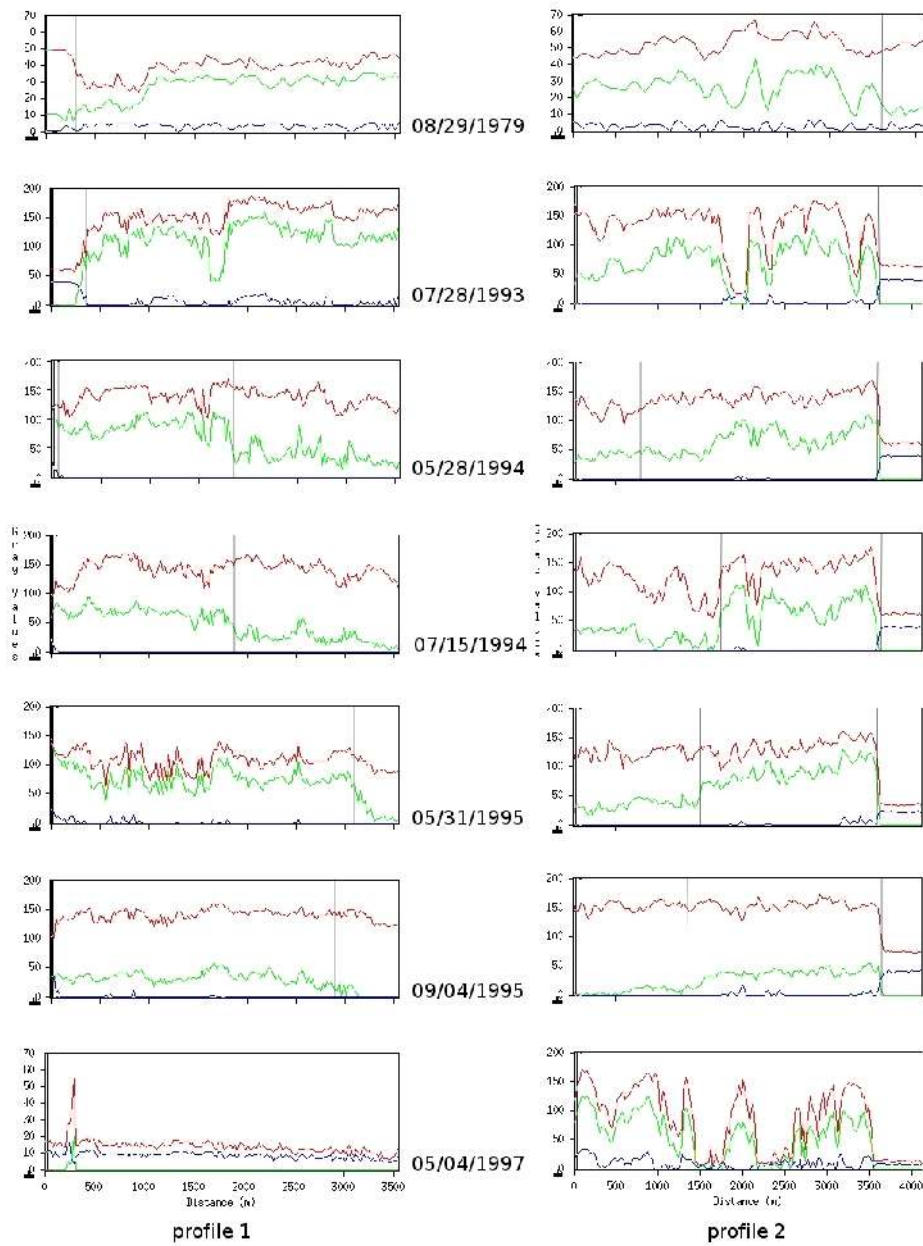


Figure 34: Pattern of Brightness (red), Greenness (green) and Yellowness (1979: blue)/Wetness (other years: blue) along profiles in the floodplain around Lake Urema, profiles show west-east-orientation

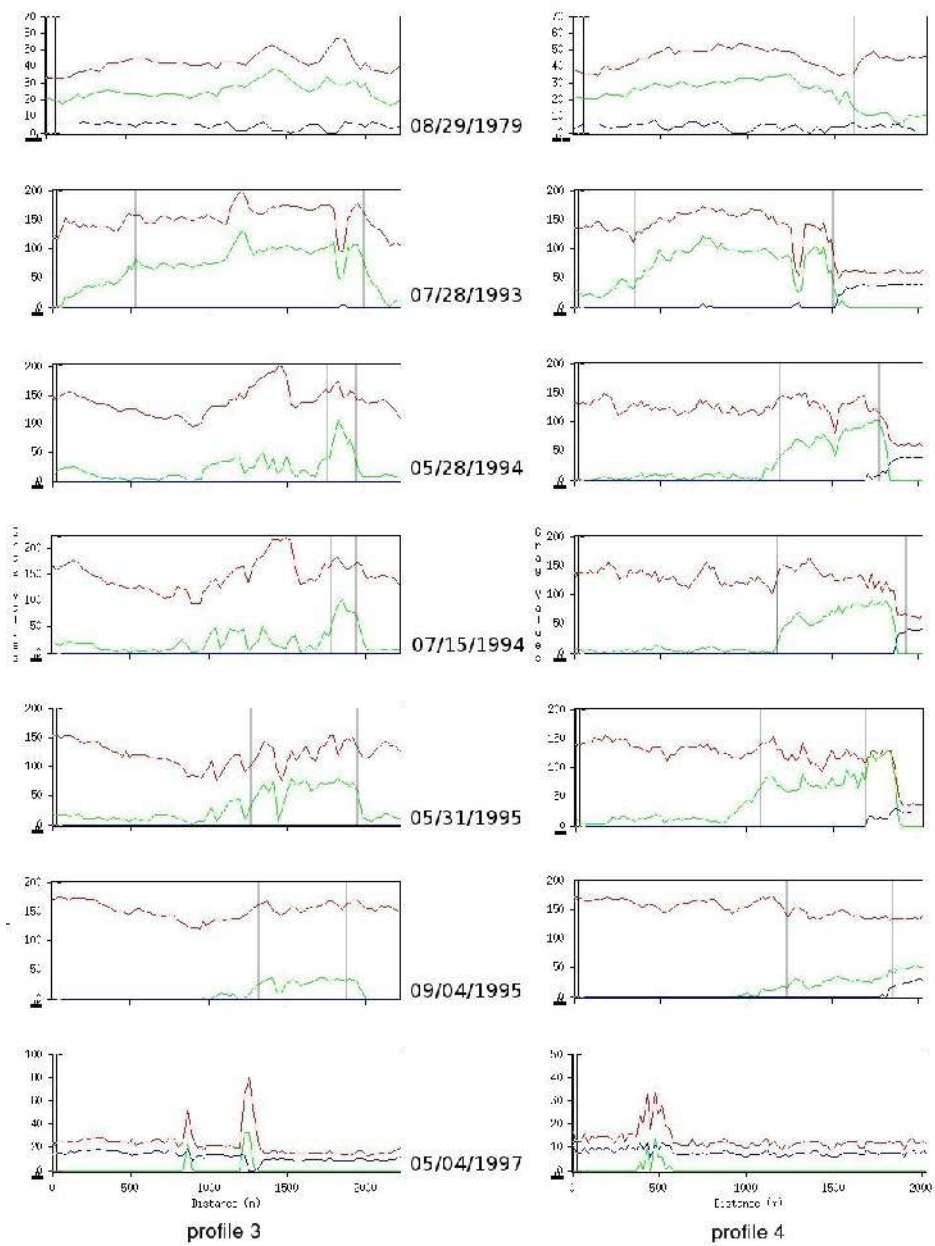


Figure 35: Pattern of Brightness (red), Greenness (green) and Yellowness (1979: blue)/Wetness (other years: blue) along profiles in the floodplain around Lake Urema, profiles show west-east-orientation

## 6.4 Hydrology

### 6.4.1 Change of the lake level height during the period of investigation

Between the 4<sup>th</sup> of September and the 28<sup>th</sup> of October the lake level height fell by 32 cm. An attempt was undertaken to estimate the water balance of Lake Urema for that time to draw conclusions about the contribution of different water sources and losses to the hydrological regime of the lake. Equation 4 was used under the assumption that the fluctuation of the lake level height over the time is caused by the change of the lake's water volume.

*Equation 4 (after MERCIER et al., 2002):*

$$dV/dt = (R+P+G_i)-(D+E+G_o)$$

whereas

V	=	lake's volume [m <sup>3</sup> ]
t	=	observation time, e.g. one year, one month
R	=	rate of surface runoff [m <sup>3</sup> /time]
P	=	rate of precipitation at the surface of the lake [m <sup>3</sup> /time]
G <sub>i</sub>	=	rate of incoming groundwater seepage [m <sup>3</sup> /time]
D	=	discharge rate [m <sup>3</sup> /time]
E	=	evaporation rate at the surface of the lake (E <sub>pot</sub> = potential evaporation) [m <sup>3</sup> /time]
G <sub>o</sub>	=	rate of outgoing groundwater seepage [m <sup>3</sup> /time]

Subsequently, the acquisition of these parameters is described.

#### Precipitation P

According to ARA-Centro, Beira, there was no precipitation in August and September 2004. Little rainfall was measured at the 12<sup>th</sup> of October (0.8 mm) and at the 31<sup>st</sup> of October (1.6 mm). The reliability of these information has to be questioned because rainfall was observed several times during the field work.

Surface runoff R, Discharge D

At the Urema River, which is the only **outflow** of Lake Urema, estimates of flow velocities were performed at the 6<sup>th</sup> of September approximately 7 km downstream from the mouth of Lake Urema [Figure 36]. At this site water plants did not yet close the river. Yet, a flow of water was not detectable.



Figure 36: WP 96; Urema River about 7 km downstream the mouth of the Lake Urema (photo: Beate Böhme)

The cross-section of the Urema River at the former hydrometric station E81 [Figure 2] was nearly closed by vegetation [Figure 37] so that a flow measurement could not be conducted.



Figure 37: Hydrometric station E 81 at the Urema River in September 2004 (photo: Beate Böhme)

At the 6<sup>th</sup> of October a flow measurement was undertaken at the Vunduzi River, which is joining the Mucombeze River, a **tributary to the Lake Urema**. The sample site is approximately 60 km upstream (air-line distance) from the mouth of the Mucombeze River into the lake.

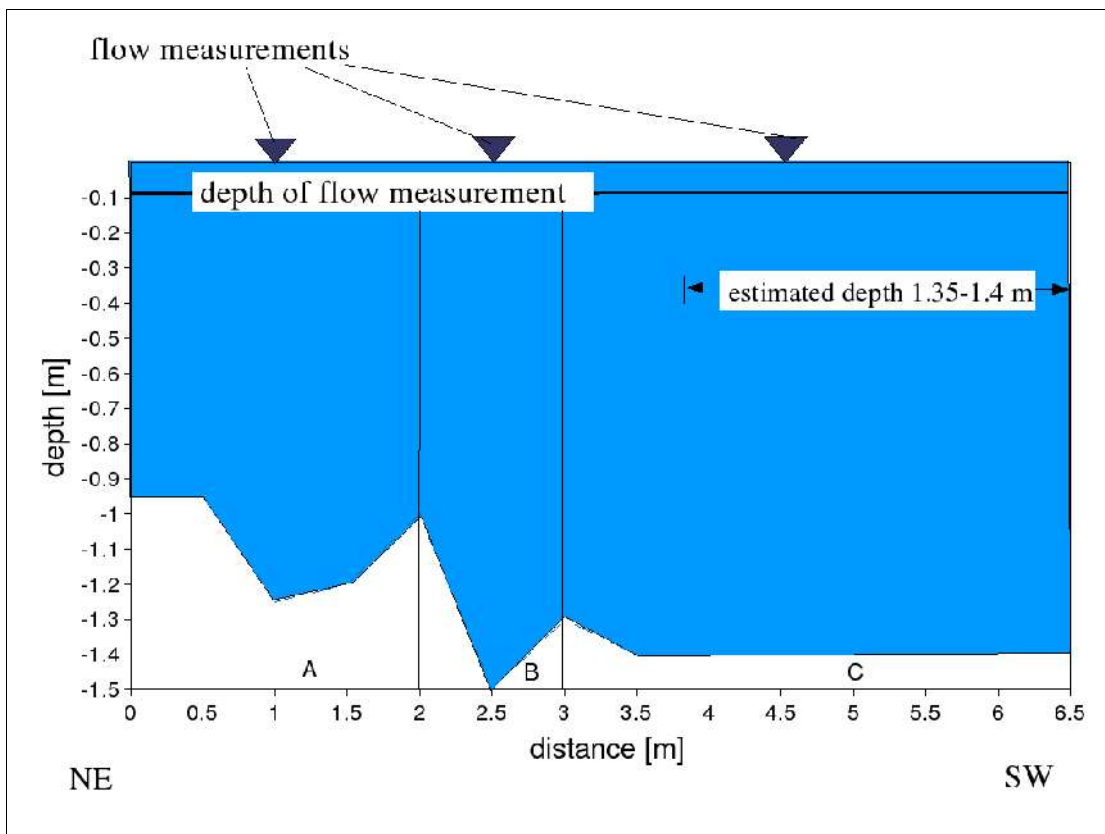


Figure 38: Cross-section of the Vunduzi River at site 318

The riverbed at site 318 was inhomogeneous: big stones and a high flow velocity made it impossible to measure the exact depth and the flow velocity within each segment [Figure 38]. The discharge of the Vunduzi River – based on the measurement with a current meter – was  $1.65 \text{ m}^3/\text{s}$  .

The result of a simple estimation of the flow velocity was  $0.3 \text{ m/s}$  and the discharge therefore  $2.33 \text{ m}^3/\text{s}$ .

#### Groundwater seepage $G_i, G_o$

Groundwater seepage could not be included in the calculations due to lack in data.

#### Evaporation $E$

For Chitengo historical data for the potential evaporation - calculated with the energy balance method - were available [COBA, 1977?]. It is supposed that the figures are from the period 1956/57-1969/70 when an A-pan was run in Chitengo.

### Conclusion

Just considering the water loss through potential evaporation and the water input through precipitation, (disregarding in- and outflow of the lake), the water table of Lake Urema (lake area approximately 18.5 km<sup>2</sup>, extent from satellite image, October 2000) should drop by 23 cm during the period from September to October [Table 8]. Actually, a drop of 32 cm was measured.

Including the inflow through the Vunduzi River (1.65 m<sup>3</sup>/s = 8,696,160 m<sup>3</sup>/September to October) and assuming that all the water is entering the lake, its level should finally rise by 0.24 m during the period from September to October (loss through potential evaporation and input through precipitation included, no outflow).

Table 8: Water loss through Potential Evaporation ( $E_{pot}$ ), water input through precipitation ( $P$ ) and surface runoff ( $R$ ) during September to October 2004, all numbers referred to an lake area of 18.5 km<sup>2</sup>

	September	October	whole period
<b>P [m<sup>3</sup>]</b>	0	44,400	44,400
<b>E<sub>pot</sub> [m<sup>3</sup>]</b>	1,831,500 m <sup>3</sup> /mon	2,405,000 m <sup>3</sup> /mon	4,236,500
<b>R [m<sup>3</sup>]</b>		1.65 m <sup>3</sup> /s	8,696,160
<b>P-E<sub>pot</sub> [m<sup>3</sup>]</b>			-4,192,100
<b>P-E<sub>pot</sub>+R [m<sup>3</sup>]</b>			4,504,060

### 6.4.2 How much rain is required to fill the lake's 1997 extent?

The volume of Lake Urema in October 2000 was estimated with 30.34\*10<sup>6</sup> m<sup>3</sup> (area 18.5 km<sup>2</sup>, mean depth 1.64 m). The water volume of the lake in May 1997 was 248.9\*10<sup>6</sup> m<sup>3</sup> bigger than in October 2000. SWECO&ASSOCIATES\_I, 2004 give numbers for the Mean Annual Precipitation (MAP) and the Mean Annual Runoff (MAR) in the catchment area of Lake Urema. In the Nhandugue subbasin the MAP is numbered with 850 mm/y, in the Urema subbasin<sup>11</sup> with 900 mm/y. The annual water input through rainfall over the whole catchment area (Urema plus Nhandugue subcatchment) comprises therefore 7,420.3\*10<sup>6</sup> m<sup>3</sup>. Using their numbers for the Mean Annual Runoff (SWECO&ASSOCIATES\_I, 2004) the annual runoff from the catchment area is 498,548\*10<sup>3</sup> m<sup>3</sup>. An increase in the lake's extent as observed in 1997 equals to 50% of the Mean Annual Runoff and three percent of the Mean Annual Precipitation in the catchment area of Lake Urema.

Using the average volume of Lake Urema, its water body is renewed 16 times per year assuming that all runoff from the catchment area is flowing into the lake. When the discharge of the Vunduzi River in the dry season 2004 is interpolated over a whole year and it is assumed that all the water is feeding the lake, the lake's volume should be renewed 1.7 times/y.

<sup>11</sup> note that SWECO&ASSOCIATES\_I (2004) confined Urema subcatchment different than done in this study

### ***6.5 Water chemistry***

Figure 39 shows the sample sites for water analyses. Three compartments of the lake system were sampled during the period of investigation: Vunduzi River, a tributary of the Mucombeze River which drains into Lake Urema; Urema River, which is the outflow of the Lake Urema, and Lake Urema itself (pelagic zone including trophogenic and tropholytic zone, inflow and outflow region and littoral zone)<sup>12</sup>.

---

<sup>12</sup> Note in the following figures that circles at the same location do not automatically belong to the same sampling. Superposition of circles of one parameter represents repetitions of measurements at different dates and times. Arrow points towards site 318 which is not in the area covered by the maps.

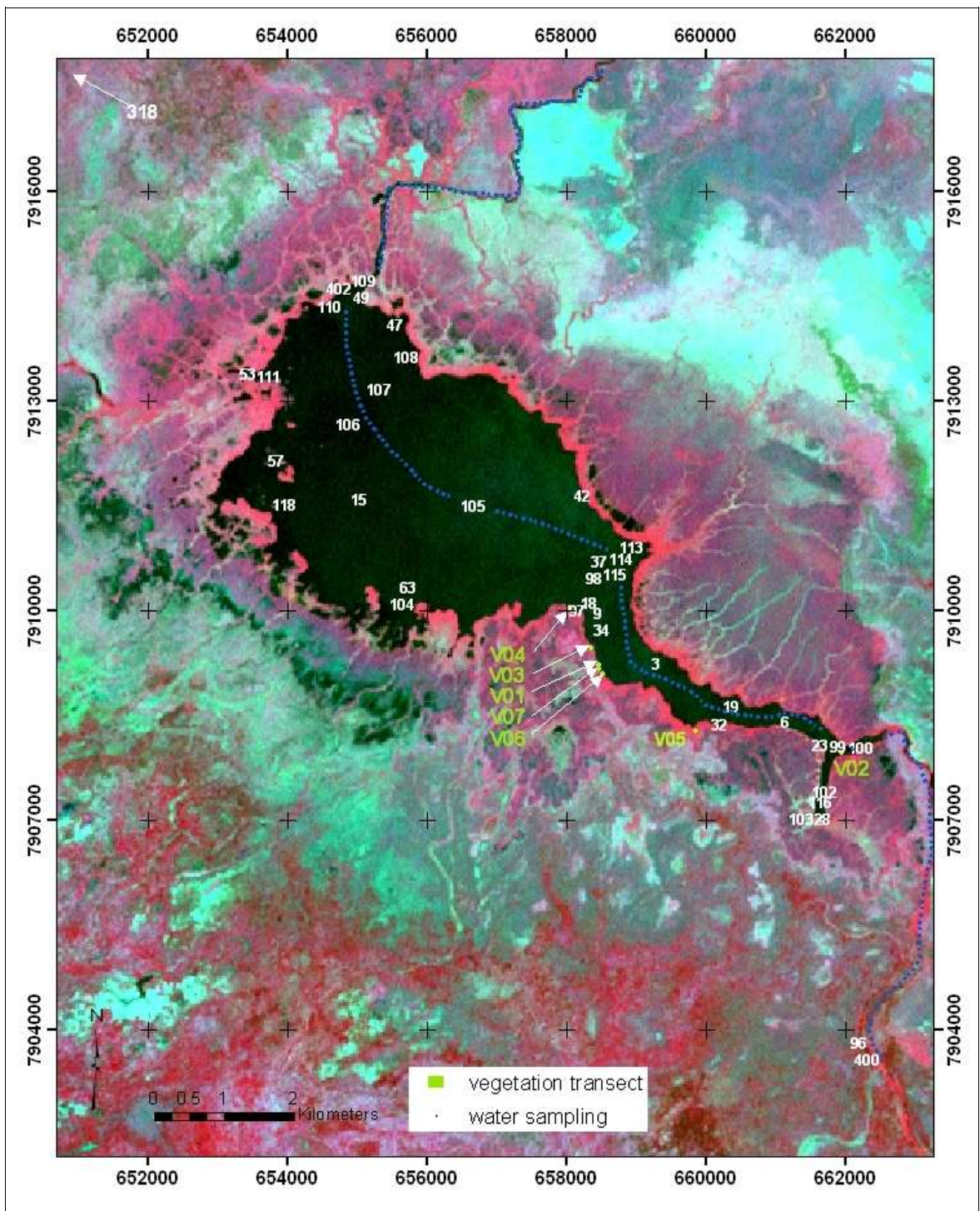


Figure 39: Sample sites at Lake Urema, white numbers are labels of water sample sites, dotted blue line is linking sites of detailed laboratory water analyses, V01-V06 are vegetation transects, background Landsat ETM+ 4/3/2, 12/30/2000, image stretch by standard deviation ( $n=2$ )

At most sample sites the **water temperature** [Figure 41] was between 24 and 28°C. Air and water temperature were correlated at the 95% confidence level [Figure 40] (Spearman Rank Correlation Coefficient  $R = 0.5995$ ,  $N = 47$ ,  $p < 0.0001$ ,  $N =$  number of observation pairs,  $p =$  level of significance).

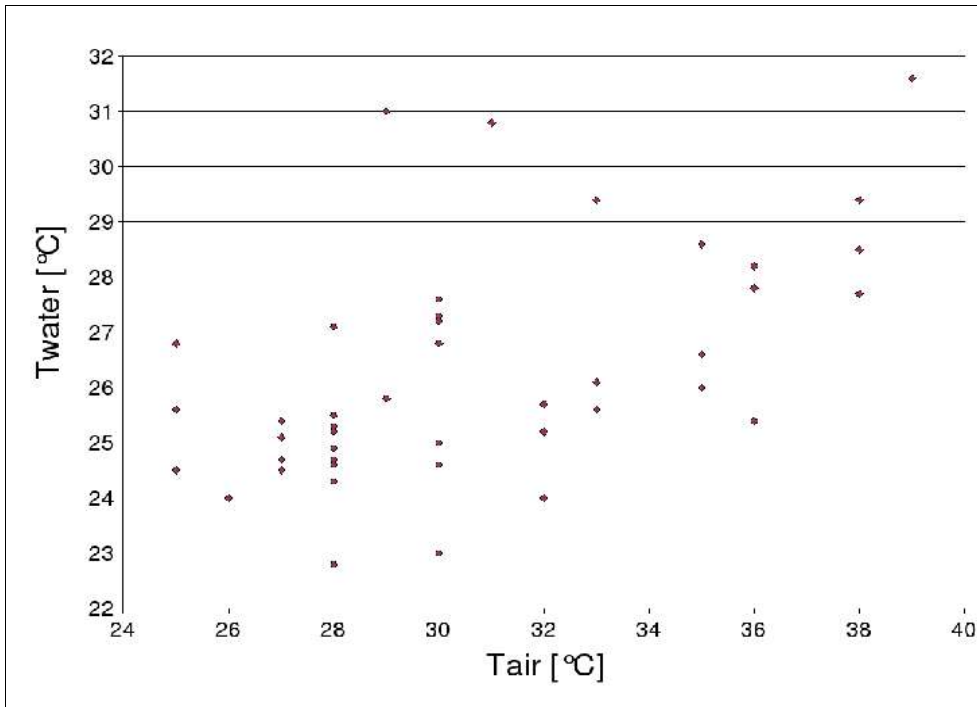


Figure 40: Air temperature vs. water temperature of Lake Urema

The **pH** of the surface water samples varied between 5.9 (moderate acidic) and 9.1 (strongly alkaline) [Figure 42] (graduation according to AG BODEN, 1996). Values of pH below 7 were measured in areas with little water circulation or stagnant conditions in bays, such as in the inflow region of the Mucombeze (49, 402) or the Sungue (111, 53), in the outflow region (99, 102, 103) or close to/within the littoral (97). Also the water of the Urema River (400, 96) was moderate acidic in comparison to the central part of the lake which showed pH values higher than 7.

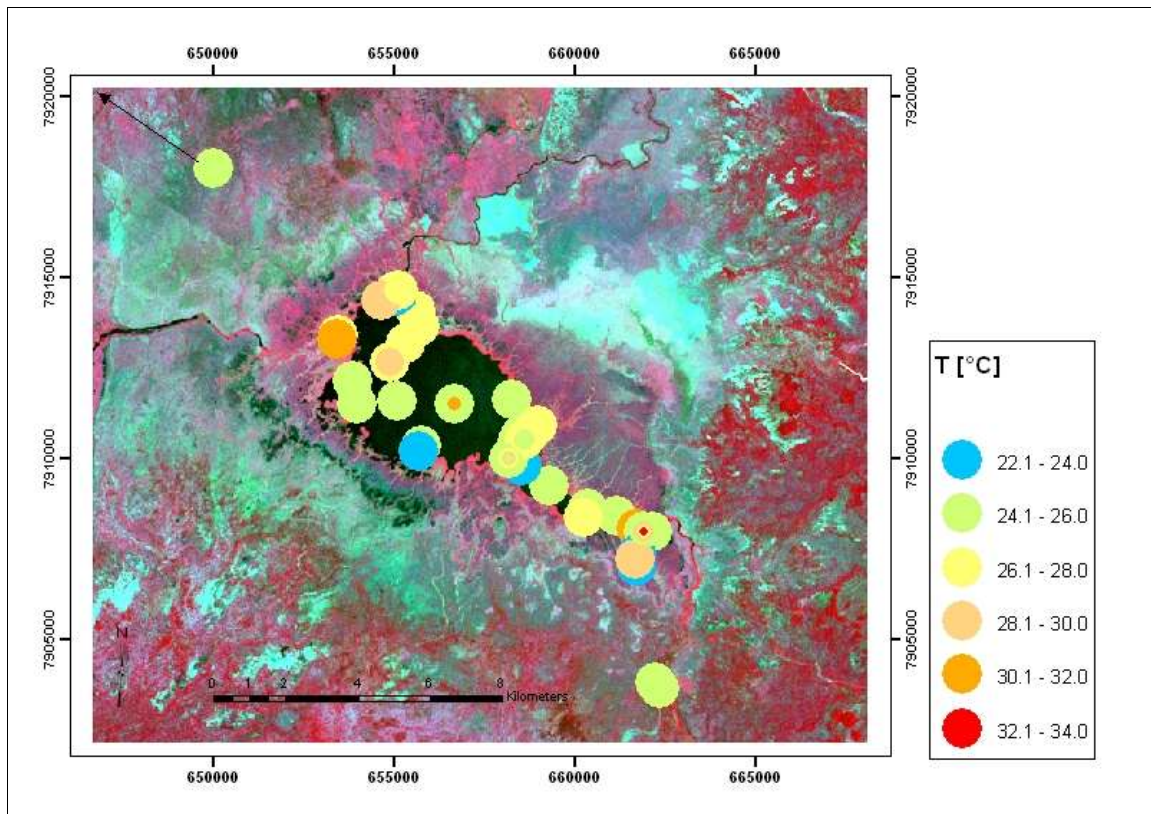


Figure 41: Measurements of water temperature at Lake Urema between 08-10/2004, Landsat ETM+ 4/3/2, 12/30/2000, image stretch by standard deviation ( $n=2$ )

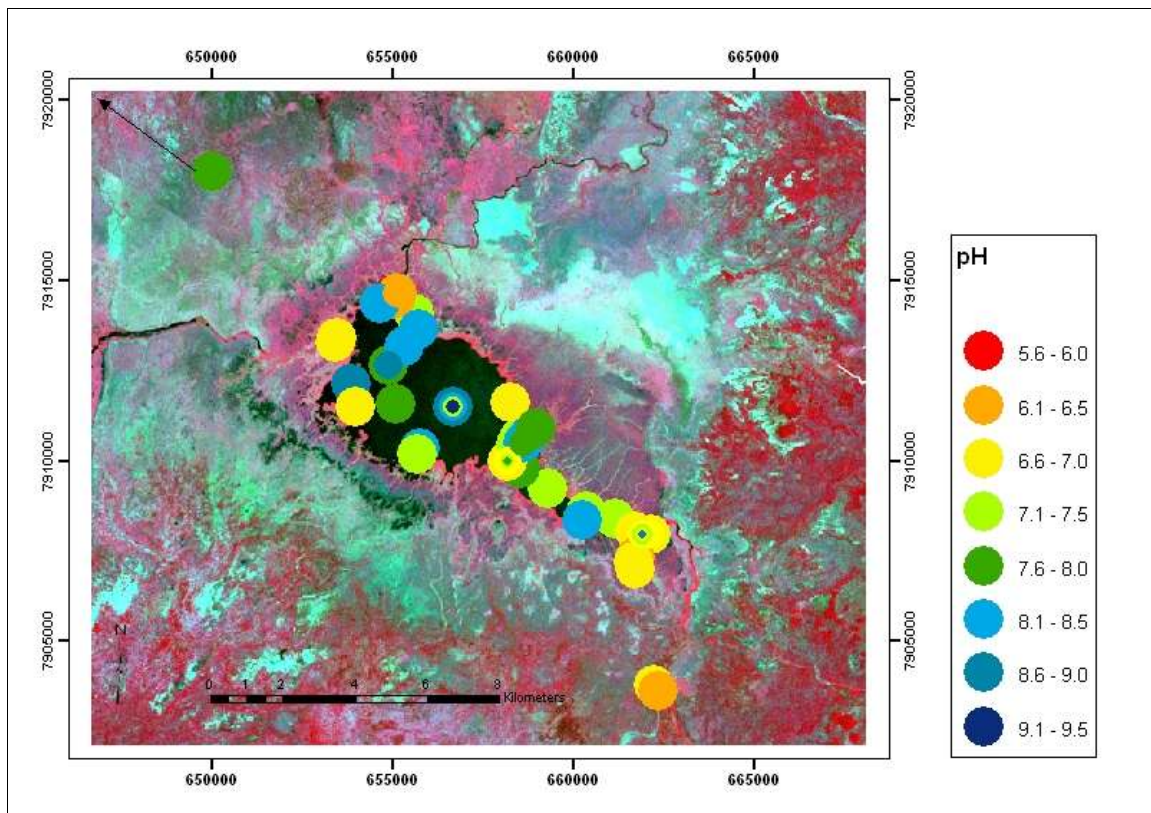


Figure 42: Measurements of pH at Lake Urema between 08-10/2004, background Landsat ETM+ 4/3/2, 12/30/2000, image stretch by standard deviation ( $n=2$ )

The values for the **electrical conductivity** [Figure 43] indicate a low mineralization of the water of Lake Urema and its tributaries. The lowest value among all measurements was in Vunduzi River (site 318), 60 km upstream of Lake Urema ( $32 \mu\text{S}/\text{cm}$ ). Conductivities below  $100 \mu\text{S}/\text{cm}$  were also measured in the inflow region of the Mucombeze River (sites 402, 49, 109). Towards the narrowing outflow region of the lake and Urema River the electrical conductivity increased to more than  $150 \mu\text{S}/\text{cm}$  (Urema River  $168.6 \mu\text{S}/\text{cm}$ ,  $160.4 \mu\text{S}/\text{cm}$ ). There is a correlation at the 95% confidence level between EC and Secchi-disc transparency (Spearman Rank Correlation Coefficient  $R = 0.5105$ ,  $N = 39$ ,  $p = 0.0016$ ).

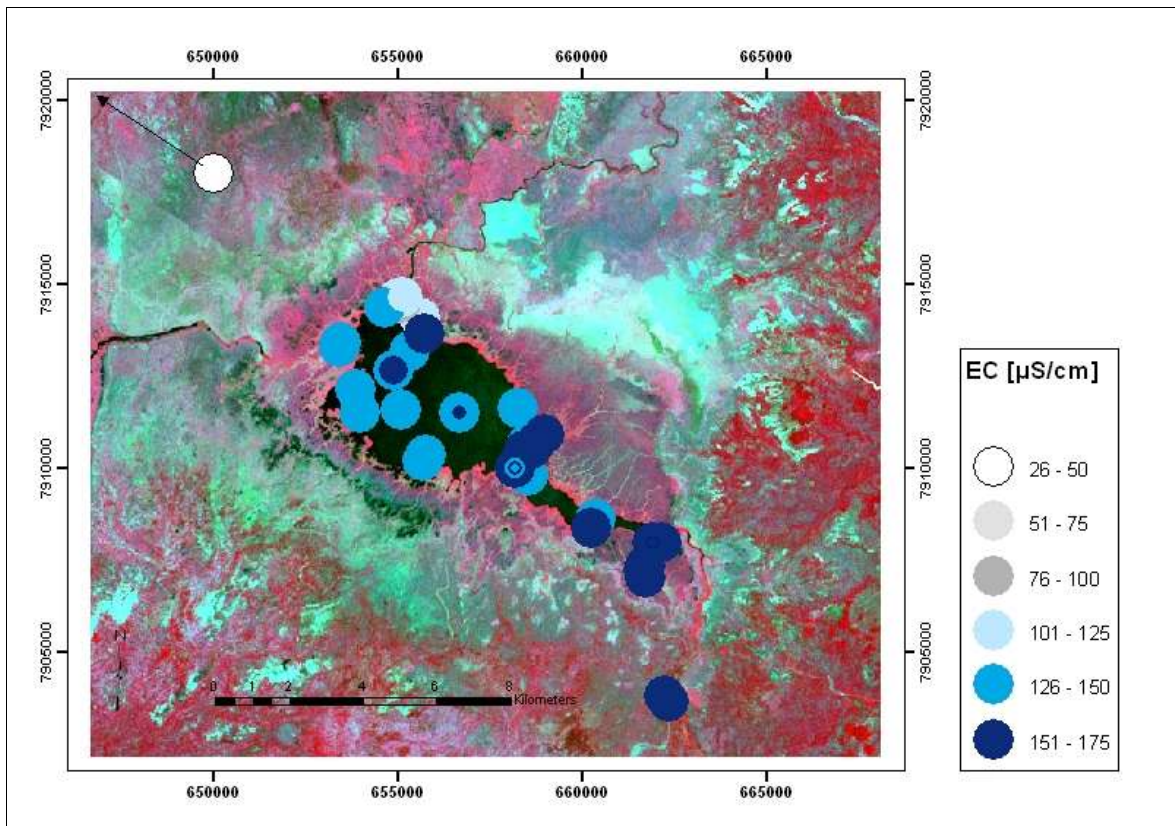


Figure 43: Measurements of electrical conductivity (EC) at Lake Urema between 08-10/2004, Landsat ETM+ 4/3/2, 12/30/2000, image stretch by standard deviation ( $n=2$ )

The **Secchi-disc transparency** varied between 0.24 and 0.7 m whereas the higher values were measured in the outflow region and the lower values in the inflow region [Figure 44]. Along the depth profile 1 (chapter 6.2.2.1) the visibility was generally between 0.3 and 0.4 m while in profile 3 and 4 it was about 10 cm higher. From the comparison of the transparency measurements during the period of investigation the conclusion could be drawn that the transparency decreased, e.g. sample site 97: 0.45 m (09/07/2004), 0.3 m (10/10/2004); site 115: 0.44 m (09/07/2004), 0.35 (10/11/2004); site 105: 0.35 m (09/09/2004), 0.25 m (10/28/2004). Nevertheless there are daily variations in transparency, depending on the sun elevation, currents and subjective influences.

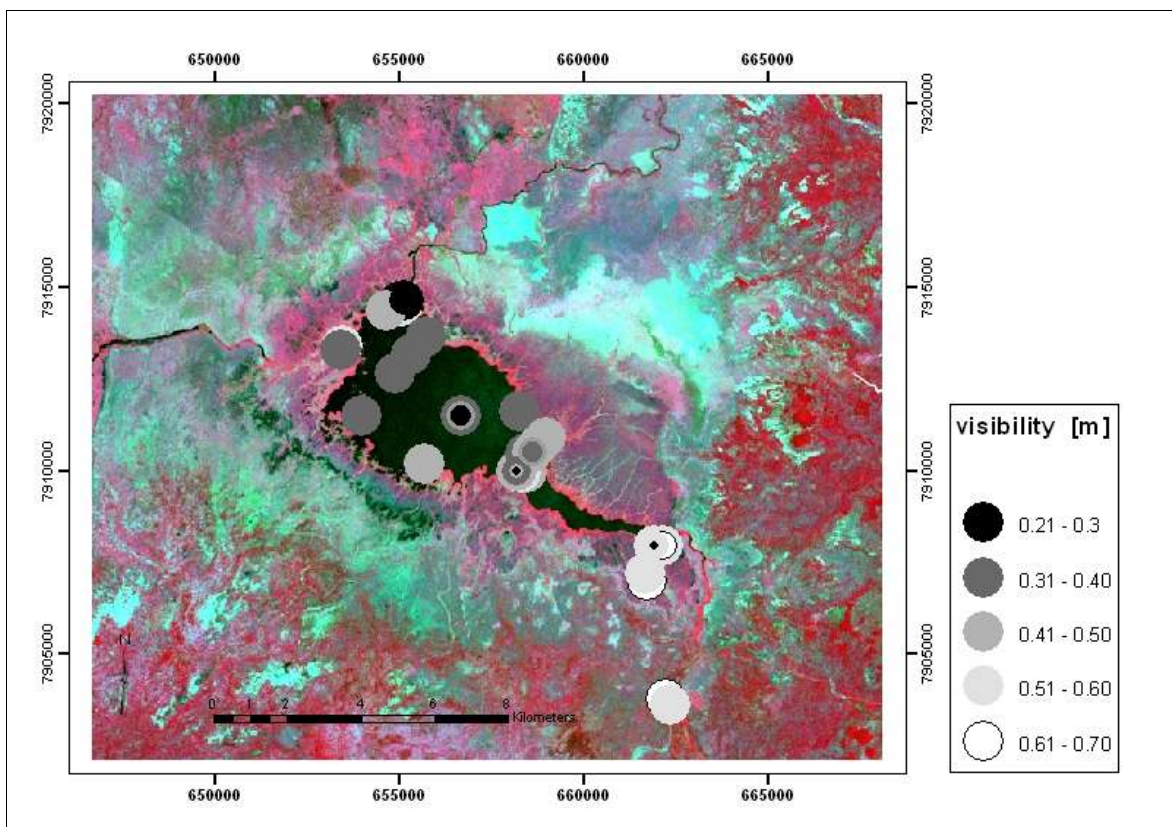


Figure 44: Measurements of Secchi-disc transparency at Lake Urema between 08-10/2004, background Landsat ETM+ 4/3/2, 12/30/2000, image stretch by standard deviation ( $n=2$ )

A general trend of decreasing transparency during the period of investigation was confirmed by visual inspection of Lake Urema as a whole. Especially the narrowing part of Lake Urema seemed to be affected by increasing turbidity.

The Secchi-disc transparency was correlated with the pH value at the 95% confidence level ( $R = 0.3613$ ,  $N = 40$ ,  $p = 0.00241$ ) and with the electrical conductivity ( $R = 0.5105$ ,  $N = 39$ ,  $p = 0.0016$ ).

The suspended matter which caused the high turbidity of the lake water, consisted mainly of fine grained clayey-silty particles, detritus and parts of plants [Figure 45]. Organisms, such as Flagellates (Protozoa) and representatives of the group of the diatoms (e.g. genera *Melosira* and *Navicula*, class Bacillariophyceae), were detected but not quantified. No representatives of green algae were observed.

The color of the water of Lake Urema was typically yellowish-greenish, in the outflow region often reddish.



Figure 45: Top view at a water filter (200 nm mesh size, magnification 8 x) after filtration of 90 ml water from site 115, lower half of picture shows scale paper: box equals to 1 mm<sup>2</sup> (photo: Beate Böhme)

The **Redox potential** indicated partly oxidizing to oxidizing conditions ( $E_h > 400$ ) [Figure 46]. Reducing conditions were nowhere observed.

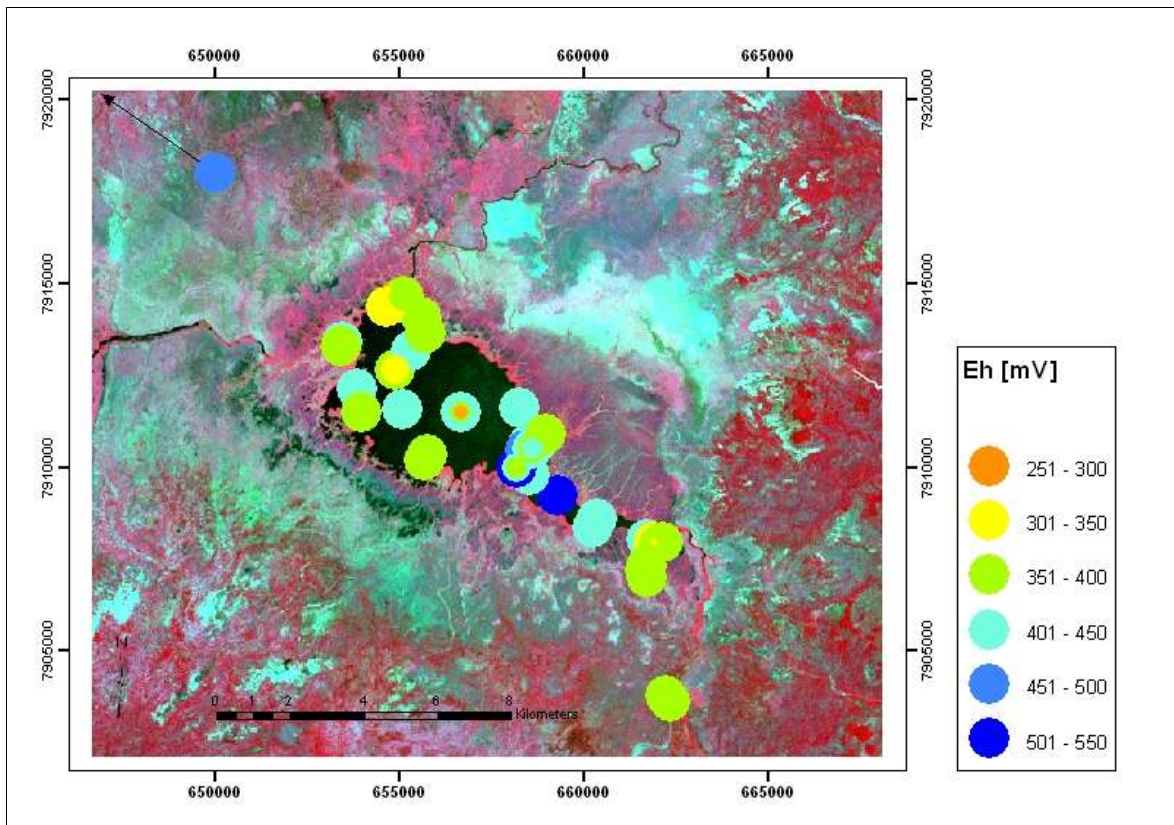


Figure 46: Measurements of redox potential at Lake Urema between 08-10/2004, background Landsat ETM+ 4/3/2, 12/30/2000, image stretch by standard deviation ( $n=2$ )

**The saturation of dissolved oxygen** (expressed as percent saturation) varied over the lake and during the period of investigation, ranging from 15% to 115% [Figure 48]. At sites 97 and 99, both located close to/within the littoral, two measurements of dissolved oxygen were conducted at different times of the day whereby the measurement in the afternoon gave a higher oxygen saturation.

97: 7.45 am: 23%, 3.30 pm: 35%

99: 10.00 am: 52%, 3.00 pm: 59%

Super-saturation of dissolved oxygen (>100%) occurred at sites 99 (10/28/04, 11.45 am), 105 (10/28/04, 09.15 am), 106 (09/16/04, 00.45 pm) and 110 (09/10/04, 01.15 pm).

The Spearman Rank Correlation Coefficient indicated a correlation between the pH and the saturation of dissolved oxygen at the 95% confidence level ( $R = 0.8956$ ,  $N = 28$ ,  $p < 0.0001$ ) [Figure 49]. The correlation between the oxygen saturation and the water temperature was also significant ( $R = 0.4380$ ,  $N = 28$ ,  $p = 0.0229$ ).

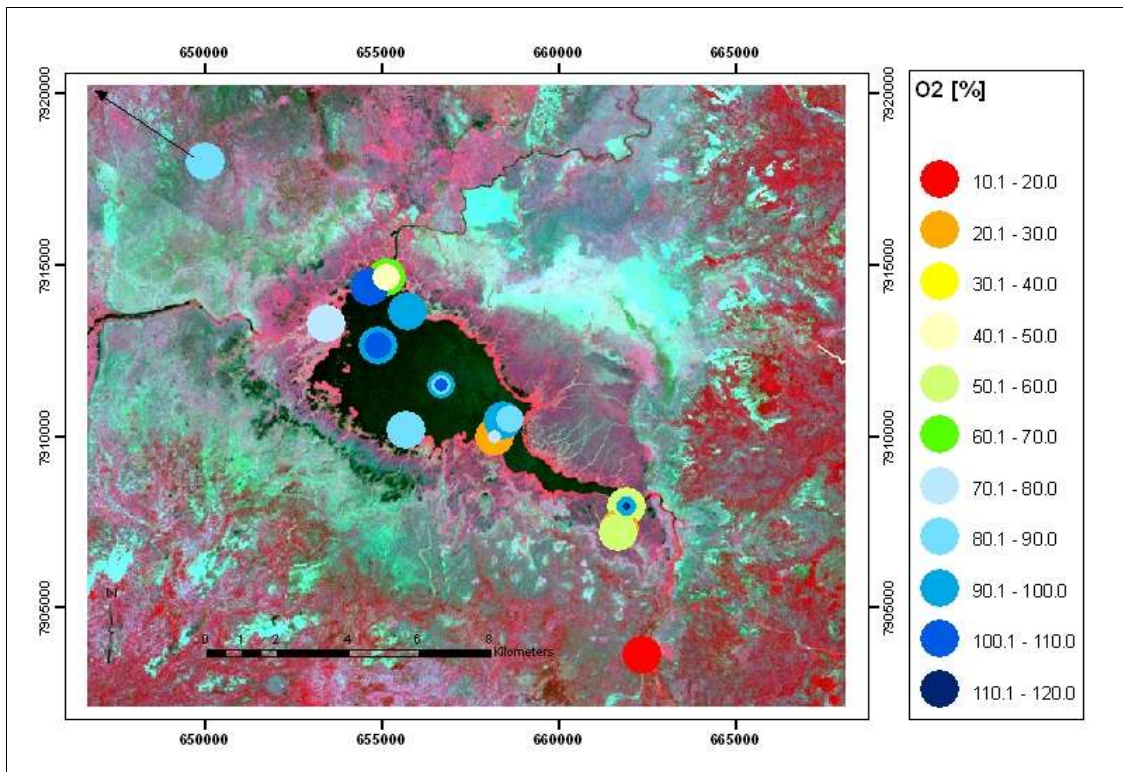


Figure 48: Measurements of saturation of dissolved oxygen at Lake Urema between 08-10/2004, background Landsat ETM+ 4/3/2, 12/30/2000, image stretch by standard deviation ( $n=2$ )

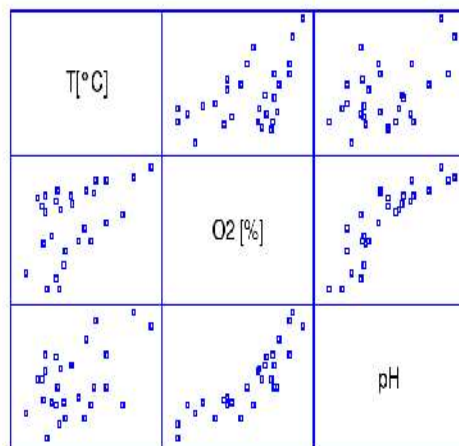


Figure 49: Correlation of saturation of dissolved oxygen, pH and water temperature, each block represents the relationship between the parameters in the adjacent fields

The **concentrations of nutrients** in the water of Lake Urema were mostly below the detection limit of the measurement device. For nitrate no concentrations above the detection limit (0.5 mg/l) were measured. Ammonium (detection limit 0.1 mg/l) was detected at a concentration of 0.2 mg/l in the Urema River. Phosphate (detection limit 0.2 mg/l) was detected at the inflow of the Mucombeze River (site 402) and at site 115 where the lake is getting narrow. The concentrations were 0.3 and 0.7 mg/l. Sulfate concentrations were below 5.5 mg/l: 97 (2.6 mg/l), 99 (2.6 mg/l), 105 (1.3 mg/l), 115 (2.6 mg/l), 318 (1.3 mg/l), 400 (5.2 mg/l).

At few sites measurements of water chemical parameters were conducted in both the trophogenic and the tropholytic zone. Values of the pH in the tropholytic zone were some 0.1 units lower than in the trophogenic zone (maximal difference to surface water 1.1 pH-unit in 106) [Table 9]. The electrical conductivity was mostly lower in the trophogenic zone than in the tropholytic zone; maximal difference comprised 68  $\mu\text{S}/\text{cm}$  (site 116). The saturation of dissolved oxygen seemed to be higher in the trophogenic zone than in the tropholytic zone, about twofold at site 99 [Table 10].

*Table 9: Water depth, pH and electrical conductivity EC in the trophogenic and tropholytic zone, site 109a and b close to each other*

sample ID	water depth [m]	T trophogenic zone [°C]	T tropholytic zone [°C]	pH trophogenic zone	pH tropholytic zone	EC trophogenic zone [ $\mu\text{S}/\text{cm}$ ]	EC tropholytic zone [ $\mu\text{S}/\text{cm}$ ]
99	1.87	28.5	25.6	7.2	6.9	164	180
105	1.43	31.6	28.6	9.1	7.3	152	155
106	1.83	28.6	26.6	9.0	7.9	152	151
109a	1.55	27.7	23.5	6.4	6.1	101	
109b	1.75	26.1	24.7	6.4	6.1	107	105
110	1.14	29.4	29.7	8.1	7.5	135	
111	1.15	30.8	30.0	6.7	6.7	147	
115	1.60	26.8	26.8	7.8	7.4	153	196
116	1.36	28.2	23.0	6.7	6.6	162	230

*Table 10: Saturation of dissolved oxygen in the trophogenic and tropholytic zone*

site ID	date	time	trophogenic zone	tropholytic zone
99	10/28/04	11:45:00 am	115	55
105	10/28/04	09:15:00 am	104	77
106	09/16/04	00:45:00 pm	102	87

In Figure 50 and Figure 51 the results of laboratory water analyses via Ion Chromatography are presented. The sampling points can be interpreted as a transect from the Vunduzi River (site 318) through the lake towards the outflow (site 400) [Figure 39].

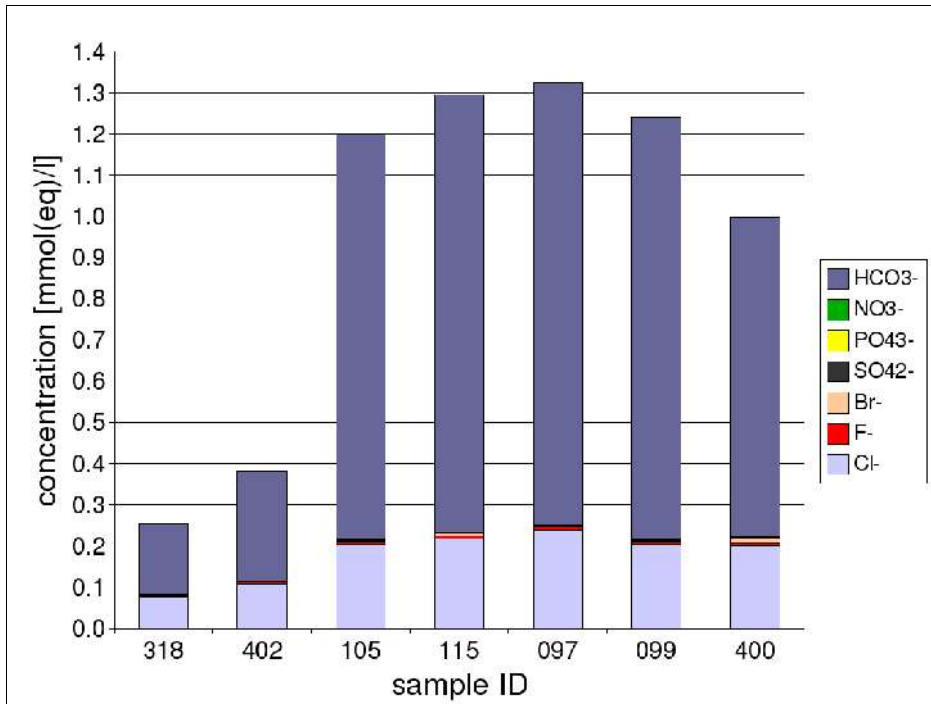


Figure 50: Concentration of major anions in the water of Lake Urema and tributaries

Hydrogen carbonate was the major anion in the water samples [Figure 50]. Concentrations were generally higher in the central part of the lake than in the Vunduzi River (site 318: 10.3 mg/l), the inflow region (site 402: 16.4 mg/l) and in the Urema River (site 400: 47.3 mg/l). Chloride, the second most common anion in Urema water, occurred with concentrations between 2.7 mg/l and 8.4 mg/l showing a similar pattern of distribution as hydrogen carbonate.

Note that the concentrations of nitrate as well as those of sulphate showed a local peak (0.14 mg/l and 0.37 mg/l) at the Vunduzi River (site 318). In the inflow region of the lake, at site 402, the nitrate concentration was similar high (0.13 mg/l) and then again in the Urema River (site 400: 0.12 mg/l). Within the lake the nitrate concentration was below 0.1 mg/l. Sulphate concentrations, except in the Vunduzi sample, were not reliable as values were close to the detection limit of the IC device.

Sodium was the dominant cation, occurring at levels of about 10 mg/l in the lake and in the Urema River and a third of this value in the Vunduzi River and half of it in the inflow region at site 402. The concentrations of potassium, calcium and magnesium were similar at sites 105, 115, 097, 099 and 400: potassium concentrations at these sites varied between 2 mg/l and 3.7 mg/l, calcium concentrations between 8.2 and 9.8 mg/l and magnesium concentrations between 2.9 and 3.9 mg/l.

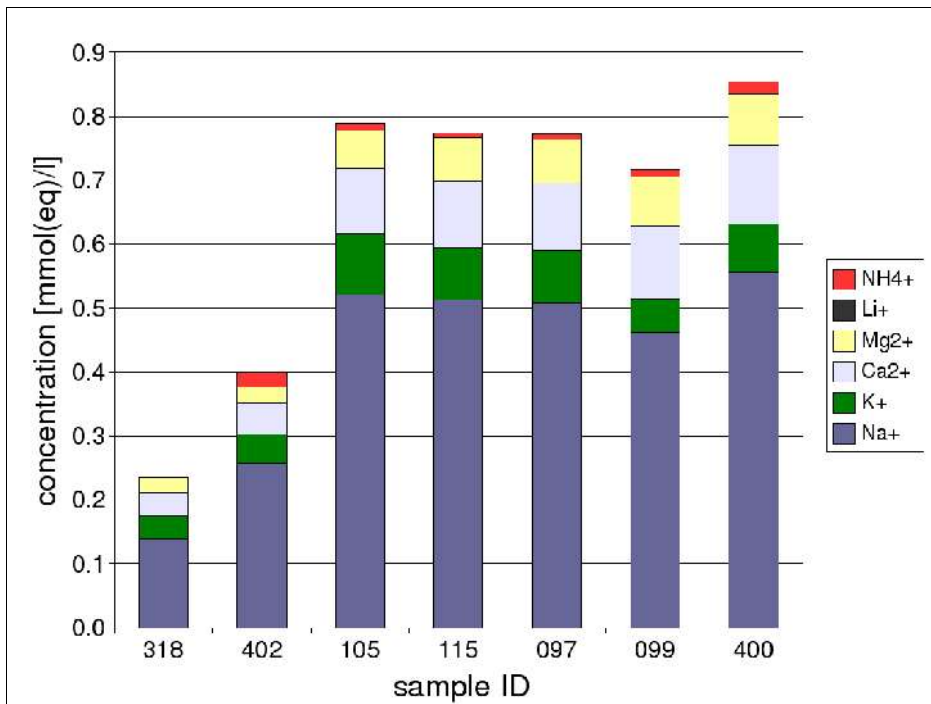


Figure 51: Concentration of major cations in the water of Lake Urema and tributaries

At sites 318 and 402 the concentrations of these major ions were approximately half the concentrations in the lake or even less.

Along the sampled transect the concentration of total dissolved solids (TDS) increased from the tributary Vunduzi River (site 318) towards the outflow of the lake and slightly decreased in the Urema River [Figure 52].

The plausibility of the water analyses can be evaluated through the comparison of the measured electrical conductivity with a conductivity value calculated with Kohlrausch's Law (calculated with an internal program of the chair of hydrogeology, TU Freiberg). The equivalent conductivities of the major an- and cations of the samples are included in this calculation. Figure 53 shows that the calculated values of the electrical conductivity were generally below the measured values. This suggests a lack of ions in the water analyses. The error of analysis was modeled in PhreeqC [Table 11] and a positive value indicates a deficiency of anions (with exception of site 097). Errors smaller than 2% testify the reliability of the analysis. The samples 318, 402 and 400 had much higher errors up to 23.5%. For samples 318 and 402 this phenomenon resulted probably from the low concentrations of water constituents close to the detection limit.

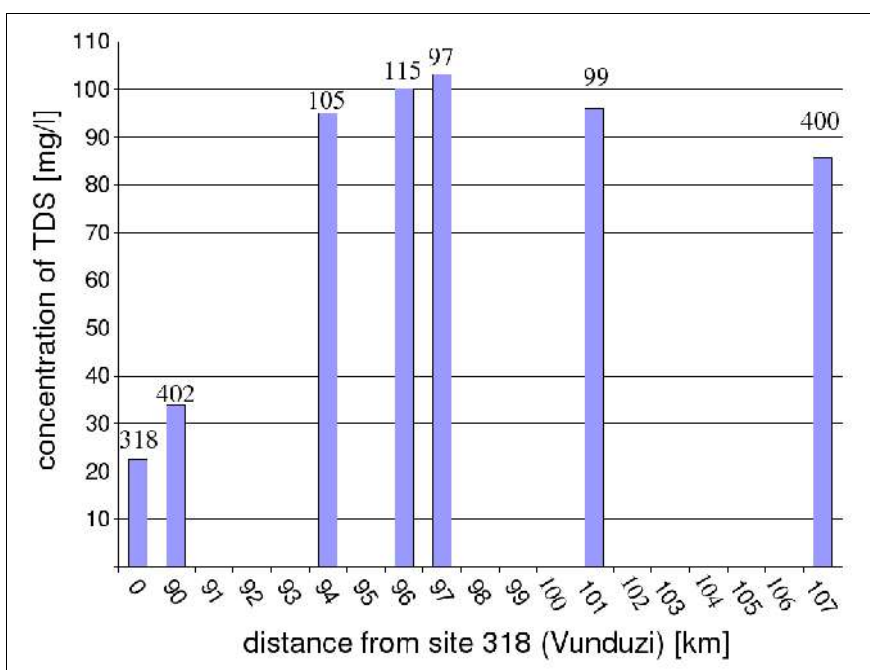


Figure 52: Concentration of total dissolved solids (TDS) along the transect through Lake Urema and its tributaries

Table 11: Error of analysis, modeled in PhreeqC, analysis is satisfying if error is below 2% (+)

sample ID	318	402	105	115	097	099	400
analysis error [%]	22.8	23.5	2.6	-0.5	-2.7	1.6	18.8
interpretation of error	deficiency of anions	deficiency of anions	deficiency of anions	+	deficiency of cations	+	deficiency of anions

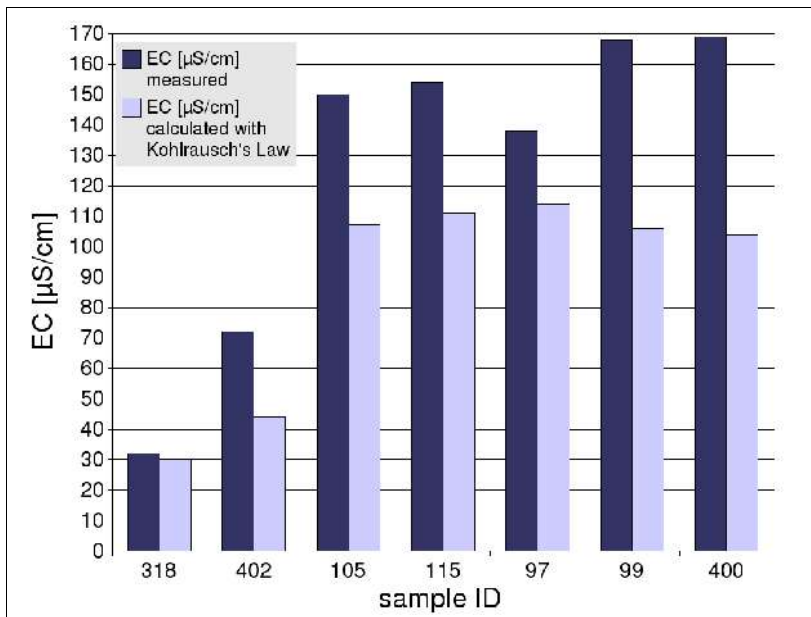


Figure 53: Comparison of the measured electrical conductivity EC with the calculated electrical conductivity

Comparing a rainwater sample from Beira (located 120 km southeast of the lake at the Indic Ocean) with the water samples from Lake Urema, its inflow and outflow, the similarity is particularly obvious for the sample from the Vunduzi River [Table 12]. The concentrations of the major ions were in most cases slightly below the values of the Vunduzi water. However, for chloride it was slightly above. Concentrations of nitrate and sulphate were significantly higher (23 and six times) in the rainwater than in the Vunduzi water.

The pH value of the rainwater sample was within the range of all lake and river water samples (pH = 5.9-8).

Table 12: Composition of rainwater in Beira, sampled in March 2005, concentration in mg/l, note: no complete analysis

T [°C]	pH	EC [µS/cm]	Na <sup>+</sup> [mg/l]	K <sup>+</sup> [mg/l]	Ca <sup>2+</sup> [mg/l]	Mg <sup>2+</sup> [mg/l]	NH <sub>4</sub> <sup>+</sup> [mg/l]	Cl <sup>-</sup> [mg/l]	SO <sub>4</sub> <sup>2-</sup> [mg/l]	NO <sub>3</sub> <sup>-</sup> [mg/l]
22.8	6.8	30.4	2.78	0.91	1.18	0.18	0.07	3.2	2.35	3.19

## 6.6 Sedimentation

### 6.6.1 Sediment coring

Five sediment cores were collected at a water depth between 0.5 m (S00) and 0.9 m (S04) [Figure 54]. The sample sites are located at the southwestern shoreline within the lower infralittoral. The thickness of the sediment cores varied between 0.17 m (S03) and 0.28 m (S02).

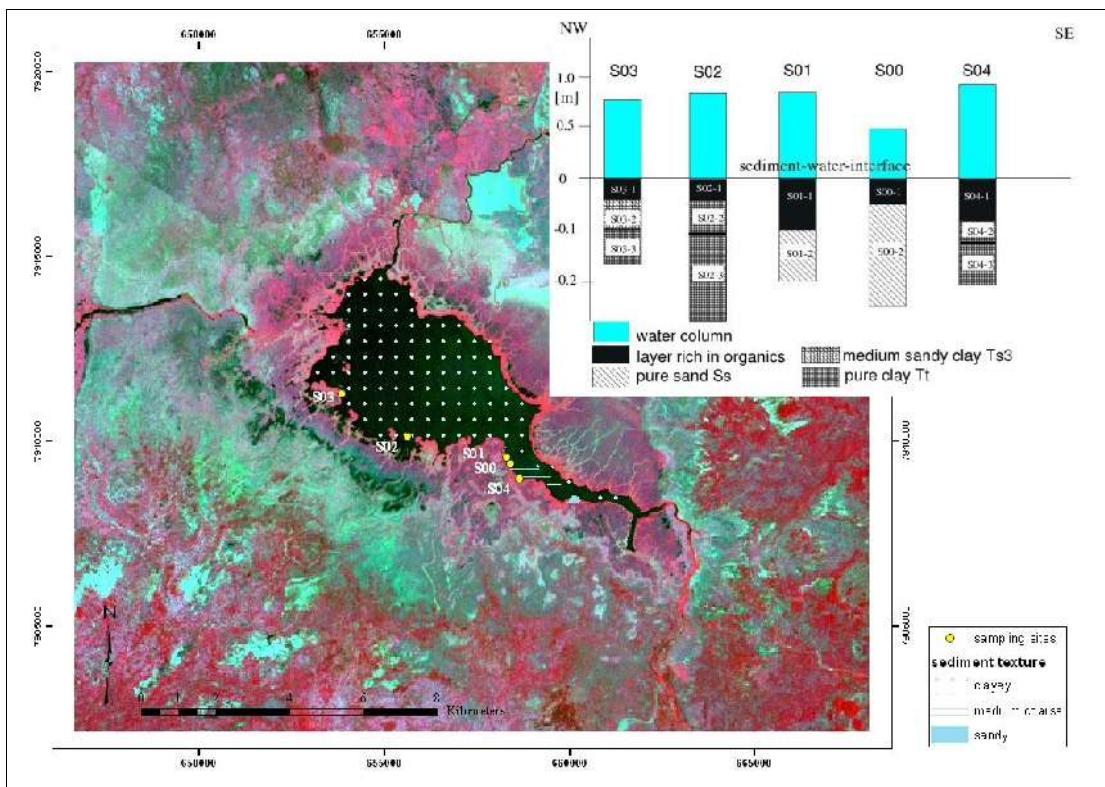


Figure 54: Location and appearance of the sediment cores at Lake Urema, sediment distribution after Januariro (2004), warden of the National Park, background picture Landsat ETM+ 4/3/2, 12/30/2000, image stretch by standard deviation ( $n=2$ )

All sediment cores show a dark brown to black organic rich top layer of 4 to 10 cm thickness. It is characterized by a mouldy smell and a mushy, liver like consistency due to a high water content and the richness in decomposed organic matter. Except some (fine) plant roots it is poor in unbroken detritus. Under the magnifying glass the matter appears to be composed of tiny light loose particles. The characteristics described here are typical for Gyttja, a coprogenous subhydic sediment containing inorganic precipitates, minerogenic matter and particulate organic matter [WETZEL, 2001]. Its theoretical organic carbon content is less than 50% but was not determined. Gyttjas can be found in well aerated, nutrient rich limnic systems [SCHEFFER, 2002].

Three types of sediment texture can be distinguished among all mineral samples.

Below the organic sediment layer the cores S00 and S01 were assigned to **pure sand Ss** (predominant grainsize 0.2-0.63 mm). The other samples were either assigned to **pure clay Tt** (S02, S04, S03-3) or to **medium sandy clay Ts3** (S03-2). Grains bigger than 2 mm were barely observed. Only in the upper part of the samples S01 and S03 some rounded grains accounted for less than one mass% of the whole sample.

Figure 54 shows a first estimation of how these sediment types are distributed over the lake.

The silt-clay fraction and the sand fraction were separately analyzed via XRD. The XRD results were set in ratio to the proportion of the clay+silt fraction and the sand fraction in the whole sediment sample.

Eight minerals were detected via XRD: quartz, kali feldspar, plagioclase, hornblende, goethite, muscovite, smectite and kaolinite. The latter three were found mainly in the silt-clay fraction (except muscovite in S04) while the others were mostly present in the sand fraction.

In sample S04 muscovite was slightly higher or equally represented in the sand fraction than in the silt-clay fraction.

According to the results of the XRD, the dominant mineral components in S00 and S01 were well-rounded quartz minerals (57 and 63 mass%), kali feldspar (16 mass%) and plagioclase (15 and 16 mass%) [Figure 55]. The clay minerals smectite and kaolinite accounted together for 3 to 5 percent. Hornblende and muscovite were present with 2 to 3 percent each.

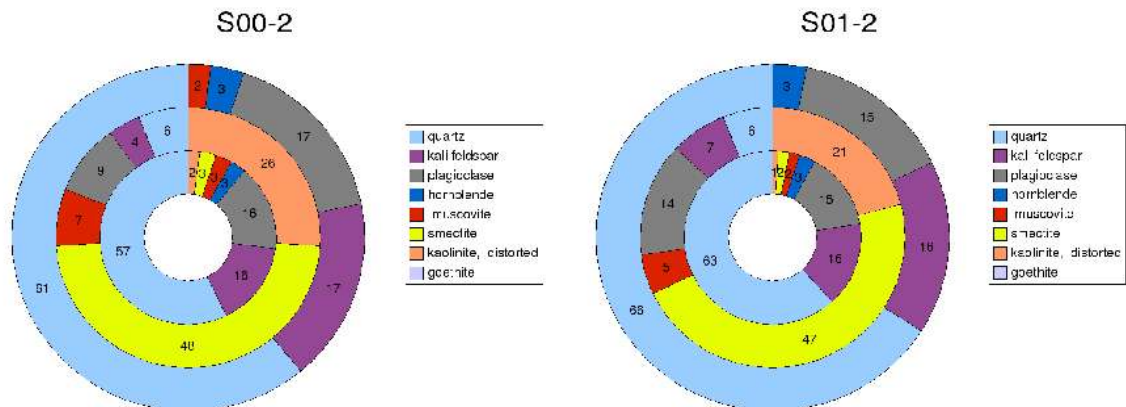


Figure 55: Mineral composition of S00-2 and S01-2 according to the results of XRD, outer segment = sand fraction (0.063-2 mm), middle segment = clay and silt fraction (<0.002-0.063 mm), inner segment = whole sample, figures rounded to whole numbers

S02 and S04 were characterized by a massive, heavy, very dark gray/black (S02) to greenish gray/black (S04) sediment with a clayey texture and shiny cutting areas. At both sample sites there was a transition layer between the organic rich top layer and the massive clayey layer. In S02 this transition zone (S02-2) measured 7 cm, in S04 (S04-2) 4 cm. It showed both a decrease in water content and organics. In comparison to the underlying layer (S02-3, S04-3) it was more rooted through and stronger inhabited by worms as worm tunnels indicated.

Signs for oxidizing conditions, e.g. rust brown spots (diameter 4-6 mm) or streaks (in worm tunnels) were observed especially in S02.

Because of the similarity of S02 and S04 with respect to their sediment texture, an analysis via XRD was only conducted for the sample S04-2 and S04-3 [Figure 56].

In contrast to the other samples, S04 had a distinct proportion of clay minerals in the sand fraction. According to the personal comments of the analyzing laboratory [KLEEBERG, 2004] cementation through goethite (11 and 18 mass%) and potentially amorph iron oxides are responsible for this characteristic.

The main difference between the upper layer S04-2 and the lower layer S04-3 is visible in the sand fraction. While in S04-2 quartz dominated with 33 mass%, in S04-3 smectite was the most common mineral with 27 mass% (quartz 18 mass%).

The mineral composition of the silt-clay fraction was similar in both samples: less than or equal to 5 mass% of quartz, kali feldspar, plagioclase and muscovite and smectite between 43 and 45 mass% of kaolinite and smectite each.

The mineral composition of S04-3 could not be referred to the whole sample due to an error in the grainsize distribution. It can be assumed that the figures are similar to those of S04-2.

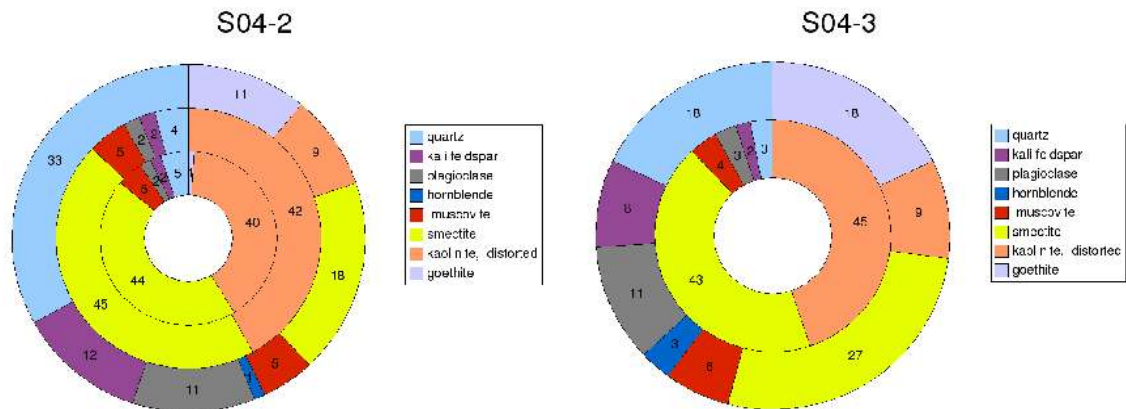


Figure 56: Mineral composition of S04-2 and S04-3 according to the results of XRD, outer segment = sand fraction (0.063-2 mm), middle segment = clay and silt fraction (<0.002-0.063 mm), inner segment = whole sample, figures rounded to whole numbers

Sample S03 is the only one where a remarkable difference in the sediment texture between the two layers S03-2 (6 cm) and S03-3 (7 cm) was observed. The upper layer was specified as medium sandy clay, the lower layer as pure clay. This difference is also reflected in the mineral composition [Figure 57]. S03-2 had a higher proportion of quartz in the sand fraction (64 mass%) than S03-3 (56 mass%). An extrapolation over the whole sample displays significant differences (S03-2: 38 mass% of quartz; S03-3: 8 mass% of quartz) due to the bigger sand fraction in S03-2. This is also alienable to kali feldspar.

Consequently, the larger clay fraction in S03-3 resulted in the double concentration of smectite and kaolinite in the whole sample in comparison to S03-2. S03-3 showed the highest content of plagioclase among all samples. Observations of few single spot-like rust signs indicated oxidizing conditions in sample S03.

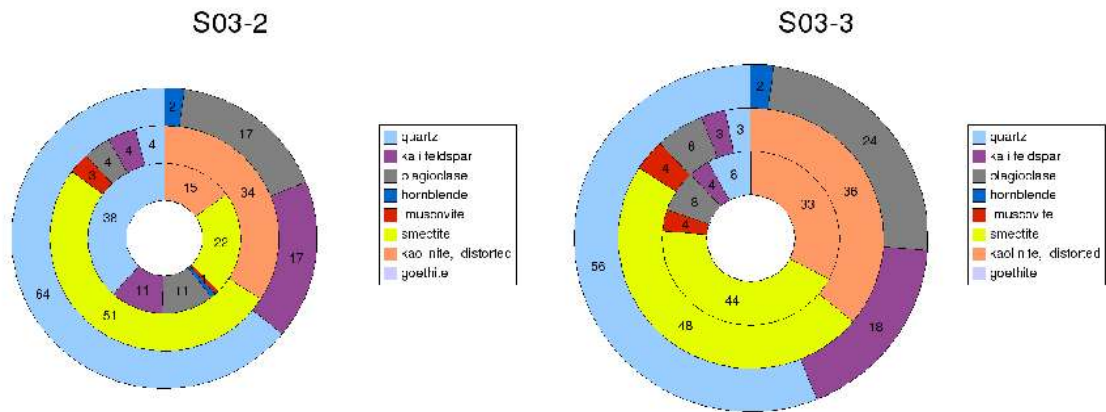


Figure 57: Mineral composition of S03-2 and S03-3 according to the results of XRD, outer segment = sand fraction (0.063-2 mm), middle segment = clay and silt fraction (<0.002-0.063 mm), inner segment = whole sample, figures rounded to whole numbers

Figure 58 summarizes the results of the mineral analyses. Two types of sediment were differentiated. S00 and S01 were dominated by their sand fraction. The sand fraction contained mainly quartz, kali feldspar, plagioclase and hornblende. S02, S03 and S04 were characterized by a clay texture and contained mainly kaolinite and smectite. S03-2 can be regarded as a transient stage between the two sediment types.

Total carbon (TC) in the sediment samples comprised basically Total Organic Carbon TOC. The concentration of Total Inorganic Carbon (TIC) was below the detection limit. Lowest concentrations of TOC were measured in the sandy samples (0.18 mass% and 0.14 mass% in S00-2 and S01-2), highest values in the clayey samples (about 2 mass% in S02 and S04) and medium values around 1 mass% TOC in S03 (medium sandy clay on top of pure clay).

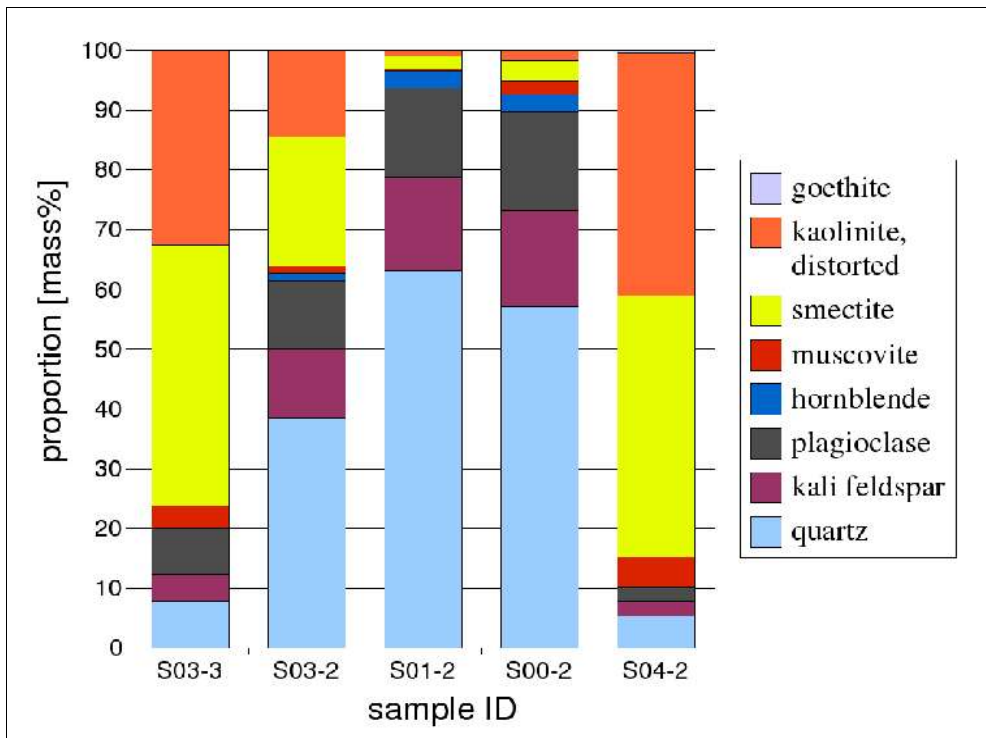


Figure 58: Mineral composition of the whole samples

Table 13: Concentration of Total Organic Carbon (TOC)

	S00-2	S01-2	S02-2	S02-3	S03-2	S03-3	S04-2	S04-3
TOC [mass%]	0.18	0.14	2	1.81	0.81	1.4	2.16	2.08

### 6.6.2 Siltation

Visual inspection of all available satellite images was conducted with respect to the development of new islands at the Lake Urema.

There were some rather small islands detected on the majority of the satellite scenes. They owe their existence to a falling water level. In 1993, the lake's extent was bigger than in most other years. Consequently the islands south of where the lake starts to narrow had disappeared. Small islands, less than five hectares in size, were visible in the southwestern part of the lake in December 2000 and at the Mucombeze inflow in May 1995. They can be composed of aquatic plants or represent dry falling lake bottom colonized by grasses or herbs.

## 6.7 Vegetation investigation

### 6.7.1 Transects

Six transects (V01, V02, V03, V04, V06, V07) along channels, presumably created by hippopotamus or elephant, were investigated according to their floristic species composition. Their location is shown in Figure 39. The transect length varied between 20 and 300 m, starting in the pelagic zone or lower littoral and ending in the seasonally inundated floodplain grassland.

In V07 the area between 0 and 50 m distance from the open water was not accessible. It is assumed that this region is similar to V06 and thus its species composition was adopted from V06.

The transects (exemplified in Figure 59, Figure 60, Figure 61) cover the following zones (notation of zones after WETZEL (2001)):

1. Pelagic zone (free open water)
2. Lower infralittoral with dominance of submerged aquatics
3. Middle infralittoral with dominance of floating aquatics and rooted aquatics with floating aerial parts
4. Upper infralittoral with dominance of rooted aquatics with floating aerial parts and emergent aquatics
5. Floodplain grassland interspersed with shrubs and trees

#### 1. Pelagic zone

Some rafts of *Eichhornia crassipes* were detached from the littoral and dislocated by wind and currents.

#### 2. Lower infralittoral

*Ceratophyllum demersum* was the dominant species within this zone. It was found in all transects with a coverage of up to 5 (V02), normally 1 to 2. The extension of this zone was on average 2 to 4 m (V01, V03, V04, V06). In V02, a transect along a path used by fishermen, the species was still detected at a distance of 12 m from the beginning of the littoral zone.

During the period of investigation it became obvious that this species was expanding over the lake. Additionally, the water turbidity was increasing, potentially correlated with the distribution of seeds of *Ceratophyllum demersum* or other aquatics [web\_15].

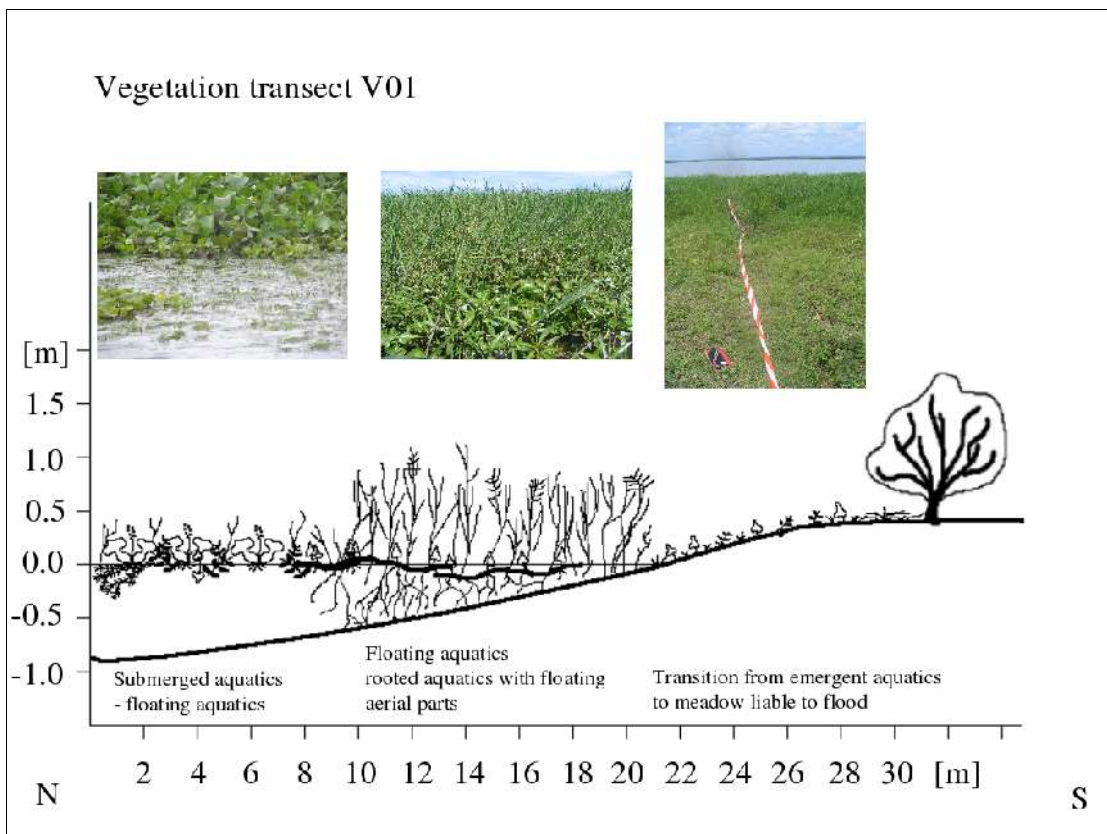


Figure 59: Vegetation transect V01 (photos: Beate Böhme)

### 3. Middle infralittoral

The zone of floating aquatics was characterized by the dominance of *Eichhornia crassipes*. Single individuals or small groups of *Azolla nilotica*, *Trapa natans* and *Pistia stratiotes* were observed in other parts of the lake (e.g. the inflow region of the Mucombeze River), but not represented in the transects. The middle infralittoral flanked the zone of submerged aquatics. The height of vegetation seldom exceeded 1 m.

*Eichhornia crassipes* formed populations with coverages up to 5 (V01).

### 4. Upper infralittoral

*Alternanthera sessilis* and *Ipomoea aquatica* were found between the floating aquatics as well as in the moist floodplain grasslands. *Cyperus pectinatus* and *Cyperus difformis* represented the group of sedges in the investigated transects. The vegetation height seldom exceeded 0.3 m.

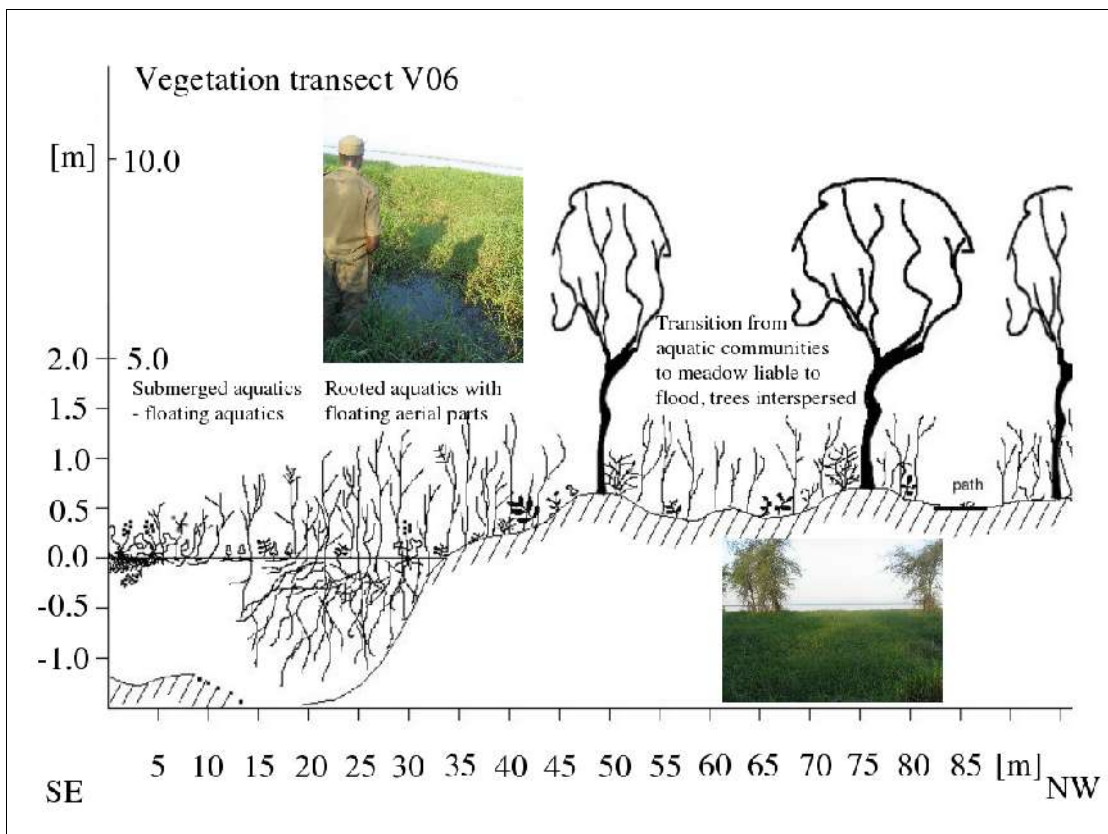


Figure 60: Vegetation transect V06, tree layer linked with inner scale (photos: Beate Böhme)

##### 5. Floodplain grassland interspersed with shrubs and trees

*Echinochloa pyramidalis* was distributed over major parts of the transects with varying coverages. In V01, V02, V03 and V06 this species was becoming dominant (coverage bigger than 4) at a distance between 6 to 10 m from the open water surface. In V04 this was already observed at a distance of 3 meters. With the dominance of *Echinochloa pyramidalis* the height of vegetation increased to over 1 m.

Dry ground began at varying distances from the open water: in V01 at 21 m, in V02 at 12 m, in V03 at 7.5 m, in V06 at 28 m and in V07 at approximately 50 m.

The transects V06 and V07 covered not only the infralittoral but also the zone of temporary inundated regions. Some shrubs and trees were interspersed into the floodplain grassland as groups or single individuals.

*Mimosa pigra?* was present in the shrub layer, while *Faederbia albida* (V06, V07) and *Kigelia africana* (V07) grew in the tree layer to a height of 15 m at dry sites. A flood mark at one individual of *Faederbia albida* was observed at a height of 0.65 m above ground.

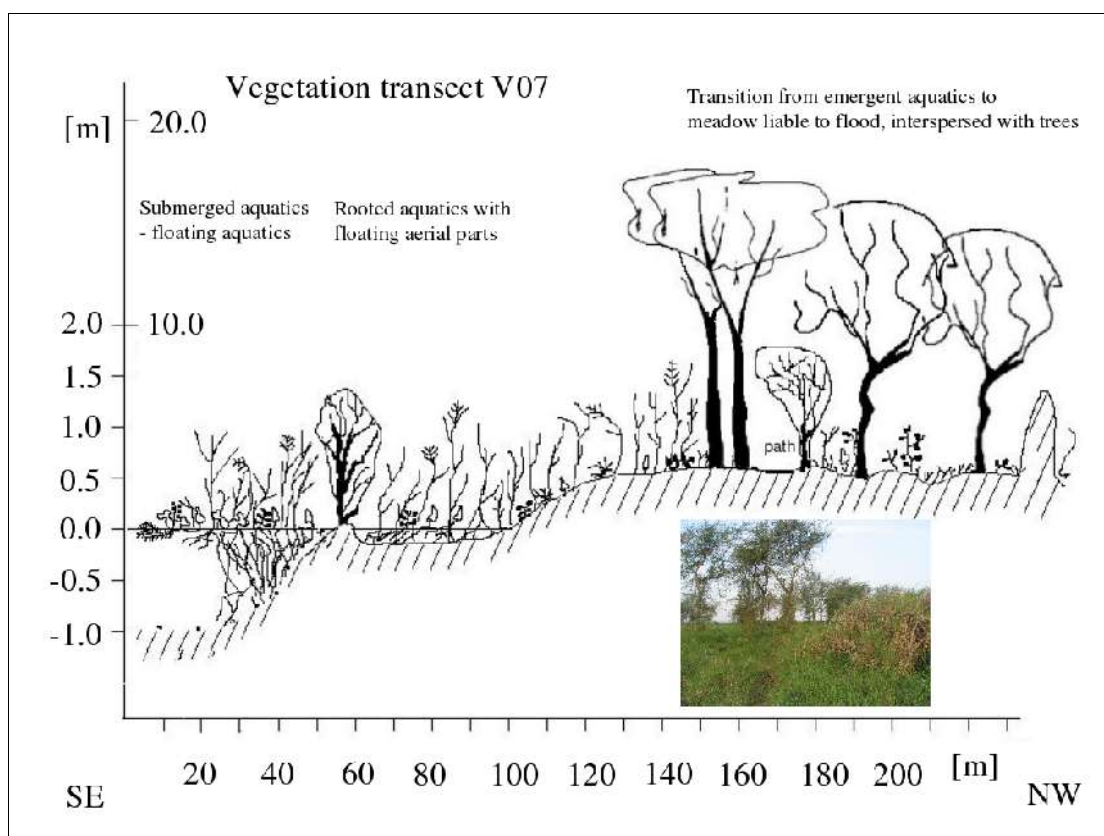


Figure 61: Vegetation transect V07, tree layer and termite hill (right image border) measured at inner scale (photos: Beate Böhme)

The paths of hippopotamus and elephant form a microrelief around the lake with differences in height of 0.5 m in the sample transects. They are partly filled with water and link aquatic and terrestrial habitats. *Ipomoea aquatica* grows mainly on the bare ground around the paths of elephant in V06. The ground coverage of this herb was mostly smaller than 50%.

### 6.7.2 Reference sites in the floodplain around Lake Urema

Reference sites are obligatory for the performance of a supervised classification (chapter 5.1.2.3). Due to limited accessibility of the floodplain grasslands and due to limited logistic facilities only a small part of the floodplain grasslands around Lake Urema was inspected.

In doing so six reference sites northwest of Mira Hippo were mapped. They represent the following vegetation classes according to the classification scheme of CUNCLIFFE (2004) and demonstrate the heterogeneity of what is referred to in general as floodplain grassland:

- Floodplain wetland – moist grassland
- Floodplain grassland to open palm-*Acacia* woodland
- Floodplain aquatic vegetation
- Floodplain open water

A flight over Lake Urema gave the chance to get a much better overview of the floodplain grasslands.

## **6.8 Fisheries**

According to personal comments from JANUARIO (2004), warden of the Gorongosa National Park, the following species of fish were identified to be living in Lake Urema.

- Sharptooth catfish (Electric catfish)
- Banded tilapia
- Redeye labeo
- Rock catfish
- Tigerfish
- Cornish jack

At least one species of turtles inhabits the lake.

- Serrated hinged Terrapin

About 300 fishes from the catches are sold weekly, mainly Rock Catfish, but also Cornish jack and Banded tilapia. Fresh fish is only sold to Muanza, which is at about 30 km distance from the lake. Gutted and smoked fish is sold mainly to Muanza, Beira and Mafambisse. The fish is caught with nets and spears from dugout canoes.

The fishermen at Lake Urema have been fishing there for several generations. Therefore they are supposed to know the lake and its ecology very well. They reported an increase in Rock catfish population since 1998 until now. In contrast the population of Banded tilapia was decreasing. The number of caught fish seems to have diminished to almost half of what was obtained in 1998. The fishermen attribute this decrease in population to the influence of drought since 1998. Rock catfish prefers small, shallow water whereas Banded tilapia prefers broader, cooler water and that makes them more susceptible to drought than Catfish.

## 7 Discussion

### 7.1 Evaluation of methods

#### 7.1.1 Remote Sensing and GIS

The delineation of the catchment area and the extraction of the river network is on the one hand controlled by the accuracy and the spatial resolution for the available DTM and on the other hand by the threshold values used in the WTRSHED module in PCI Geomatica [JENSEN & DOMINGUE, 1988]. The vertical resolution of the SRTM data is one meter. This **resolution** can be already critical in areas with small elevation differences such as at the floor of the rift valley. For the modeling of the drainage network a threshold of 5000 cells was used. Generally, the density of the network increases as the threshold value decreases.

The calculation of the **water volume** for the flood event in May 1997 can be only as accurate as the topographical data from SRTM are. Own measurements with a Trimble DGPS gave an elevation of 18.69 m a.s.l. (vertical precision 0.862 m)<sup>13</sup> for a site close to the lake while the SRTM data showed an altitude of 23 m a.s.l. The difference of more than 4 m between these two results probably arises from inaccuracies of the SRTM data. Yet, their overall accuracy was sufficient for the tasks to be solved in this study.

Using a **supervised classification** for the delineation of the open water surface of the Lake Urema and the floodplain grasslands was an appropriate approach. Extracting the lake's contour with a threshold for the **NDVI** was also feasible. The lake's extents from the NDVI were mostly larger than those extracted with the classification procedure. The results of the supervised classification are supposed to be more reliable because the definition of an overall boundary value for the NDVI is too strict, especially when the multi-temporal image dataset is not radiometrically normalized. This constrains a direct comparison of gray values from different images. A normalization is recommended by MUNYATI (2000) in his multi-temporal remote sensing study on the Kafue Flats, Zambia.

The **residuals** of the geometric registration of the satellite scenes were smaller than 2 pixel (in Landsat TM, pixel size 30 m x 30 m). Ground control points were mainly road junctions as well as river bends. Residuals smaller than two pixel were barely achievable because the 1:50 000 topographical maps were from 1960 (the 1:250 000 were from 1997/98) and many roads and river courses have changed since then. Therefore, variations of the lake's extent can not be detected with an accuracy better than two pixel.

---

<sup>13</sup> real-time corrected, location 658409.838, 7909395.8600; 9/14/2004, 03:48:12PM

In the course of this study the floodplain grasslands around Lake Urema were regarded as a more or less homogeneous unit. CUNCLIFFE (2004) in accordance with TINLEY (1977) and own observations demonstrated the diversity of the Urema Floodplain ecosystem.

The use of a **Tasseled Cap Transformation** on satellite imagery produces images with three channels which can be interpreted as Brightness, Greenness and Wetness/Yellowness. This approach has proven to be suitable for the monitoring of the ecological responses of the floodplain grasslands. The Tasseled Cap Transformation is sensitive towards atmospheric influences. Therefore an atmospheric correction prior to the transformation process is recommended. For the Landsat TM scene from 09/1995 no haze correction was conducted by ATCOR2. Therefore it is possible, that the Greenness values are lower than in the other years.

It has to be kept in mind that some of the satellite scenes had gaps in their spectral coverages due to missing or not assignable bands. Therefore the procedures NDVI and Tasseled Cap Transformation could not be applied on all images ahead of the classification process. These gaps also prevented the extraction of the class “floodplain grassland” through supervised classification of the Landsat TM scene from 1996. The Landsat MSS scene (1979) did not allow a distinct delineation of the floodplain grassland.

Elaborate pre-processing of the data would possibly have reduced the described error sources. However, for the purpose of this study the applied procedures were sufficiently accurate.

The generated **ASTER DTM** had a good relative quality but was too erroneous for absolute height measurements in the flat terrain of the rift valley floor. It has to be proven whether the collection of additional Ground Control Points (GCPs) and Tie Points will improve accuracy.

### **7.1.2 Field sampling and mapping**

The major constraints for the field work were the simple sampling methods on the one hand and on the other hand the limited logistic facilities and the available time.

**Sediment coring** was limited to the shallow parts of the lake close to the shoreline and therefore may not be representative for the rest of the lake. However, information from local people confirmed the widespread distribution of clayey sediments over the lake. It would have been desirable to sample the sediments deeper than 30 cm but this was not possible with the available equipment.

**Vegetation analyses** were restricted to paths of hippopotamus, elephants and one of fisherman because an abundant population of crocodiles is inhabiting the lake. Therefore, the vegetation transects were located at somewhat disturbed sites (especially V02 by fishermen). It was attempted to avoid the investigation of the vegetation close to the path. Fragmentary plant species lists result from the lack of appropriate field guides.

The reference sites for the supervised classification were limited to the area southwest of the lake because of limited time and accessibility. Reference site 4 is not really representative for pristine floodplain grassland. By its even-aged stands of *Abutilon* sp. it was identified as secondary growth on fallow fields (in accordance with observations of TINLEY (1977)). The final flight over the lake gave a better overview over the extension of the floodplain grasslands.

The results of the **bathymetric survey** have a horizontal resolution of about 2 m. At least one additional depth profile perpendicular to the other four profiles should have been done. For a satisfying modeling of the lake basin more depth measurements in between the four profiles would have been necessary.

The methods related with the **hydrology and hydrochemistry** are discussed in the next section.

### 7.1.3 Hydrology and hydrochemistry

The calculation of the **water balance** of Lake Urema for the period of investigation was based on several assumptions and simplifications and is therefore more an estimation than an exact number. Some uncertainties are as follows:

- The flow measurement at the Vunduzi River was associated with some uncertainties as the river cross-section was very inhomogeneous. Only one measurement was carried out during the period of investigation. It is conjecturable that not all water of the Vunduzi River will feed the lake. A part will get lost on its course, such as by seepage or evapotranspiration. Possibly, other tributaries than the Vunduzi River delivered water to Lake Urema at that time but were not investigated.
- The available current meter was not calibrated and probably not sensitive enough for discharge measurements in the Urema River.
- The data for the evaporation are from more than 30 years ago. Possible climate changes since then could have caused changes of the amount of water lost by evaporation. Additional evapotranspiration from the floodplain grassland may not be disregarded.
- Subsurface flow and groundwater seepage were disregarded due to the lack in data.
- Precipitation data for the period of investigation did not always agree with own observations. Several times rainfall was noted at Lake Urema but not at the climate station in Chitengo.

The runoff factor of 7% for the Urema and the Nhandugue catchments, given in SWECO&ASSOCIATES\_I (2004), has to be adopted carefully. Water storage in the lake and the surrounding floodplains was not sufficiently incorporated in the modeling. However, for this study the figures given in SWECO&ASSOCIATES\_I (2004) were used.

Concentrations of **nitrate, ammonium, sulphate and phosphate** were mostly below the detection limit of the measurement device. Determinations of other water constituents, such as of dissolved silicic acids, were not conducted during the field investigations. Concentrations of dissolved silicic acids are generally high in tropical freshwater [WETZEL, 2001] and should therefore be a part of the water analysis.

As some of the major ions (nitrate, sulphate, lithium) were not detectable in the unaltered water sample, enrichment procedures (by evaporation) were applied. Comparing the concentrations of calcium and magnesium before and after the enrichment, discrepancies of up to 550% were observed and ascribed to the precipitation of carbonates. Therefore the results from the IC measurements of the unaltered samples were used for these two ions. Lithium and sulphate concentrations were still very close to the detection limit after the enrichment and results for these ions are not reliable.

#### **7.1.4 Sediment analyses**

According to SCHLICHTING et al. (1995) an error of analysis smaller than 3% is acceptable for the determination of grainsize distributions. The errors for the samples S02 and S04 were about 4%, the errors for the other samples below 3%. However, the error of about 4% did not affect the final declaration of the samples as pure clays.

#### ***7.2 Does Lake Urema undergo changes?***

MERCIER et al. (2002) gives an overview of geophysical processes that may result in lake level height fluctuations of continental lakes. These are changes in water temperature or composition, surface pressure changes, water circulation processes, wind-driven events and tides. However, the importance of these factors is supposed to be negligible for African lakes. Instead, tectonic processes, such as earthquakes, are considered to be more important. Even more attention is paid to the variability of precipitation regimes and evaporation conditions over pristine lakes and their catchment areas.

Already BURLISON et al. (1977) attempted to solve the question whether a drying up of the area of the Gorongosa National Park occurred. A flow reduction of the perennial Vunduzi River in the Park, the increasing drying up of annual rivers in the dry season, a reduction of the flooding period during the rainy season and a lowering of the water table were indications for such a development. The authors discussed climate and land use changes, changes in the flooding between the Urema and Zambeze catchments due to the closure of the Kariba dam on the Zambeze (1958) and seismological activity as possible reasons. All these factors seemed to contribute to the drying up, but no ranking of their importance was given by the authors. Rainfall changes in the catchment area seemed to have only temporary effects due to “cyclical variations in precipitation patterns.”

Following, the results of own investigations on the current state of Lake Urema in the dry season 2004 and its development over the last 20 years are presented.

The lake's extent as it was derived from satellite images did not show any trend in the period between 1979 and 2000. Already slight fluctuations in the lake level height are supposed to cause considerable variations in the lake's extent due to the very flat surrounding. Thus, the conclusion is drawn, that Lake Urema did not undergo large fluctuations of the lake level height between 1979 and 2000. The standard deviation of the lake's extent (from classification) was 2.8 km<sup>2</sup>, the average lake size 20.5 km<sup>2</sup>.

On the topographical map from 1960 (DINAGECA) Lake Urema has an extent of only 7.9 km<sup>2</sup>. This figure is not plausible because Lake Urema should then have increased by 17.2 km<sup>2</sup> from 1960 to 1979. Between 1979 and 2000 it did not undergo such extreme changes. The lake's extent showed similar dimensions when different methods were applied to extract the shoreline (NDVI, supervised classification). Thus the results are considered to be consistent and reliable.

Unfortunately, the relation between the inter-annual variability of precipitation and the lake's extent could not be evaluated due to the lack of precipitation data for this period. However, it is known that Mozambique experienced several El Niño/Southern Oscillation (ENSO) events in the last twenty years: e.g. a warm phase event with severe droughts in 1991-92 and in 1994-95 [EASTMAN et al., 1996] (for definitions of ENSO, cold and warm events see web\_19). They were not reflected by the lake's extent.

In May 1997, Lake Urema had five times its average size. The water surplus equals to three percent of the modeled annual precipitation in the catchment area (SWECO&ASSOCIATES\_I, 2004). The sudden rise in the lake level height and the extent of Lake Urema can be associated with three cyclones which have caused extensive flooding in Mozambique in the rainy season 1996/1997. This is visible in the interpolated, estimated rainfall diagrams from NOAA/CPC - USAID/FEWS - USGS/EDC for the period 1993 to 1998 [Figure 62] [web\_6].

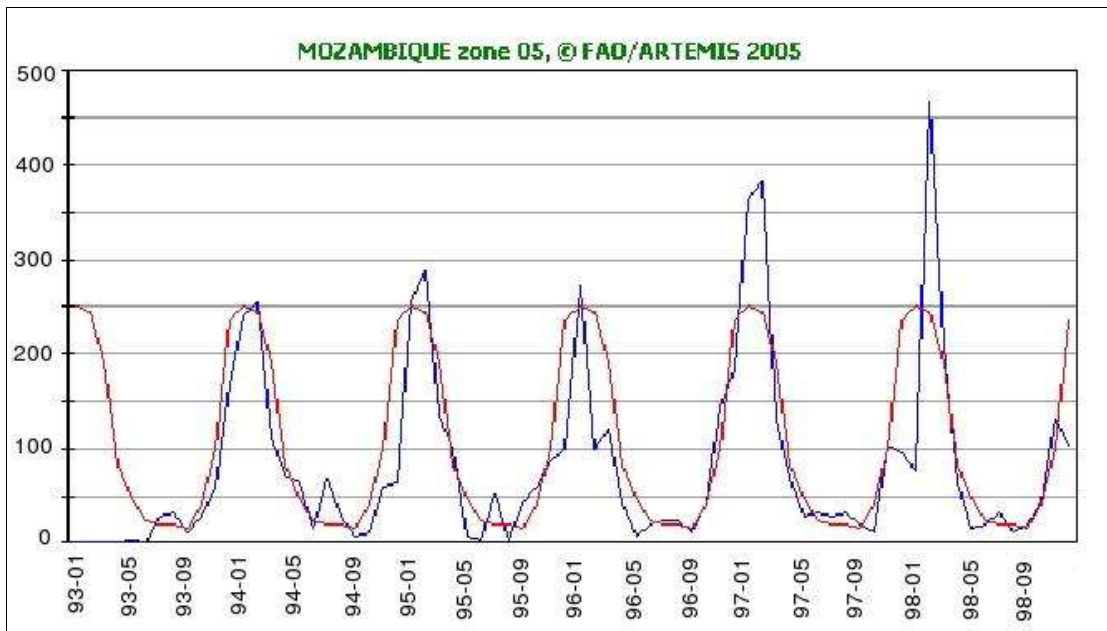


Figure 62: : Interpolated, estimated rainfall for climate zone 05 for the period 1993 to 1998, from web\_6, red line = average over period; blue line = measured rainfall in selected period

A period of investigation of 20 years is probably too small for the discussion of climate driven changes of the extent of Lake Urema. SWECO&ASSOCIATES\_I, 2004 discuss: “21 years of data on river runoff in southern Africa is, however, generally too short to give reliable long-term flow characteristics. The reason is that the region suffers from clear cycles in the climate where wet and dry periods alternate. Normally at least 30 years are therefore considered to be required for good estimates of e.g. mean annual runoff.”

The intra annual variations of the open water surface in the years 1994, 1995 and 2000 were less than one square kilometer. Yet, among the available scenes there was none from the peak of the rainy season (December to February) which could demonstrate the maximal extent of the lake.

In the following chapter control mechanisms for the hydrological regime of Lake Urema beside of climatic reasons are discussed.

### ***7.3 Which factors influence the hydrological regime of Lake Urema?***

#### **7.3.1 Neo-tectonics**

Seismic activity is present in the catchment area of Lake Urema. Four shallow earthquakes were recorded close to the lake and the Urema River in the 1980s but no evaluation of possible consequences was done. Neo-tectonic movements *could* play a role for the hydrological regime of the lake, e.g. through landslides and spillage, but no evidences are at hand. The presence of hot springs proves the seismic activity of the rift.

### 7.3.2 Morphology and Sedimentation

Its origin makes Lake Urema to a kind of Reservoir Lake which owe their existence per definition to an “impounding structure” [WETZEL et al., 2000]. The alluvial fan of the Pungoe River is this impounding structure in the study area. It dams up the drainage from the adjacent rift escarpments and the rift floor to form Lake Urema. Only a small outlet is left for the lake's drainage. This “bottleneck” is controlled by the fan of the Muredeze River which originates at the Cheringoma Plateau. The term “alluvial plug” [TINLEY, 1977] describes this circumstance adequately. Other alluvial fans limit the Urema Basin from the east, north and west. As illustrated during the anomalous flood event in May 1997, these fans are both a morphological barrier for the extent of the lake and a natural dam, controlling its outflow.

The morphology of reservoir basins is typically characterized by a detritic drainage system and a narrow, elongated form of the lake [WETZEL, 2001]. This is true for Lake Urema [Figure 25]. A shoreline development significantly bigger than 2 is representative for flooded river valleys [WETZEL et al, 2000]. This parameter amounts to 3.1 for Lake Urema.

Due to its low location on the rift valley floor, Lake Urema serves as a local base level for erosion and deposition (in accordance with TINLEY, 1977).

From the size and the slope of alluvial fans one can draw conclusions about the size of the stream itself, its load and thereby the intensity of weathering in its catchment area [AHNERT, 1998]. Large fans such as those from the Pungoe, Nhandugue and Nhampasa are formed where much mechanical weathering in the catchment occurs and much bedload is delivered.

The input of sediments from the rift escarpments plays obviously a major role for the existence of Lake Urema and the floodplain ecosystem. Therefore, a bathymetrical survey of the lake's basin as well as sediment analyses were conducted to get an idea of the sedimentation pattern.

Two sediment textures were distinguished. These are on the one hand pure sand and on the other hand pure clay. One sample shows a transition type. The Hjulström diagram (in AHNERT, 1998) provides estimations of flow velocities which enable erosion, transport or deposition of particles of a certain diameter. The critical velocity for the erosion of particles of 0.002 mm diameter (clay) is approximately 100 to 240 cm/s. Transport occurs at velocities below that value. For deposition of clays water has to stagnate. The sand fraction with diameters between 0.2 and 0.63 mm can be eroded at velocities above 15 to 30 cm/s. The critical velocity for deposition is about 1.3 to 4.5 cm/s. Sediment transport occurs between these boundary values. The widespread distribution of clayey sediments over large parts of the lake and the occurrence of sandy sediments in the narrowing part of the lake towards its outflow suggest a temporally and spatially constrained pattern of transport and deposition.

The deposition configuration and types as well as the incised lake floor (shown by bathymetric profiles) concur with the hypothesis that the axial part of the lake is characterized by a more energetic flow and the lateral areas by calm conditions. Web\_14 (2004) recommend a length-to-width-ratio of minimum 2:1 for improving the sediment trapping efficiency of impoundments (Lake Urema: ratio 2.5:1). The functioning of Lake Urema as a sediment trap is proven by the increasing transparency towards the lake's outflow controlled through in situ measurements of the Secchi-disc transparency. McCARTHY et al. (1991) described a decrease in turbidity downstream of Dxhereaga lediba (lake) in the Okavango Delta resulting from sediment settling, although this lake is much smaller (diameter approximately 500 m) than Lake Urema.

The underlying geology and the soils in the catchment area have to be included into the interpretation of the mineralogical composition of the sediments.

Free carbonates were not detected in the samples. The dominant minerals in the sandy samples were quartz, kali feldspar, hornblende and plagioclase while kaolinite, smectite and muscovite were dominant in the clayey samples.

**Quartz** components, **mica** and **feldspars** are supposed to originate from the gneisses and migmatites of the Bárue formation (introduced e.g. through Nhandugue River, in accordance with TINLEY, 1977) or from the gabbros and granites of the Gorongosa Mountain. In soils which developed on acidic igneous and metamorphic rocks, quartz, orthoclase and muscovite are likely to occur because of their stability towards weathering. Subsequently these minerals will be recovered in river and lake sediments. This suggests that the constituents of the samples S00 and S001 originated from the granites and gneisses west of the rift valley.

**Goethite** probably results from iron-oxide enriched ferrallitic/fersiallitic soils of the Gorongosa Mountain or the Midlands.

Under tropical conditions **kaolinite** and **smectite** result mainly from the intensive weathering of feldspars [JASMUND, 1993]. With increasing intensity of weathering of primary minerals, silica is more and more lost while new formed clay minerals dominate. Three phases of residual soil development in tropical soils can be distinguished [FOOKES, 1997]. The first stage of this process are fersiallitic soils (occurring in the Midlands according to TINLEY, 1977). Quartz, alkali feldspars and muscovite remain unaffected, released silica and bases are retained in the soil profile. The main new clay mineral is smectite, especially where drainage is impeded. The second phase are ferruginous soils and the third phase are ferrallitic soils (as described for the Gorongosa Mountain in TINLEY, 1977) where all primary minerals – except quartz - are weathered and much of silica and bases are removed. The remaining silica build up kaolinite with alumina.

In the tropics, montmorillonite (a subtype of smectites) will form instead of kaolinite in slucks or basins with insufficient drainage [JASMUND, 1993]. Such conditions are present at the floor of the rift valley with its small gradients.

With decreasing silica concentration smectite will turn to kaolinite. According to TINLEY (1977), the clayey soils of the rift valley floor (Vertisols) contain mainly montmorillonite. Smectites were very present in samples S02, S03 and S04.

The co-existence of kaolinite and smectite in the same sediment sample represents different stages of soil development or different catchment areas. It is supposed that smectites are either introduced from the vertisols of the rift valley floor or from the ferrallitic soils of the Midlands, and Kaolinite from the ferrallitic soils of the Gorongosa Mountain.

### 7.3.3 Quantity of surface water

In October 1971, TINLEY (1977) measured a discharge of 0.6 m<sup>3</sup>/s at the Vunduzi River whereas a discharge of 1.65 m<sup>3</sup>/s was estimated in October 2004. The mean outflow of Lake Urema through the Urema River in October 1956/57-1978/79 was 2.61 m<sup>3</sup>/s [ARAC, 2004]. Some efforts were undertaken to detect any outflow of Lake Urema during field investigations in the dry season 2004, but water stagnated. This can be ascribed to low water condition or/and the closure of the Urema River through sediments or vegetation. The latter was observed during field trips.

Although there was no outflow of the lake detected during that time, a non-negligible discharge of the Vunduzi River was observed. This rises the question where the water is “disappearing”.

The water balance for the dry season 2004 has to be understood as a first estimate. After temporal interpolation of all water inputs (discharge of Vunduzi River, precipitation) and water losses (evaporation) the lake level height should theoretically raise by 0.24 m in the period from September to October. Actually, the lake level height sank by 0.32 m. It is assumed that infiltration in the underground occurs, as well as the spread of surface water into the adjacent floodplain grasslands and extensive evapotranspiration. The low mineralization of the lake water suggests that an enrichment of dissolved solids through evaporation does not happen on a high level. However, the rate of 16 complete renewals per year must be considered to be too high and the estimation of two complete circulations per year from the Vunduzi discharge is more reliable. It is supposed that major circulations occur during flooding while only small circulations happen in the dry season and therefore enable the deposition of fine-grained sediment. The increasing concentrations of TDS towards the outflow of the lake suggest that there is at least a small water flow in the lake in the dry season.

OWEN (2004) emphasizes the delayed peak runoff of the Urema River in comparison to the peak rainfall which is “typical of surface water retention in wetlands and lakes and for permeable catchments that have high groundwater recharge.” In contrast to the Urema River the rivers draining the crystalline basement have a faster runoff component.

Field investigations which were carried out later in the year (in the dry season as well as in the rainy season) proved that surface water flow was little and also groundwater levels in the catchment area were dramatically low [STEINBRUCH, 2004]. This supports own observations at the Urema River and also at the Sungue River.

### **7.3.4 Water chemistry**

According to the classification system of the Ramsar Convention [web\_17] Lake Urema is a permanent freshwater lake (> 8 ha). It is supposed to be a “warm polymictic” lake which is per definition [WETZEL, 2001] characterized by frequent periods of circulation with small annual temperature variations.

However, evidences for this supposition are rare because Lake Urema was only sampled during the dry season and not over its complete depth. Stratification of the water body is supposed to be weak and of short duration due to the small area and depth of the lake, the mixing through wind and the activity of animals (crocodiles, hippopotamus).

Short term fluctuations (episodic, seasonal, inter-annual) in water column nutrient levels of Lake Urema can be generally expected from freshwater input, physical disturbance, macrophyte growth, mineralization and nutrient uptake. Therefore the sampling results from the dry season 2004 have to be understood as indications for processes but not as fixed values.

The water analyses of the Vunduzi River, Lake Urema and the Urema River show a low mineralization (20-100 mg/l TDS, 32-171  $\mu\text{S}/\text{cm}$ ), comparable to that of rainwater or poorly mineralized groundwater (100-300  $\mu\text{S}/\text{cm}$ , KÖLLE, 2003).

The concentrations of dissolved inorganic macro nutrients such as nitrate, ammonium, sulphate and ortho-phosphate in the study area were mostly below the detection limit of the measurement devices. This nature is common for freshwater ecosystems, especially when they are characterized by a high primary productivity of the surrounding floodplain grasslands. In pristine, well oxygenated systems (saturation 80-120%) more than 80% of inorganic nitrogen typically occurs as nitrate [DWAFa, 1996]. Ammonium arises from the decomposition of organic matter by heterotrophic bacteria and is contained in excretory products of higher aquatic animals. Under oxidizing conditions it is converted into nitrate (nitrification). The high proportion of ammonium in the water samples in comparison to nitrate suggests that a major part of nitrate is consumed by the vegetation during the period of growth and ammonium is relatively enriched. The higher nitrate concentration in the Vunduzi River in comparison to the central part of the lake enforces this assumption. The increased sulphate concentration at that site can also result from anthropogenic influences as local people use the river for washing.

Montaneous regions of crystalline rocks, such as the Gorongosa Massif and the Bárue Midlands, have typically low phosphate concentrations. Therefore high concentrations in phosphorous were not expected. Pristine water in RSA are below 1g/l [DWAFA, 2004]. Phosphate can be introduced in lentic systems by erosional processes because it is mainly associated with the suspended matter.

Carbon, nitrogen and phosphorous occur not infrequently in organic form in freshwater ecosystems, such as as DOC, DON and DOP [CONNELL & HAWKER, 1991]. However, only DOC was measured in the samples of Lake Urema. The major sources of organic carbon are photosynthesis by aquatic macrophytes, macroalgae and phytoplankton and terrestrial detritus.

In the Urema River (site 400), in the outflow region of Lake Urema (site 99) as well as within the littoral (site 97), DOC values were higher than in the central part of the lake and in the inflow region (sites 105, 115, 318, 402). At the sites 400 and 99, which showed little water movement, higher concentrations of DOC were related to a higher electrical conductivity (EC), a lower pH and a lower saturation of dissolved oxygen. Probably this is due to the formation of organic acids and CO<sub>2</sub> and the consumption of oxygen through decompositional processes and biochemical oxidations. The positive correlation between the saturation of dissolved oxygen and pH was statistically significant. Sites 97, 105, 115 and 318 (Vunduzi River) showed a lower electrical conductivity and a higher saturation of dissolved oxygen. This observation can be attributed to oxygen solution in the turbulent water of the Vunduzi River and the permanent mixing in the central part of the lake. In the littoral zone (site 97) oxygen saturations were increased (especially in the afternoon) due to photosynthetic activity.

Generally, the electrical conductivity increased from the inflow to the outflow of Lake Urema. Enrichment through evaporation and decomposition of organic matter are considered to be the major reasons. As the water transparency also increased towards the outflow of the lake the electrical conductivity was positively correlated with Secchi-disc transparency (pretended correlation).

The few samplings of the tropholytic zone showed that the pH and the saturation of dissolved oxygen were lower there than in the trophogenic layer. Electrical conductivity was higher. This indicates decompositional processes in the tropholytic zone.

The following section attempts to investigate the effects of the population of hippopotamus on the nutrient pool of Lake Urema. Hippopotami are described as a key species in the Urema Floodplain system [TINLEY, 1977], though their numbers have dramatically decreased during the civil war.

GREY & HARPER (2002) estimated in their study about Lake Naivasha, Kenya, a dunging rate of hippo at one per night on land. The maximum dung wet weight was approximately 8 kg. The authors assumed that a hippo ingests 40 kg biomass per night, excretes 8 kg faeces on the catchment and the remainder in the lake.

A population of 2500 hippos at Lake Urema (including direct tributaries) (November 1968, TINLEY, 1977) would have introduced 29,200 tonnes of dung into the lake annually. Nitrogen accounts for 1.5% of dung dry weight, carbon 37% (dung wet weight = 5.8 x dry weight). Consequently, the annual input of nitrogen into Lake Urema was at that time approximately 75.5 tons. Assuming a lake area of 19 km<sup>2</sup> (area of October 2000) and a water depth of 1.6 m the water body of Lake Urema comprises 30.4\*10<sup>6</sup> m<sup>3</sup> (= 30.4\*10<sup>9</sup> l). If all nitrogen was converted into nitrate (334.2 t) and no removal of nitrate occurred, the concentration of nitrate after one year should be 11.0 mg/l. A population of 62 hippos thus would rise the nitrate concentration by 0.27 mg/l.

ARMAN et al. (1975) number the nitrogen concentration of faecal of non-ruminants (e.g. warthog, hippopotamus) with 5.9 g N/kg faecal dry mass. This value was determined in the course of experiments about nitrogen-balance trials with grass fodder. Using the excretion numbers of hippos after GREY & HARPER (= 32 kg wet dung per night per individual; dung wet weight = 5.8 x dry weight), the annual nitrogen input of 2500 hippos into the lake comprises 29.7 t. Consequently the nitrate concentration after one year would have risen by 4.3 mg/l. 62 hippos would have caused a rise by 0.1 mg/l.

These nitrate concentrations are close to the detection limit of simple field measurement devices (0.5 mg/l). The influence of hippopotamus on the eutrophication of Lake Urema can be therefore disregarded. However, substantial nutrient balances must also consider nutrient sinks such as the uptake by plants.

Based on its organo-leptic properties, such as Secchi-disc transparency and color, the water of Lake Urema and Urema River can be assigned to “whitewaters” as propagated by TINLEY (1977). Values of pH of “whitewaters” should be about 6 at the peak of the dry season. Own measurements gave values of about 7. The rivers originating at the Gorongosa Mountain, such as the Vunduzi River, are classified by TINLEY (1977) as “clearwaters” with a pale green color, a high transparency and a pH between 5.5 and 6. The pH value of the Vunduzi River in the dry season 2004 was not significantly lower than the pH values of the lake as is should be according to TINLEY'S classification.

After all, the water of Lake Urema belongs to the bicarbonate type which is characterized by a CO<sub>2</sub>-HCO<sub>3</sub><sup>-</sup>-CO<sub>3</sub><sup>2-</sup> buffering system.

The majority of the analyzed parameters of the seven water samples were below or within the SAWQG (South African Water Quality Guidelines) target range for aquatic systems, irrigation water use and domestic use [DWA Fa/b/c, 1996]. Only the concentration of dissolved organic carbon was above the target range of 0-5 mg C/l (maximum 7.35 mg C/l at site 99 close to the outflow region of the lake), except for the samples 318 at the Vunduzi River and 402 in the inflow region of the lake.

The average summer inorganic phosphorous concentration as well as the concentration of inorganic nitrogen are indicators for the trophic state of a limnic system. With respect to the concentration of inorganic nitrogen Lake Urema is assigned to oligotroph systems (<0.5 mg/l) [DWAFA, 1996]. With respect to the average summer inorganic phosphorous concentration it shows eutrophic conditions (25-250 µg/l).

The comparison of historical water chemical analyses of the Urema River (in SWECO&ASSOCIATES\_VI, 2004) with actual data shows that the concentration of sulphate was significantly lower in the dry season 2004 than in the 1970s.

### **7.3.5 Groundwater fed?**

The low concentrations of major an- and cations allow to hypothesize

1. that the water feeding Lake Urema is ground water which is in contact with hardly soluble underground and/or which has a short contact time with the underlying geology because of a high permeability
2. that Lake Urema is fed by surface water.

Because of a short retention time the lake water is not significantly enriched through evaporation. The general absence of saline surface water can also be due to transpiration exceeding by far the evaporation as it was suggested by McCARTHY & ELLERY (1998) for the swamps of the Okavango Delta.

It is supposed that both water sources play a role for the chemical characteristics of the lake water.

*explanation to point 1:* Groundwater from the western rift escarpements could originate from fractures and fissures intersecting the main rift-parallel fracture system of the crystalline rocks. The quartz sands of the Cheringoma Plateau on the eastern side of the rift can form groundwater traps when they lay over a clayey subsoil (perched groundwater). This local phenomenon is described in TINLEY (1977). The seaward dip of the strata of the Cheringoma Plateau will allow preferential groundwater flow eastwards towards the sea.

Water in contact with granite, siliceous sands and well leached soils has typically a concentration of dissolved solids below 30 mg/l [DWAFA, 2004]. The catchment area of the Okavango River, taken as an example, is underlain by windblown Kalahari sands and bedrock outcrops consisting primarily of granite. Thus, its concentration of dissolved solids is typically around 40 mg/l.

The Bárue Midlands as well as the Gorongosa Mountain consist of hardly soluble material: gneiss, granite, migmatites. Sands and limestones occur in the Cheringoma Plateau. The Vunduzi River had a concentration of 22.5 mg TDS/l and the sample site 115 in the central part of the lake 100.1 mg TDS/l. These results coincide with the specifications in DWAFa (1996).

There is still the question about groundwater infiltrating through the coarse sediments at the rift flanks. OWEN (2004) draws the conclusion from historical flow data and a rainfall-runoff-modeling of the Urema River that groundwater flow and surface storage in wetlands should be responsible for the excess of runoff in comparison to rainfall in several months.

If there is a significant subsurface flow to Lake Urema, it has to be checked out whether it has the same catchment boundaries as the surface drainage basin which was modeled in the course of this thesis. Phreatic divides are particularly important in areas which are underlain by relatively permeable rock such as the alluvia of the rift valley floor.

*explanation to point 2:* The comparison of the water from the Vunduzi River with rainwater from Beira showed a similarity (e.g. electrical conductivity below 50  $\mu\text{S}/\text{cm}$ ), although this was not statistically proven due to the small amount of data. Chloride concentrations in the rainwater were higher than in the lake and river water, probably due to sea spray. Concentrations of nitrate and sulphate were significantly higher in Beira, probably due to the impact of industrial emissions.

### **7.3.6 Ecological responses of Lake Urema**

Due to the flat terrain of the rift valley floor (less than  $0.1^\circ$  seawards dipping) the tributaries originating at the rift escarpments and on the floor of the rift valley feed extensive swampy areas (floodplain grasslands), ponds and the shallow Lake Urema.

The intra-annual response of the grasslands surrounding the lake was subject of the interpretation of Tasseled Cap transformed satellite scenes providing three channels coded as Brightness, Greenness and Wetness/Yellowness. The images from 1994 and 1995 demonstrated the regression of the shoreline of the lake from wet to dry season. Following this zone is a belt characterized by high Greenness values (= floodplain grasslands). Its vitality is probably supported by a) infiltration of lake water into the underground, b) the spreading of lake water into the floodplain and c) the water retention in ponds and channels after the end of the flooding.

This zone showed significantly lower Greenness values in September 1995. This could be due to drier conditions and/or due to the lacking haze correction for this scene. Unclassified stripes in this scene, located between the open water and the floodplain grasslands, were supposed to be shallowly flooded areas (swamps). The existence of such belts is an indication for drought which would prove the lower Greenness values in September 1995.

TINLEY (1977) anticipated bush encroachment into the floodplain grasslands because of the channelling activity of hippopotamus and the resulting drainage of water holding ponds. The opposite development, diminished bush encroachment, should be expected on the long term as a consequence of the decimation of this key species. On a short term, these channels will maintain their draining function.

It is expected that the rehabilitation of the hippo population will lead to an increase in water turbidity because hippopotami churn up the sediments and keep them in suspension.



Figure 63: Hippo path in the floodplain southwest of Lake Urema close to Mira Hippo (visible in upper middle of the photo, note green belt around Lake Urema during dry season 2004 (photo: Beate Böhme)

The species composition of the littoral zone of Lake Urema can serve as an indicator for water quality. The low nutrient concentrations agree with the observation of relatively small populations of *Eichhornia crassipes*. Although this species was widely distributed over the lake it can not be regarded as an invasive species. With adequate nutrient supplies, high temperatures and irradiance levels, *Eichhornia crassipes* can spread over large areas in floodplain lakes, whereby it occludes the water surface, limits growth of phytoplankton and submerged macrophytes and ingests nutrients [CONNELL & HAWKER, 1991]. Finally, it provides large amounts of detritus when decaying and enhances the spread of schistosomiasis.

*Ceratophyllum demersum* was widely distributed in the littoral zone. It is a species that indicates neutral or alkaline water. Because of its adaptation to relatively low light intensities it can tolerate shade better than most aquatic plants which may be essential for surviving in the turbid water of Lake Urema.

A siltation process, possibly expressed through the development of islands, could not be shown on the satellite scenes. There were small islands on some satellite images visible but their presence seemed to be more dependent on the lake level height than to be the result of increasing sedimentation.

#### ***7.4 Will Lake Urema disappear?***

From the evaluation of the satellite images from 1979 to 2000, there was no trend for an increase or decrease of the lake's extent detectable. The extensive flooding in 1997 was a result of anomalous rains. The buffering capacity of the ecosystem seems to be working although it is not yet fully understood what is controlling the system.

However, two major threats – both short term and long term – have to be discussed (partly in accordance with TINLEY (1977) and SWECO&ASSOCIATES\_V (2004)):

##### 1) Sedimentation and maintenance of local base levels

Lake Urema owes its existence to alluvial fans which limit the Urema Basin. The benefit of the sediment input from the adjacent mountains can turn into a threat for the wetland system when it results in the siltation of the shallow lake due to increased sediment input from the catchment area. This could arise from increasing erosion after forest clearings. The local base level at the outlet of Lake Urema triggers whether Lake Urema will be able to keep its water or whether it will drain through the Urema River. It is supposed (in accordance with TINLEY, 1977) that at the confluence of the Urema River with the Muredeze River there is the first local base level. Under certain conditions “the Muaredzi stream [Muredeze, the author] which joins the Urema River at the lake's outlet floods into the lake and only when the lake water have reached sufficient height to cross the sill formed by the Muaredzi alluvial plug do the water reverse and flow back down the Urema River.” [TINLEY, 1977].

The second local base level is the confluence of the Urema River with the Pungoe River. A change in gradient between the lake basin and the Pungoe River will either result in accelerated or decelerated drainage. Accelerated drainage is related to an increase in gradient, e.g. when the lake's basin is filled with sediments or when the Pungoe River is deeper incised at the confluence with the Urema River [LYNAM, 2004]. The latter process could be a consequence of the construction of the Bué Maria Dam at the Pungoe River. The construction of this impoundment is a major water resources development goal for hydro power production, irrigation, increase of low floods, flood control and increase in tourism [SWECO&ASSOCIATES\_V, 2004]. The planned reservoir will have a storage capacity of 987 Mm<sup>3</sup>, an area of 67.9 km<sup>2</sup> and the dam will have a height of 70 m [SWECO&ASSOCIATES\_V, 2004]. It will act as a sediment trap and therefore will increase the flow velocity of the Pungoe River behind this construction. Faster drainage of the Pungoe River probably leads to an incision in its course and therefore to a lowering of the base level at the confluence with the Urema River.

TINLEY (1977) described that during high flooding the Pungoe River was able to dam up the outflow from the Urema catchment and therewith maintained the critical height of the lake's outlet by increased sediment accumulation. Such events would be impeded by a regulation of the Pungoe River.

## 2) Water input

As was observed during the period of investigation, the Vunduzi River which is originating at the Gorongosa Mountain, is one of the important (the only?) surface water sources for Lake Urema in the dry season. Deforestation in the catchment area could result in reduced infiltration and enhanced occurrence of flush floods, possibly limiting the water supply to the wetland system [TINLEY, 1977]. Extreme events such as cyclones, are capable to influence the water input to the wetland in both directions: drying or flooding (e.g. in 1997).

## 8 Conclusions and recommendations

The evaluation of time series of satellite images covering a period of 20 years does not indicate any shrinking or even disappearance of Lake Urema. The results from this multi-disciplinary study conclude that its extents and dynamics are largely controlled by morphological barriers buffering the drainage and in turn influence the whole ecosystem. The profiles through the Tasseled Cap transformed satellite images together with the results from the supervised classification witnessed the response of the wetland ecosystem to proceeding drying of the floodplain grasslands towards the peak of the dry season and therefore proved to be a valuable monitoring instrument.

The water feeding the lake is lowly mineralized and its retention time is supposed to be small (few months). The configuration of sediment depositions and sediment types as well as the incised lake floor (showed by bathymetric profiles) concur with the hypothesis that the axial part of the lake is characterized by a more energetic flow and the lateral areas are quiescent regions.

Many of the factors triggering the floodplain ecosystem are potent during the rainy season (erosion & deposition, turnover of water body) and should be therefore investigated at that time. However, the field work of this study was carried out in the dry season 2004 due to logistical problems associated with the rainy season. Further field studies are essentially combined with Remote Sensing and GIS.

Based on this study, further work should focus on the following points:

- **Contribution of groundwater**

Groundwater flow and the groundwater recharge rate in the catchment area should be quantified. This will enable a more reliable calculation of the water balance.

- **Hydrology in the catchment area**

A consistent nomenclature for the rivers in the catchment area of Lake Urema facilitates future work. During literature studies the occurrence of two Vunduzi Rivers and one Vanduzi River was confusing. Historical hydrological data from the Pungoe River catchment were recently evaluated with satisfying results. Future work should focus on the maintenance of existing and the establishment of new hydrometric gauging stations.

- **Siltation**

To quantify the current rate of siltation of Lake Urema two aspects should be considered, namely the **sediment delivery from the catchment area** and the **sediment deposition** in the Urema Basin.

- **Pollution**

It has to be investigated whether gold mining activity is a relevant source of pollution in the catchment area of Lake Urema. SWECO&ASSOCIATES\_VI (2004) detected a local deterioration of the water quality in the Pungoe River Basin in Mozambique due to gold mining operations.

- **Morphology of the lake's catchment area**

An actual high resolution DTM should be compared with that extracted from available aerial photographs from the 1970s. This will enable the verification of possible morphological changes in the Urema Floodplain and in the catchment area of Lake Urema, e.g. as a result of seismic activity or channeling activity of hippopotamus.

- **Vegetation changes**

Floodplain grasslands are susceptible to changes of environmental conditions, such as of water availability and flood regime. Thus they can be used as indicators in ecosystem monitoring, including field studies and remote sensing.

An integrated approach, comprising the catchment area of the wetland system, is of fundamental importance in obtaining data that are required in formulating its protective atmosphere.

## 9 Sources

- AD-HOC-ARBEITSGRUPPE BODEN 1994. *Bodenkundliche Kartieranleitung*. 4<sup>th</sup> edition Hannover
- AHNERT, F. 1998. *Introduction to Geomorphology*. London: Arnold.
- ALLEE, R.J. & JOHNSON, J.E. 1999. *Use of satellite imagery to estimate surface chlorophyll a and Secchi disc depth of Bull Shoals Reservoir, Arkansas, USA*. - Int. J. Remote Sensing, 20(6), pp. 1057-1072.
- Administração Regional de Águas Centro (ARAC) 2004. Spreadsheet with flow data of Urema River.
- ARMAN, P., HOPCRAFT, D. & McDONALD, I. 1975. *Nutritional studies on East African herbivores. - 2. Losses of nitrogen in faeces*. - Br. J. Nutr., 33(265), pp. 265-276.
- Breen, C.M., Quinn, N.W. & Mander, J.J. 1997. *Wetlands Conservation and Management in Southern Africa: Challenges and Opportunities*. Summary of the SADC Wetlands Conservation Survey Reports. The IUCN Wetlands Programme.
- BRUNE, G.M. 1953. *Trap Efficiency of Reservoirs*. - Trans. Am. Geophys. Union, 34(3), pp. 407-418.
- BURLISON, J., CARTER, J. & WILLIAMS, T. 1977. *Report to the Ministry of Agriculture on an investigation into some of the Ecological problems of Gorongosa National Park*. Maputo: Centro de Ecologia, Instituto de Investigação Científica de Moçambique, Universidade Eduardo Mondlane.
- CAMPBELL, J.B. 2002. *Introduction to Remote Sensing*. 3<sup>rd</sup> edition London, N.Y.: Taylor & Francis.
- COBA. PROFABRIL, 1977 (?). *Esqueme Geral da Bacia do Rio Pungoe Vol. VI*. Lisboa: Dir. Prov. Serviços Hidráulicos.
- CONNELL, D.W. & HAWKER, D.W. 1991. *Pollution in tropical aquatic systems*. Boca Raton: CRC Press.
- CUNLIFFE, R. 2004. GM SAFMA. *Vegetation classification of Gorongosa National Park and Surrounds*. The Millennium Ecosystem Assessment (MA). University of Zimbabwe.
- D.N.A. & UNICEF 1987. *Hydrogeological Map of Mozambique*, scale 1:1,000,000 and the explanatory notes.
- DIRECÇÃO NACIONAL DE GEOGRAFIA E CADASTRO (DINAGECA) 1997/1998. *Topographical maps*, scale 1:250 000, folhas 67, 68, 72, 73.
- DIRECÇÃO NACIONAL DE GEOGRAFIA E CADASTRO (DINAGECA) 1960?. *Topographical maps*, scale 1:50 000 (Provisória), folhas 808, 809, 810, 811, 825, 826, 827, 828, 841, 842, 844.
- DOXARAN, D., FROIDEFOND, J.-M. & CASTAING, P. 2002. *A reflectance band ratio used to estimate suspended matter concentrations in sediment-dominated coastal waters*. - Int. J. Remote Sensing, 23 (23), pp. 5079-5085.
- DWAFa, DEPARTMENT OF WATER AFFAIRS AND FORESTRY 1996. *South African Water Quality Guidelines*. Vol. 7: Aquatic Ecosystems.
- DWAFb, DEPARTMENT OF WATER AFFAIRS AND FORESTRY 1996. *South African Water Quality Guidelines*. Vol. 1: Domestic Use.
- DWAFc, DEPARTMENT OF WATER AFFAIRS AND FORESTRY 1996. *South African Water Quality Guidelines*. Vol. 4: Agricultural Use: Irrigation.

- EASTMAN, R.J., ANYAMBA, A. & RAMACHANDRAN, M. 1996. *The Spatial Manifestation of ENSO Warm Phase Events in Southern Africa*. IDRISI GIS 96, Salzburger Geographische Materialien, 25.
- EDIÇÃO DOS SERVIÇOS DE GEOLOGIA E MINAS DA PROVÍNCIA DE MOÇAMBIQUE, LOURENÇO MARQUES, 1968a. *Carta Geológica*, Escala 1 : 250 000, Folha (SUL-E-36)/Q, Grau Quadrado 1834, Vila Paiva de Andrada – Inhaminga, Portugal Província de Moçambique.
- EDIÇÃO DOS SERVIÇOS DE GEOLOGIA E MINAS DA PROVÍNCIA DE MOÇAMBIQUE, LOURENÇO MARQUES, 1968b. *Carta Geológica*, Escala 1 : 250 000, Folha (SUL-E-36)/X, Grau Quadrado 1934, Beira – Vila Machado, Portugal Província de Moçambique.
- FERNANDES, J.F. 1968. *Os solos do Parque Nacional da Gorongosa*. IIAM Comunicações No 19.
- FOOKES, P.G. 1997. *Geological Society Professional Handbooks: Tropical Residual Soils*. A Geological Society Engineering Groups Working Party Revised Report. London: The Geological Society.
- FRAZIER, P.S. & PAGE, K.J. 2000. *Water Body Detection and Delineation with Landsat TM Data*. - Photogrammetric Engineering & Remote Sensing, 66(12), pp. 1461-1467.
- GREY, J. & HARPER, D. M. 2002. *Using stable Isotope analyses to identify allochthonous inputs to Lake Naivasha mediated via the Hippopotamus gut*. - Isotopes Environ. Health Stud., 38(4), pp. 245-250.
- IGN.FI CENACARTA 1999. *Land Use / Land Cover Database*. Maputo
- JASMUND, K. & LAGALY, G. 1993. *Tonminerale und Tone: Struktur, Eigenschaften, Anwendungen und Einsatz in Industrie und Umwelt*. Darmstadt: Steinkopff.
- JENSON, S.K. & DOMINGUE, J.O. 1988. *Extracting Topographic Structure from Digital Elevation Data for Geographic Information System Analysis*. - Photogrammetric Engineering and Remote Sensing, 54(11), pp. 1593-1600.
- KÖLLE, W. 2003. *Wasseranalysen – richtig beurteilt*. 2<sup>nd</sup> edition Weinheim: WILEY-VCH Verlag.
- KLEEBERG, R. 2005. Unpublished explanatory notes to the results of the XRD analyses of sediment samples of Lake Urema, collected by Beate Böhme. Mineralogisches Labor, TU Bergakademie Freiberg, Germany
- KLOIBER, S.M., BREZONIK, P.L., OLMANSON, L.G. & BAUER, M.E. 2002. *A procedure for regional lake water clarity assessment using Landsat multispectral data*. - Remote Sens. Environ., 82, pp. 38-47.
- LÄCHELT, S. 2004. *Geology and Mineral Resources of Mozambique*. Maputo: Direcção Nacional de Geologia Moçambique.
- LYNAM, T., CUNLIFFE, R., MAPAURE, I. & BWERINOFI, I. 2003. *Assessment of the value of woodland landscape function to local communities in Gorongosa and Muanza Districts, Sofala Province, Mozambique*. CIFOR, Bogor, Indonesia.
- MARTINELLI, G., DONGARRA, G. JONES, M.Q.W. & RODRIGUEZ, A. 1995. *Geothermal features of Mozambique – country update*. - Proceedings of the World Geothermal Congress, Florence, Italy, pp. 251-273.
- MATIZA, T. & CRAFTER, S.A. (eds.) 1994. *Wetland Ecology and Priorities for Conservation in Zimbabwe*. - Proceedings of a Seminar on Wetlands Ecology and Priorities for Conservation in Zimbabwe. Harare, Zimbabwe.
- HALDORSEN, S., RIISE, G., SWENSEN, B. & SLETTEN, R.S. 1997. *Environmental isotopes as tracers in catchments*. In Saether, O.M. & de Caritat, P. (eds.) 1997. *Geochemical processes, weathering and groundwater recharge in catchments*. Rotterdam: Balkema, pp. 185-210.

- McCARTHY, T.S. & ELLERY, W.N. 1998. *The Okavango Delta*. - Trans. Roy. Soc. S. Afr., 53(2), pp. 157-182.
- McCARTHY, T.S., STANISTREET, I.G. & CAIRNCROSS, B. 1991. *The sedimentary dynamics of active fluvial channels on the Okavango fan, Botswana*. - Sedimentology, 38, pp. 471-487.
- MERCIER, F., CAZENAVE, A. & MAHEU, C. 2002. *Interannual lake level fluctuations (1993-1999) in Africa from Topex/Poseidon: connections with ocean-atmosphere interactions over the Indian Ocean*. - Global and Planetary Changes, 32, pp. 141-163.
- MERTES, L.A.K., SMITH, M.O. & ADAMS, J.B. 1993. *Estimating Suspended Sediment Concentrations in Surface Waters of the Amazon River Wetlands from Landsat Images*. - Remote Sens. Environ., 43, pp. 281-301.
- NELLIS, M.D., HARRINGTON, J.A. & WU, J. 1998. *Remote Sensing of temporal and spatial variations in pool size, suspended sediment, turbidity, and Secchi depth in Tuttle Creek Reservoir, Kansas, 1993*. - Geomorphology, 21, pp. 281-293.
- MUNYATI, C. 2000. *Wetland change detection on the Kafue Flats, Zambia, by classification of a multitemporal remote sensing image dataset*. - Int. J. Remote Sensing, 21 (9), pp. 1787-1806.
- OWEN, R. 2004. *GM SAFMA Hydrogeology condition and trend report*. The Millenium Ecosystem Assessment (MA). Mineral Resources Centre, University of Zimbabwe.
- RICHTER, R. 2005. *Atmospheric / Topographic Correction for Satellite Imagery (ATCOR-2/3 User Guide, Version 6.1)*. Wessling: DLR – German Aerospace Center.
- ROWAN, J.S. 1995. *The Erosional Transport of Radocaesium in Catchment Systems: A Case Study of the Exe Basin, Devon*. In Foster, I., Gurnell, A. & Webb, B. 1995. *Sediment and Water Quality in River Catchments*. Chichester: John Wiley & Sons, pp. 331-351.
- SCHIEFFER, F. 2002. *Lehrbuch der Bodenkunde / Scheffer/Schachtschabel*. 15<sup>th</sup> edition Heidelberg: Spektrum Akademischer Verlag.
- SCHLICHTING, E., BLUME, H.-P. & STAHR, K. 1995. *Bodenkundliches Praktikum*. 2<sup>nd</sup> edition Berlin, Wien: Blackwell Wissenschaftsverlag.
- SHUMWAY, C.A. 1999. *Forgotten Waters: Freshwater and Marine Ecosystems in Africa: Strategies for Biodiversity Conservation and Sustainable Development*. The Biodiversity Support Program of Boston University, New England Aquarium, U.S. Agency for International Development.
- SUTHERLAND, R.A. & BRYAN, R.B. 1991. *Sediment budgeting: A case study in the Katorin Drainage Basin, Kenya*. Earth Surface Processes and Landforms, 16, pp. 383-398.
- SWECO&ASSOCIATES\_I. 2004. Development of the Pungwe River Basin. Joint Integrated Water Resources Management Strategy. Monograph Report. Annex I. Sector Study on: Surface Water Resources of the Pungwe River Basin. - client: Government of the Republic of Mozambique, Government of the Republic of Zimbabwe, Swedish International Development Cooperation Agency (Sida).
- SWECO&ASSOCIATES\_III. 2004. Development of the Pungwe River Basin. Joint Integrated Water Resources Management Strategy. Monograph Report. Annex III. *Sector Study on: Hydrological Data Quality & Modelling*. - client: Government of the Republic of Mozambique, Government of the Republic of Zimbabwe, Swedish International Development Cooperation Agency (Sida).
- SWECO&ASSOCIATES\_IV. 2004. Development of the Pungwe River Basin. Joint Integrated Water Resources Management Strategy. Monograph Report. Annex IV. *Sector Study on: Groundwater Recources*. - client: Government of the Republic of Mozambique, Government of the Republic of Zimbabwe, Swedish International Development Cooperation Agency (Sida).

SWECO&ASSOCIATES\_V. 2004. Development of the Pungwe River Basin. Joint Integrated Water Resources Management Strategy. Monograph Report. Annex V. *Sector Study on: Dams and other Hydraulic Works*. - client: Government of the Republic of Mozambique, Government of the Republic of Zimbabwe, Swedish International Development Cooperation Agency (Sida).

SWECO&ASSOCIATES\_VI. 2004. Development of the Pungwe River Basin. Joint Integrated Water Resources Management Strategy. Monograph Report. Annex VI. *Sector Study on: Water Quality and Sediment Transport*. - client: Government of the Republic of Mozambique, Government of the Republic of Zimbabwe, Swedish International Development Cooperation Agency (Sida).

SWECO&ASSOCIATES\_X. 2004. Development of the Pungwe River Basin. Joint Integrated Water Resources Management Strategy. Monograph Report. Annex X. *Sector Study on: Conservation Areas, Wildlife and Tourism*. - client: Government of the Republic of Mozambique, Government of the Republic of Zimbabwe, Swedish International Development Cooperation Agency (Sida).

TINLEY, K.L. 1977: *Framework of the Gorongosa Ecosystem*. PhD. Thesis, Faculty of Science, University of Pretoria, South Africa.

WETZEL, R.G. 2001. *Limnology – Lake and River Ecosystems*. 3<sup>rd</sup> edition San Diego: Academic Press.

WETZEL, R.G. & LIKENS, G.E. 2000. *Limnological analyses*. 3<sup>rd</sup> edition New York: Springer.

ZHANG, X. & ZHANG, Y. 1995. *Use of Caesium-137 to investigate Sediment Sources in the Hekouzhen-Longmen Basin of the Middle Yellow River, China*. In Foster, I., Gurnell, A. & Webb, B 1995. *Sediment and Water Quality in River Catchments*. Chichester: John Wiley & Sons, pp. 353-362.

#### DIN

DIN ISO 11277: 2002-08: Bodenbeschaffenheit: Bestimmung der Partikelgrößenverteilung in Mineralböden – Verfahren mittels Siebung & Sedimentation

#### URL sources

web\_1 Carr Foundation <http://www.gorongosa.net/index.asp> (access 07-19-2005)

web\_4 Envirotrade [http://www.envirotrade.co.uk/Pages/gorongosa\\_biocarbon.htm](http://www.envirotrade.co.uk/Pages/gorongosa_biocarbon.htm) (access 07-19-2005)

web\_6 FAO METART [http://metart.fao.org/~~/gbr/ARTEMIS.exe\\$ProdMenu?Ctry=MOZ](http://metart.fao.org/~~/gbr/ARTEMIS.exe$ProdMenu?Ctry=MOZ) (access 06-10-2005)

web\_7 Fernerkundung Freiberg [http://www.geo.tu-freiberg.de/fernerkundung/fe\\_lehre.html](http://www.geo.tu-freiberg.de/fernerkundung/fe_lehre.html) (access 07-19-2005)

web\_8 GEO:connexion <http://www.geoconnexion.com/magazine/article.asp?ID=869> (access 07-19-2005)

web\_10 Global Land Cover Facility Shuttle Radar Topography Mission <http://glcf.umiacs.umd.edu/data/guide/technical/srtm.shtml> (access 07-19-2005)

web\_11 Harvard Seismology CMT Catalog <http://www.seismology.harvard.edu/CMTsearch.html> (access 07-19-2005)

web\_12 Land Processes Distributed Active Archive Center <http://edcdaac.usgs.gov:80/gtopo30/gtopo30.asp> (access 07-19-2005)

web\_13 NASA Shuttle Radar Topography Mission <http://www2.jpl.nasa.gov/srtm> (access 07-19-2005)

web\_14 Pennsylvania Department of Environmental Protection [http://www.dep.state.pa.us/dep/deputate/minres/districts/Eng\\_Manual/chapter3.html](http://www.dep.state.pa.us/dep/deputate/minres/districts/Eng_Manual/chapter3.html) (access 07-19-2005)

web\_15 Rook, E.J.S. <http://www.rook.org/earl/bwca/nature/aquatics/ceratophyllum.html> (access 07-19-2005)

web\_17 The Ramsar Convention on Wetlands <http://www.ramsar.org> (access 07-19-2005)

web\_19 UCAR [http://www.isse.ucar.edu/el\\_nino/glossary.html](http://www.isse.ucar.edu/el_nino/glossary.html) (access 07-19-2005)

web\_20 USGS SRTM <http://seamless.usgs.gov/>

personal communication

FALKER, D., Carr Foundation, Gorongosa National Park Restoration Project, Chitengo, Mozambique, March 2005

HAHNEWALD, M. 2005: Technical University Bergakademie Freiberg, Soil and Water Conservation Unit, July 2005

JANUARIO, F., Warden of Gorongosa National Park, Chitengo, Mozambique, October 2004

LYNAM, T. Institute of Environmental Studies, University of Zimbabwe, Harare, Zimbabwe, August 2005

STEINBRUCH, F., Centro de Informação Geográfica, Universidade Católica de Moçambique (CIG UCM), Beira, Mozambique, March 2005

graphics

NIEMEYER, I. 2004. created object orientated image classification in eCognition Enterprise. Professorship for photogrammetry and geomonitoring Technical University Bergakademie Freiberg

WOBBE, F. 2005. produced map of southern Africa and Mozambique in GMT 3.4.4

## 10 Acknowledgments

The accomplishment of this work (as part of the prerequisite for the award of my degree in geology at the Technical University Bergakademie Freiberg) received an enormous amount of assistance and cooperation from a number of individuals and institutes both here Germany and Mozambique. During the entire implementation period a lot of people helped and supported me in a variety of ways. I am indebted to all of them. Here I would like to distinguish and express my special thanks to the following:

Dipl. Geol. **Franziska Steinbruch** (Centro de Informação Geográfica, Universidade Católica de Moçambique (CIG UCM), Beira, Mozambique) for her support in every aspect of this work especially during my stay in Mozambique. Her hospitality gave me a lot of inspiration and comfort.

My supervisors; **Prof. Broder Merkel** (Chair for Hydrogeology), **Prof. Richard Gloaguen** (Remote Sensing Group), **PD Dr. Hermann Heilmeier** (Interdisciplinary Ecological Centre (IÖZ)) for their enormous and unquantifiable discussions, ideas and encouragements both during my study as well as in the course of this thesis.

**Fernando Januario** (warden at Gorongosa National Park) for both his moral and physical protection in “Mira Hippo”. He shielded me in the field through his wealthy experiences in African Wildlife.

**Roberto Zohlo** (former director of the Gorongosa National Park) for the initiation of this work, his practical support and many valuable advices.

**Jose Paulino Capece and the team of the Gorongosa National Park** for the organization and logistical support during my period of stay at the Gorongosa National Park.

I would like to emphasize that this work received a collaborative assistance from different institutes and organizations. From this point of view I would like to thank;

- Centro de Informação Geográfica, Universidade Católica de Moçambique (CIG UCM), Beira, Mozambique
- Chair for Hydrogeology, Remote Sensing Group, Soil and Water Conservation Unit (Faculty of Geoscience, Geotechnique and Mining), Interdisciplinary Ecological Centre (IÖZ), all located at the Technical University Bergakademie Freiberg (TUBAF), Germany
- Ministry of Tourism in its responsibility for the Gorongosa National Park in Sofala Province, Mozambique
- Deutscher Akademischer Austauschdienst e.V. (DAAD)

- Administração Regional de Águas Centro (ARAC), Beira, Mozambique
- Instituto Nacional de Meteorologia (INAM), Maputo, Mozambique
- SUBTECH Diving & Marine Co., Durban, Republic of South Africa
- Zentrum für GeoInformatik (ZGIS), Salzburg, Austria

for financial support, data and provision of equipment.

The support and understanding from the following people can not be underestimated;

- Jan Böttger
- André Günther for his “survival tips” and the encouragements during the “peak phases” of the thesis
- Kurt Herklotz: Interdisciplinary Ecological Centre (IÖZ), TUBAF, for equipping me with all necessary techniques to get familiar with the water and sediments of Lake Urema
- Hans-Joachim Peter: Chair for Hydrogeology, TUBAF, and Monika Hahnewald, Soil and Water Conservation Unit, TUBAF, for the water- and sediment analyses
- Dave Falker, Carr Foundation, for giving me the chance to see Lake Urema from above, for keeping me from starving in Mira Hippo and for many interesting safaris
- Tim Lynam, Institute of Environmental Studies, University of Zimbabwe: for constructive discussions and the delivery of elevation data
- staff and other students at the Remote Sensing Group at TUBAF: particularly Florian Wobbe for his experience with all kinds of computer problems and his wonderful graphics in GMT, Anna Görner for sharing her experiences with PCI Geomatica and Michael Buchwitz for his help with the confusing rift geology

Among others are **Christine Cellarius** and **Dirk Tietens**, **Ludgar Kaup** and **Brit Zohlo**. They made me feel at home during my stay at Beira and Chitengo.

Lastly and most importantly, I would have not been privileged to write this thesis without the love, caring, trust and affection from my family and friends. With profound gratitude I say thanks to you all!